NASA CONTRACTOR REPORT

NASA CR-2665

NASA CR-2665

SPECTRAL REFLECTANCE AND RADIANCE CHARACTERISTICS OF WATER POLLUTANTS

C. T. Wezernak, R. E. Turner, and D. R. Lyzenga

Prepared by
ENVIRONMENTAL RESEARCH INSTITUTE OF MICHIGAN
Ann Arbor, Mich. 48107
for Langley Research Center

NATIONAL AERONAUTICS AND SPACE ADMINISTRATION • WASHINGTON, D. C. • APRIL 1976

1. Report No. NASA CR-2665	2. Government Accession No.	3. Recipie
4. Title and Subtitle Spectral Reflectance and Radiance Characteristics of Water Pollutants		5. Report Date April 1976
		6. Performing Organization Code
7. Author(s) C.T. Wezernak, R.E. Turner, and D.R. Lyzenga		8. Performing Organization Report No. 112000-9-F
9. Performing Organization Name and Address Environmental Research Institute of Michigan Infrared and Optics Division P.O. Box 618 Ann Arbor, Michigan 48107		10. Work Unit No.
		11. Contract or Grant No. NAS1-13589
12. Sponsoring Agency Name and Address National Aeronautics and Space Administration Langley Research Center Hampton, Virginia 23665		13. Type of Report and Period Covered September 1974-June 1975
		14. Sponsoring Agency Code

15. Supplementary Notes

Langley Technical Monitor: David E. Bowker

Final Report

16. Abstract

Spectral reflectance characteristics of water pollutants and water bodies were compiled using the existing literature. Radiance calculations were performed at satellite altitude for selected illumination angles and atmospheric conditions. The work described in this report was limited to the reflective portion of the spectrum between 0.40 μm to 1.0 μm.

17. Key Words remote sensing, water pollutants, water bodies, reflectance, radiance		18. Distribution Statement UNCLASSIFIED - UNLIMITED Subject Category 45	
19. Security Classif. (of this report) UNCLASSIFIED	20. Security Classif. (of this page) UNCLASSIFIED	21. No. of Pages 230	22. Price* $7.75

*For sale by the National Technical Information Service, Springfield, Virginia 22161

NOTICES

Sponsorship. The work reported herein was conducted by the Environmental Research Institute of Michigan for the National Aeronautics and Space Administration, Langley Research Center, Hampton, Virginia 23665, Contract No. NAS1-13589. Dr. D. Bowker was Technical Monitor. Contracts and grants to the Institute for the support of sponsored research are administered through the Office of Contracts Administration.

Disclaimers. This report was prepared as an account of Government-sponsored work. Neither the United States, nor the National Aeronautics and Space Administration (NASA), nor any person acting on behalf of NASA

(A) Makes any warranty or representation, expressed or implied with respect to the accuracy, completeness, or usefulness of the information contained in this report, or that the use of any information apparatus, method, or process disclosed in this report may not infringe privately owned rights; or

(B) Assumes any liabilities with respect to the use of, or for damages resulting from the use of any information, apparatus, method, or process disclosed in this report.

As used above, "person acting on behalf of NASA" includes any employee or contractor of NASA, or employee of such contractor, to the extent that such employee or contractor of NASA or employee of such contractor prepares, disseminates, or provides access to any information pursuant to his employment or contract with NASA, or his employment with such contractor.

PREFACE

The general objectives of the program were to describe the spectral reflectance characteristics of water pollutants and water bodies using information derived from the existing literature; and to convert the spectral reflectance data so compiled into radiance data at satellite altitude for selected illumination angles and atmospheric conditions.

The work described in this report was limited to the reflective portion of the electromagnetic spectrum between 0.40 μm to 1.0 μm. Information is included for the following general categories:

1. Water Bodies
2. Phytoplankton-Chlorophyll
3. Suspended Solids
4. Oil
5. Municipal Effluent
6. Industrial Effluents

The amount of suitable material in the professional literature was found to be very limited. Information is generally lacking regarding the optical properties of surface waters and water pollutants. The material presented in this report is regarded simply as an initial effort in the development of a suitable data base which can serve as the basis for the development of remote sensing systems for monitoring the aquatic environment.

CONTENTS

FIGURES

TABLES

TABLE	TITLE	PAGE
143	Steel Mill Effluent, Radiance, Visibility 23 km	193
144	Steel Mill Effluent, Radiance, Visibility 40 km	194
145	Steel Mill Effluent, Radiance, Visibility 60 km	195
146	Paper Mill Sulfite Liquor, 8% Solids, Reflectance	196
147	Paper Mill Sulfite Liquor, 8% Solids, Radiance, Visibility 15 km	197
148	Paper Mill Sulfite Liquor, 8% Solids, Radiance, Visibility 23 km	198
149	Paper Mill Sulfite Liquor, 8% Solids, Radiance, Visibility 40 km	199
150	Paper Mill Sulfite Liquor, 8% Solids, Radiance, Visibility 60 km	200
151	Chemical: Chlor-Alkali, Reflectance	201
152	Chemical: Chlor-Alkali, Radiance, Visibility 15 km	202
153	Chemical: Chlor-Alkali, Radiance, Visibility 23 km	203
154	Chemical: Chlor-Alkali, Radiance, Visibility 40 km	204
155	Chemical: Chlor-Alkali, Radiance, Visibility 60 km	205
156	Tannery Effluent, Reflectance	206
157	Tannery Effluent, Radiance, Visibility 15 km	207
158	Tannery Effluent, Radiance, Visibility 23 km	207
159	Tannery Effluent, Radiance, Visibility 40 km	208
160	Tannery Effluent, Radiance, Visibility 60 km	208

SPECTRAL REFLECTANCE AND RADIANCE CHARACTERISTICS OF WATER POLLUTANTS

By C.T. Wezernak, R.E. Turner, and D.R. Lyzenga
Environmental Research Institute of Michigan

1
INTRODUCTION

The data needs in limnology, oceanography, and water pollution control are very extensive and span a broad spectrum of physical, chemical, and biological measurements. The aquatic environment is clearly a dynamic and complex heterogeneous system. As a result, a wide-range of instrumental techniques and analytical procedures are required.

Water pollutants are substances introduced into the aquatic environment which adversely alter the quality of this environment. Water quality is expressed in terms of a set of physical, chemical, and biological parameters. In general, water quality analysis does not lend itself to simple analytical procedures. As a result, the potential of remote sensing for water quality analysis, in the chemical sense, is severely limited.

The term monitoring as applied to water resources and water pollution control embraces a vast array of functions and procedures for detection, measuring, and analyzing materials on the surface of the water, materials suspended in the water, and materials dissolved in the water. Expressed in general terms, monitoring is performed for the following purposes:

(1) establishment of water quality baselines
(2) detection of spills, discharges, and seeps of polluting substances into the aquatic environment
(3) identification of pollutant sources
(4) determination of the extent of the pollutant and tracking its

movement

(5) evaluation of the effect of pollutants on designated beneficial uses of the water resource and the total ecology

(6) characterization of autochthonous and allochtonous materials and/or substances in solution, suspension, and in the form of surface films, for various environmental and resource management purposes.

Clearly, a wide range of surveillance and analytical techniques are needed to acquire the necessary physical, chemical, and biolo cal data required in water quality monitoring. The limitations of conventional point-sampling methods are particularly evident in programs dealing with large environmental systems such as estuaries, and Great Lakes, and the oceans of the world. Many of the above monitoring functions are amenable to remote sensing analysis.

Fundamental to the design of remote sensing instrumentation and the development of interpretive techniques intended for monitoring the aquatic environment from satellite altitudes is information regarding the spectral reflectance and radiance characteristics of water pollutants and various water bodies. Although other characteristics, particularly thermal properties, are equally important to the problem; the work described in this report was limited to the reflective portion of the electromagnetic spectrum between 0.40 μm to 1.0 μm. The objectives of the program were:

(1) Using information derived from the existing literatur , to define the spectral reflectance characteristics of water pollutants and water bodies.

(2) To convert the spectral reflectance data into radiance data at satellite altitude, for selected illumination angles and atmospheric conditions.

Although the existing remote sensing literature is very extensive, much of the data contained in the literature consists of imagery and/or data which is uncalibrated and collected under undefined conditions. Nevertheless, in spite of the numerous difficulties and limitations associated with extracting information from the existing literature, the data which is presented in the sections which follow provides important insights regarding the reflectance characteristics of surface waters and the modifications in these characteristics resulting from the introduction of pollutants into surface waters. Data regarding specific pollutants is also presented. However, it must be recognized that the apparent reflectance of aqueous solutions and suspensions is related to receiving water characteristics.

Reflectance data were converted to radiance data at satellite altitude for a specific set of conditions. A description of the atmospheric model used and conditions for which calculations were made, is presented in the sections which follow.

2

RADIATIVE TRANSFER AND ATMOSPHERIC MODEL

2.1 THE ATMOSPHERIC STATE

In the remote sensing of Earth's surface by means of electromagnetic radiation reflected from terrain objects, the atmosphere will scatter and absorb the radiation and, hence, alter the intrinsic radiation characteristics of the object being investigated. The resultant radiation received by a sensor depends upon factors such as viewing geometry, time of year, surface conditions, and atmospheric state. The state of the atmosphere is discussed in the section which follows.

2.1.1 COMPOSITION OF THE ATMOSPHERE

The state of the atmosphere at any location and at any time can be defined by a unique set of parameters fully describing all aspects of the atmosphere. However, all aspects are not relevant to this discussion, but only thoese aspects which are of key importance to remote sensing applications. Thus, micro-fluctuations in density or ion content are of no importance; however, visibility is an important factor. The goal, therefore, is a somewhat limited specification of parameters which can be used to define the state of the atmosphere. For purposes of the present study, the major concerns are the scattering and absorbing properties of gases and particulates that exist in our atmosphere.

Atmospheric Gases

By definition, the visible portion of the electromagnetic spectrum is that part of it to which the human eye is most sensitive; thus it is not surprising that this part of the spectrum undergoes little absorption by the atmosphere. The major permanent gaseous components of our atmosphere are molecular oxygen, nitrogen, and argon. These gases absorb very little radiation in the visible and near-infrared part of the spectrum; only variable components such as water vapor, carbon dioxide, ozone, sulfur dioxide, nitrogen compounds, methane, and other trace gases absorb such radiation to any extent. Of these variable components, ozone, water vapor, and carbon dioxide are the most important absorbers of radiation in the near-infrared. For the purposes of this study, we shall consider only ozone in the Chappuis bands in the region 0.44 to 0.74 μm and assume that all other radiation in the region 0.40 to 2.0 μm is not absorbed by gases. Since the gaseous absorption regimes of the various atmospheric components are well known, it is relatively easy to select those spectral regions within which absorption is at a minimum. More detailed studies of atmospheric gases have been done by Goody [1] and Zuyev [2].

Throughout the visible part of the spectrum, ozone is the primary gaseous absorber. There are variable amounts in the troposphere, but the general altitude variation is known [3]. A profile of the ozone number density is illustrated in Figure 1. Note that the maximum density occurs at an altitude of about 23 km.

Aerosols

One may define an aerosol as a semi-permanent suspension of solid or liquid particles in the Earth's atmosphere. Typical aerosol distributions would be hazes, clouds, mists, fogs, smokes, and dusts. It is the aerosol component of the atmosphere which is quite variable. Depending upon location and time, aerosols can have many compositions, sizes, shapes, and densities. In condensation processes, the predominant composition is water (for which the refractive index is well known). Depending upon the history of the distribution, however, various contaminants can mix with water and water vapor in the formation of droplets to produce a composition quite different from that of water. The major primary source of atmospheric aerosols on a world-wide basis is sea spray [4]; other primary sources are wind-

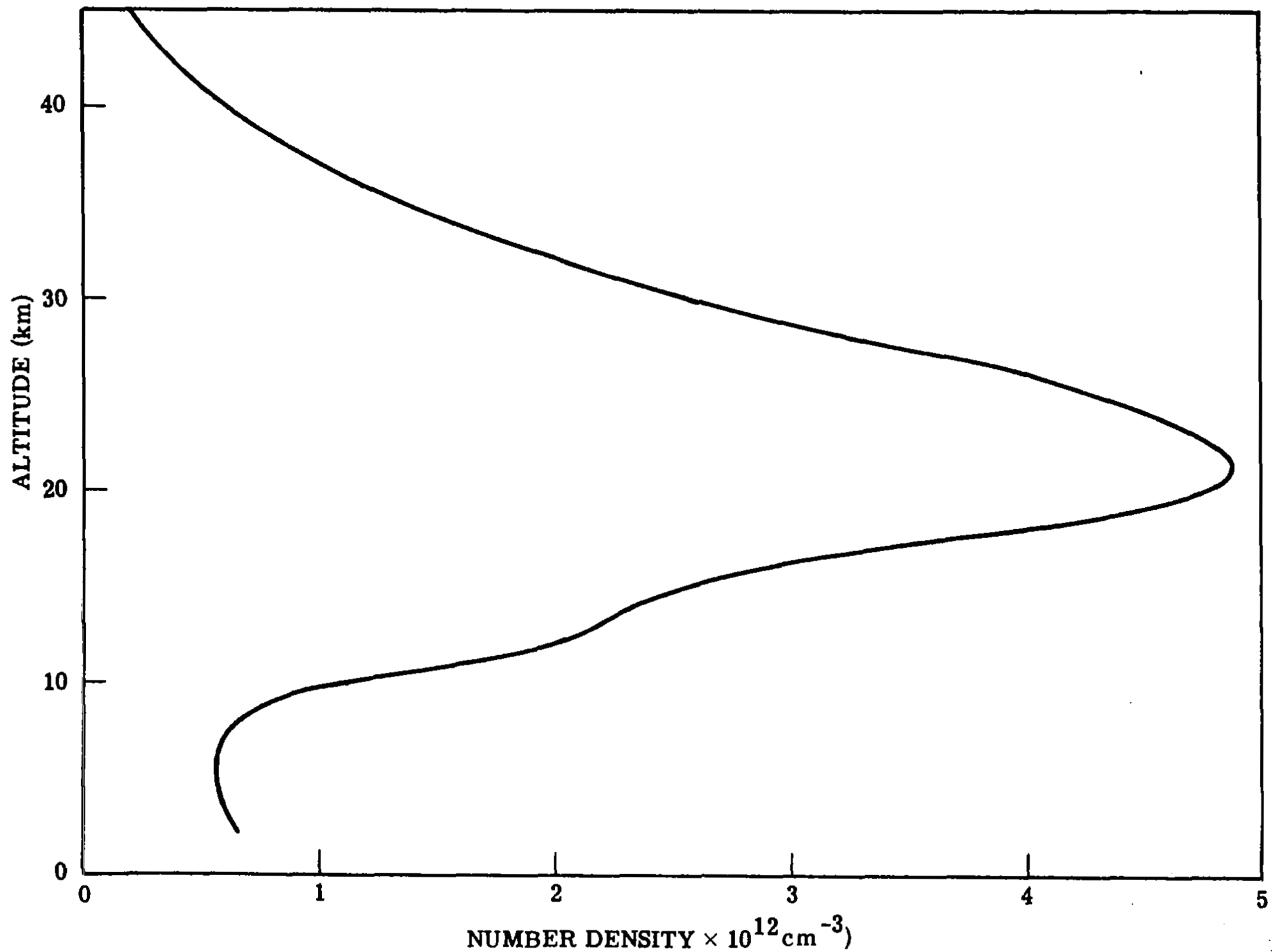

FIGURE 1. ALTITUDE PROFILE FOR OZONE DENSITY

blown dust and smoke from forest fires. While the composition of world-wide aerosol distribution can be estimated, this composition can nevertheless vary over a wide range depending upon its proximity to various local sources. The only ways in which the composition can be determined is by direct in situ sampling of the air in a particular location or by radiometric techniques. Much in situ sampling has been done by Volz [5,6], Grams et al. [7], and Flanigan and Delong [8]. As a result of their work and that of others, the mean world-wide aerosol can be considered to have a real refractive index of about 1.5 and an imaginary part between 0.01 and 1.0. Hence,

$$m(\lambda) = m_1 - im_2 \tag{1}$$

where m_1 and m_2, respectively, are the real and imaginary part of the refractive index, and λ is the wavelength. For realistic atmospheric conditions,

$$1.33 \lesssim m_1 \lesssim 1.55 \tag{2}$$

and

$$0 < m_2 \lesssim 1.0 \tag{3}$$

which are roughly independent of wavelength.

Particles also come in various sizes. Generally, however, they can be put into three categories: the Aitken nuclei with radii between 10^{-7} and 10^{-5} cm, the large particles with radii between 10^{-5} and 10^{-4} cm, and the so-called giant particles with radii greater than 10^{-4} cm. In most hazes, the optically active region is made up of those particles in the large or giant categories. Junge [9] showed that most aerosol distributions follow the simple power law:

$$N(z,r) = C(Z)\ r^{-\nu} \tag{4}$$

where N(z,r) is the particle number density for radius, r, at altitude, z, ν is the exponent of the power law. Experimentally, ν has been found to vary from 2 to 5 for various tropospheric aerosol distributions. Also, other investigators have found a better fit to the particulate data by using the modified gamma distribution,

$$N(z,r) = ar^{\alpha}\ \exp(-br^{\gamma});\ 0 \leq r < \infty \tag{5}$$

where a, α, b, and γ are parameters which describe the distribution.

Diermendjian [10] has used this function to characterize different hazes. The following is a list of the hazes Diermendjian considered and the relevant parameters;

Haze Type	a	α	γ	b
M	5.3333×10^4	1	1/2	8.9443
L	4.9757×10^6	2	1/2	15.1186
H	4.0000×10^5	2	1	20.0000

Haze M, used to describe a marine or coastal haze, has a peak in the distribution at r = 0.05 μm. The haze L represents a continental distribution and has a peak at r = 0.07 μm. The haze H model can be used to represent a stratospheric aerosol or dust layers; it has a peak at 0.10 μm. A graph of the three hazes is illustrated in Figure 2. We shall make use of these hazes in the detailed analysis of atmospheric radiation.

For the liquid aerosols it can be assumed that the particles are spherical or nearly spherical in shape. For solid particles, however, the shape may assume any form. A number of investigators [11,12,13]

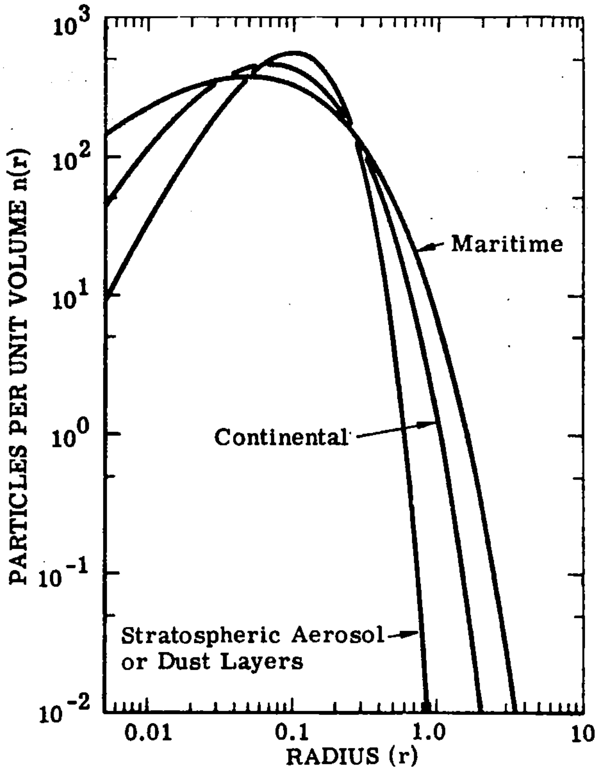

FIGURE 2. HAZE-TYPE DISTRIBUTION FUNCTIONS USED. Units depend on the particular model.

have studied the influence of particle shape on the scattering of radiation. The scattering of electromagnetic radiation by odd-shaped particles has a different pattern from that produced by spherical particles; but given a polydisperse collection of odd-shaped particles; the nature of the different is not clear. Most of the work on radiation in atmospheres concerns spherical aerosols; we shall follow suit and neglect the complications of particle shape.

Thus far we have considered the composition, sizes, and shapes of aerosol particles, but in order to define the atmospheric state we must also know the concentration of particles. Wiegand [14] was the first to measure the vertical profile of an aerosol number concentration of condensation nuclei. As a result of his measurements and many others cited in Ivlev [15], it was found that the concentration of condensation nuclei obeys an exponential law with altitude. It was also determined that a zone of increased concentration of large particles exists in the 17 to 23 km altitude range (Junge layer) and in a probable layer under the tropopause at 9 to 10 km. These layers are relatively stable compared to the lower part of the troposphere. As an example of an aerosol model atmosphere, Zuyev [2] has constructed the following altitude-dependent, number density-distribution-function for aerosols:

$$N(z) = \begin{cases} N(0)e^{-bz}; & z \leq 5 \text{ km} \\ 0.03; & 5 \text{ km} \leq z \leq 15 \text{ km} \\ 0.03e^{0.06z}; & 15 \text{ km} \leq z \leq 20 \text{ km} \\ 0.01e^{-0.09z}; & z \geq 20 \text{ km} \end{cases} \tag{6}$$

where N(z) and N(0), respectively, are the number densities at altitude z and the Earth's surface (altitude 0).

In conclusion, we can say that the most significant aspect of aerosol particles in the atmosphere is their high degree of variability in composition, size distribution, and especially in number density. All the models in the current literature deal with a highly approximate average-condition from which large deviations can occur in real situations. The many details of aerosol science will not be considered in this report. For a more complete study of the physics and chemistry of aerosols, see Mason [16], Fuchs [17], Davies [18], or Green and Lane [19].

2.1.2 TURBIDITY

Having examined the basic characteristics of the gases and aerosol particles composing the atmosphere, we now consider those parameters which relate to attenuation of radiation passing through the atmosphere.

If a collimated beam of monochromatic radiation is incident upon a scattering and absorbing medium, then the intensity of the beam at distance x is given by

$$I(x) = I(o)e^{-\kappa x} \tag{7}$$

where I(o) is the beam intensity at the origin. The quantity κ, called the volume extinction coefficient, is equal to the sum of the volume absorption and volume scattering coefficients. Since attenuation of radiation in the atmosphere is caused primarily by molecular scattering, scattering and absorption by water droplets, and also by dust particles, Linke [20] proposed that the attenuation be measured by taking the ratio of the total integrated attenuation coefficients to the pure Rayleigh integratec coefficients. Thus,

$$t(\lambda) = \frac{\int_0^\infty \kappa_R(\lambda)dz + \int_0^\infty \kappa_w(\lambda)dz + \int_0^\infty \kappa_d(\lambda)dz}{\int_0^\infty \kappa_R(\lambda)dz} \tag{8}$$

where $\kappa_R(\lambda)$, $\kappa_w(\lambda)$, and $\kappa_d(\lambda)$ are the volume extinction coefficients for Rayleigh, water aerosol, and dust particle scattering, respectively. Thus, the turbidity, $t(\lambda)$, is a measure of the departure of a real atmosphere from the ideal pure Rayleigh atmosphere. Equation (8) can also be written as

$$t = 1 + W + R \tag{9}$$

where W is the humid turbidity factor and R is the residual turbidity factor. For a pure atmosphere free of water and dust, t = 1. Values of the turbidity vary from 3.59 for a continental tropical air mass in the summer months to 2.16 for a sea arctic air mass in winter. Tables of typical turbidity values are given by Kondratyev [21] for many locations and weather conditions. The turbidity is a function of altitude is shown in Figure 3 [22]; this figure was constructed from data collected by Elterman [23] in optical searchlight measurements. The maximum near the tropopause is the result of convective activity causing particles to concentrate at that stable position.

2.1.3 VISIBILITY

Visibility in meteorology referes to the transparency of the atmosphere to visible radiation. Usually characterized by a quantity, V, called visual range, it depends upon the optical properties of the atmosphere, the properties of both the object

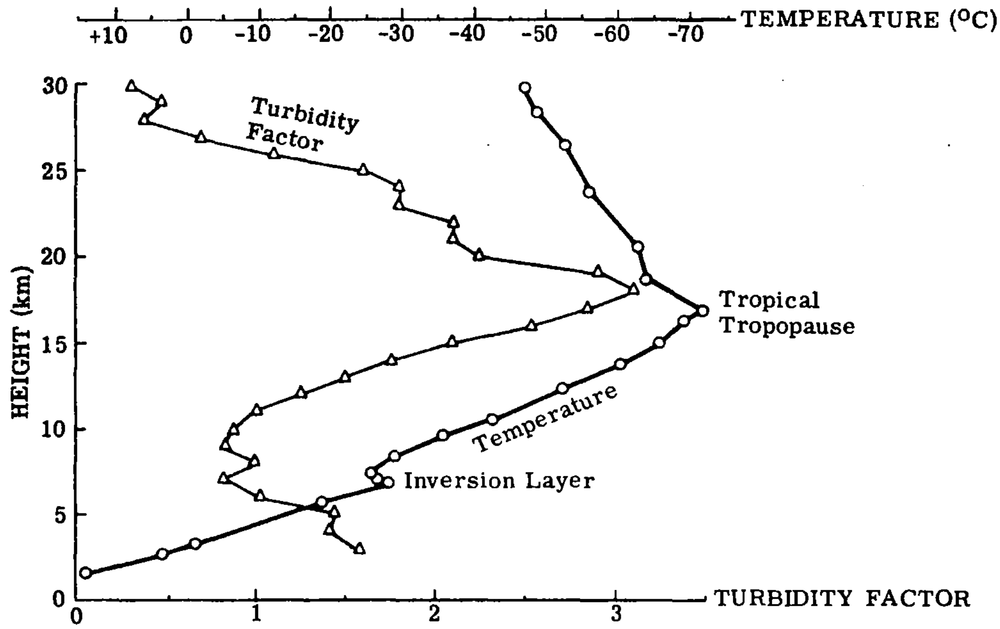

FIGURE 3. AEROSOL AND TEMPERATURE PROFILES FOR 4-5 NOVEMBER 1964

sighted and its background, and illumination conditions. Middleton [24] derives the so-called air-light equation given by

$$L = L_o e^{-\kappa x} + L_p(1-e^{-\kappa x}) \tag{10}$$

where L_o is the intrinsic radiance of the object

L_p is the radiance along an infinite path through the atmosphere

κ is the volume extinction coefficient

Tverskoi [25] derives a contrast equation:

$$C = \frac{C_o}{1+\frac{1}{b_o}(e^{\kappa x}-1)} \tag{11}$$

where C_o is the ratio of the difference between background and intrinsic radiances to background radiances, and b_o is a brightness factor. This equation can be simplified:

$$C = C_o e^{-\kappa x} \tag{12}$$

The visual range in km is that distance at which the relative contrast is 2%, i.e.,

$$(C/C_o) = 0.02 = e^{-\kappa V} \tag{13}$$

or

$$V = \frac{\ell n\ 0.02}{\kappa} = \frac{3.912}{\kappa} \tag{14}$$

Equation (14) is usually taken as the defining equation for visual range at a wavelength of 0.55 μm, which is near the peak of the human visual-response curve.

2.2 OPTICAL PARAMETERS

The physical state of the atmosphere was considered in the preceding section. In this section the appropriate atmospheric optical parameters used in radiative-transfer model are defined and calculated.

2.2.1 SCATTERING THEORY

Radiation which passes through a homogeneous medium free of any discontinuities will cause waves to interfere in such a way that no scattering takes place. Realistic media at temperatures above absolute zero, however, have discontinuities such as crystal impurities, density fluctuations, and various sized particles. The earth's atmosphere is such a medium. An assumption is made, moreover, that all scatterings are independent; that is, that there is no phase relation between scattered waves. For this to be true, the distance between scattering centers must be at least several times the size of the scattering centers themselves. This condition is certainly fulfilled for atmospheric hazes and even for dense fogs. The basic optical quantities needed for radiative-transfer analysis are examined in terms of this physical setting.

Rayleigh Scattering

The theory of light scattering in the atmosphere originated when Lord Rayleigh [26] found an explanation for the blue color of the clear sky. It is now known that this hue is the result of the scattering of radiation from density fluctuations, rather than from molecules as had been assumed earlier. If we have a plane electromagnetic wave with electric field strength

$$\vec{E}(\vec{r}, t) = \vec{E}_o e^{i(\vec{k}\cdot\vec{r} - \omega t)} \tag{15}$$

where $\vec{k}$ is the complex propagation vector

$\vec{r}$ is a coordinate position vector

ω is the angular frequency

then this wave impinging upon a scattering center whose size is much smaller than the wavelength of the radiation will produce scattered waves in an effect called Rayleigh scattering. The scattering cross-section can be obtained by integrating the Poynting vector over a period of oscillation. The result is

$$\sigma_R(\lambda) = \frac{8\pi^3(m^2 - 1)^2}{3N^2\lambda^4} \cdot \frac{6 + 3\delta}{6 - 7\delta} \tag{16}$$

where N is the molecular number density

λ is the wavelength

δ is an anisotrophy parameter to account for polarization effects

m is the refractive index of the medium

Of importance here is the $1/\lambda^4$ dependence of the cross-section, a characteristic of radiation from an oscillating dipole field.

It can also be shown that the scattering pattern is described by the following formula:

$$p(\cos \chi) = \frac{3}{4} (1 + \cos^2 \chi) \tag{17}$$

in which χ is the angle between the incoming direction and the scattered direction. The function $p(\cos \chi)$, which is called the scattering phase function, is normalized to unity over all 4π steradians, that is,

$$\int_{\Omega} p(\cos\ \chi)\ d\Omega = 1 \tag{18}$$

where Ω is the solid angle.

Mie Scattering

The scattering of electromagnetic radiation by homogeneous dielectric spheres is called Mie scattering. In principle, determining the scattering and absorption cross-sections and the scattering phase function is straightforward. First, the wave equation is solved inside and outside the sphere; then the solutions are matched at the boundary to determine the constants. The intensity of the radiation scattered into an angle χ is given by

$$I = \frac{\lambda^2}{4\pi^2 R^2} \frac{|S_1|^2 + |S_2|^2}{2} I_o \tag{19}$$

where R is the distance from the sphere, and I_o is the incident intensity. The scattering amplitudes $|S_1|^2$ and $|S_2|^2$ are given by

$$S_1 = \sum_{\ell=1}^{\infty} \frac{2\ell + 1}{\ell(\ell + 1)} [a_\ell \pi_\ell + b_\ell \tau_\ell] \tag{20}$$

$$S_2 = \sum_{\ell=1}^{\infty} \frac{2\ell + 1}{\ell(\ell + 1)} [a_\ell \tau_\ell + b_\ell \pi_\ell]$$

In Equation (20) a_ℓ and b_ℓ, which are the Mie coefficients, are given by

$$a = \frac{\psi'_\ell(mx)\psi_\ell(x) - m\psi_\ell(mx)\psi'_\ell(x)}{\psi'_\ell(mx)\zeta_\ell(x) - m\psi_\ell(mx)\zeta'_\ell(x)} \tag{21}$$

$$b = \frac{m\psi'_\ell(mx)\psi_\ell(x) - \psi_\ell(mx)\psi'_\ell(x)}{m\psi'_\ell(mx)\zeta_\ell(x) - \psi_\ell(mx)\zeta'_\ell(x)} \tag{22}$$

where m and x, respectively, are the complex refractive index and size parameters - that is, $m = m_1 - im_2$ and $x = 2\pi r/\lambda$ when r is the particle radius. The functions ψ_ℓ and ζ_ℓ are the Riccati-Bessel functions, and a prime indicates differentiation with respect to the argument. The π_ℓ and τ_ℓ functions are given by

$$\pi_\ell(\cos\chi) = \frac{dP_\ell(\cos\chi)}{d\cos\chi} \tag{23}$$

and

$$\tau_\ell(\cos\chi) = \cos\chi\pi_\ell(\cos\chi) - \sin\chi\frac{d\pi_\ell(\cos\chi)}{d\cos\chi} \tag{24}$$

where $P_\ell(\cos\chi)$ is a Legendre polynomial. The scattering cross-section is

$$\sigma_s(\lambda, r, m) = \pi r^2 Q_s(x, m) = \frac{\lambda^2}{2\pi}\sum_{\ell=1}^{\infty}(2\ell + 1)\ [|a_\ell|^2 + |b_\ell|^2] \tag{25}$$

where $Q_s(x,m)$ is called the scattering efficiency factor. The total (scattering plus absorption) cross-section is

$$\sigma_t(\lambda, r, m) = \pi r^2 Q_t(x, m) = \frac{\lambda^2}{2\pi} \sum_{\ell=1}^{\infty} (2\ell + 1)\mathrm{Re}(a_\ell + b_\ell) \tag{26}$$

where $Q_t(x,m)$ is the total efficiency factor. Likewise, the absorption cross-section is then

$$\sigma_a(\lambda, r, m) = \sigma_t(\lambda, r, m) - \sigma_s(\lambda, r, m) \tag{27}$$

with a corresponding efficiency factor $Q_a(x,m)$. As in the Rayleigh case, a scattering phase function can be defined:

$$P(\cos \chi) = \frac{1}{2\pi x^2 Q_s(x, m)} [|S_1|^2 + |S_2|^2] \tag{28}$$

Calculating all the functions given above for various refractive indices and size parameters is quite involved. Nevertheless, computer programs have been written which allow the performance of this analysis. Having obtained a program written by J.V. Dave, we used it to calculate the cross-sections and phase functions. For example, we have calculated the scattering efficiency factor for homogeneous spheres of refractive indices m = 1.29, 1.29 - 0.0465i, and 1.28 - 1.37i. The results are shown in Figure 4. It should be noted that the efficiency factor is greatest for the real index (that is, when there is no absorption) and decreases with increasing imaginary index. The absorption efficiency factor has also been calculated for m = 1.28 - 0.0465i and 1.28 - 1.37i. Here the efficiency factor is large for a

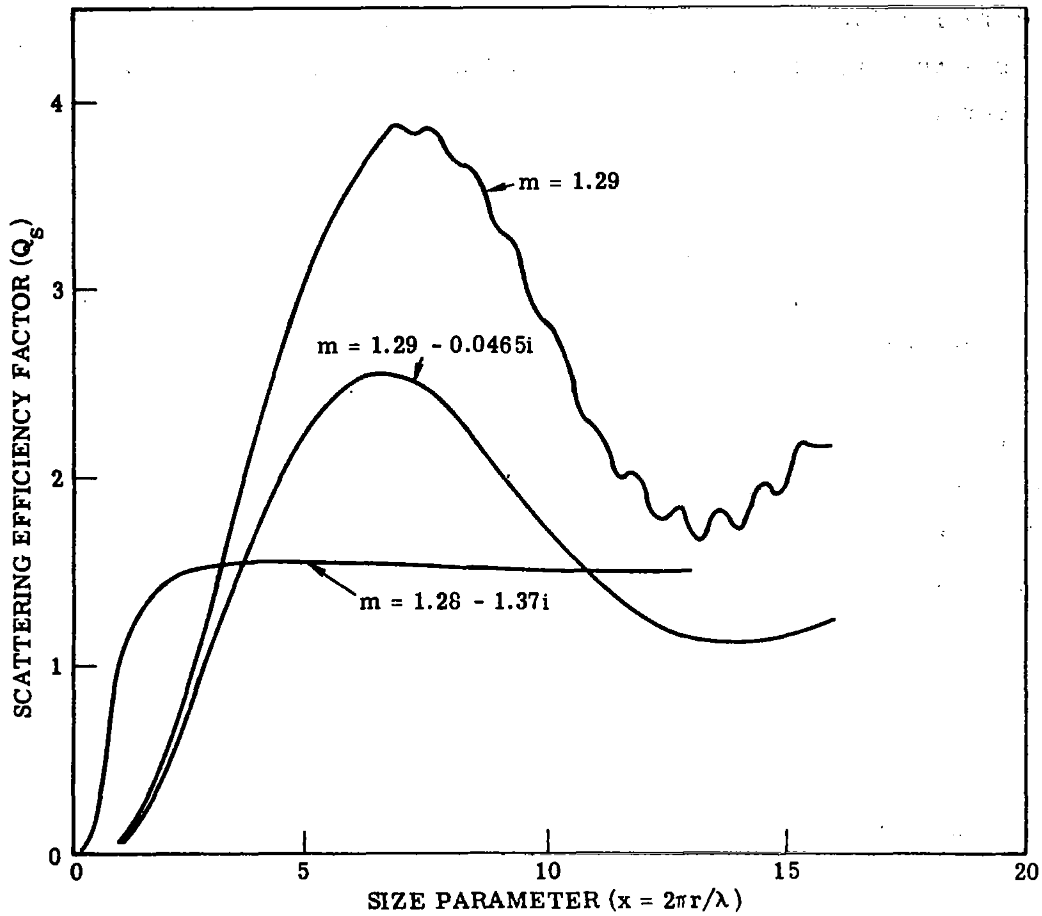

FIGURE 4. SCATTERING EFFICIENCY FACTOR FOR HOMOGENEOUS SPHERES OF COMPLEX REFRACTIVE INDEX m

high imaginary index and small particles, as illustrated in Figure 5. Finally, the total efficiency factor is shown in Figure 6 for the same set of refractive indices. Thus, it can be seen that efficiency factors vary strongly for different refractive indices and size parameters.

2.2.2 ATTENUATION COEFFICIENTS

Knowing the cross-sections, one can then calculate the scattering, absorption, and extinction coefficients by multiplying the cross-sections by the particle number density. For real atmospheric conditions characterized by haze, fogs, and dusts, there is a distribution of particle sizes. (One distribution, characterized in Section 2.1.1 is the modified gamma distribution.) Thus, for a polydispersion, one must integrate over particle size to obtain the absorption, scattering, and extinction coefficients:

$$\alpha_A(\lambda, m, z) = \int_0^\infty \sigma_{a,A}(\lambda, m, r)n(z, r)dr \tag{29}$$

$$\beta_A(\lambda, m, z) = \int_0^\infty \sigma_{s,A}(\lambda, m, r)n(z, r)dr \tag{30}$$

$$\kappa_A(\lambda, m, z) = \int_0^\infty \sigma_{t,A}(\lambda, m, r)n(z, r)dr \tag{31}$$

where α, β, and κ denote absorption, scattering, and extinction coefficients, A designates aerosol; and $n(z,r)$ is the aerosol-particle number density at altitude z for particles in size range Δr at size r. The number density is normalized as follows:

$$N(z) = \int_0^\infty n(z, r)dr \tag{32}$$

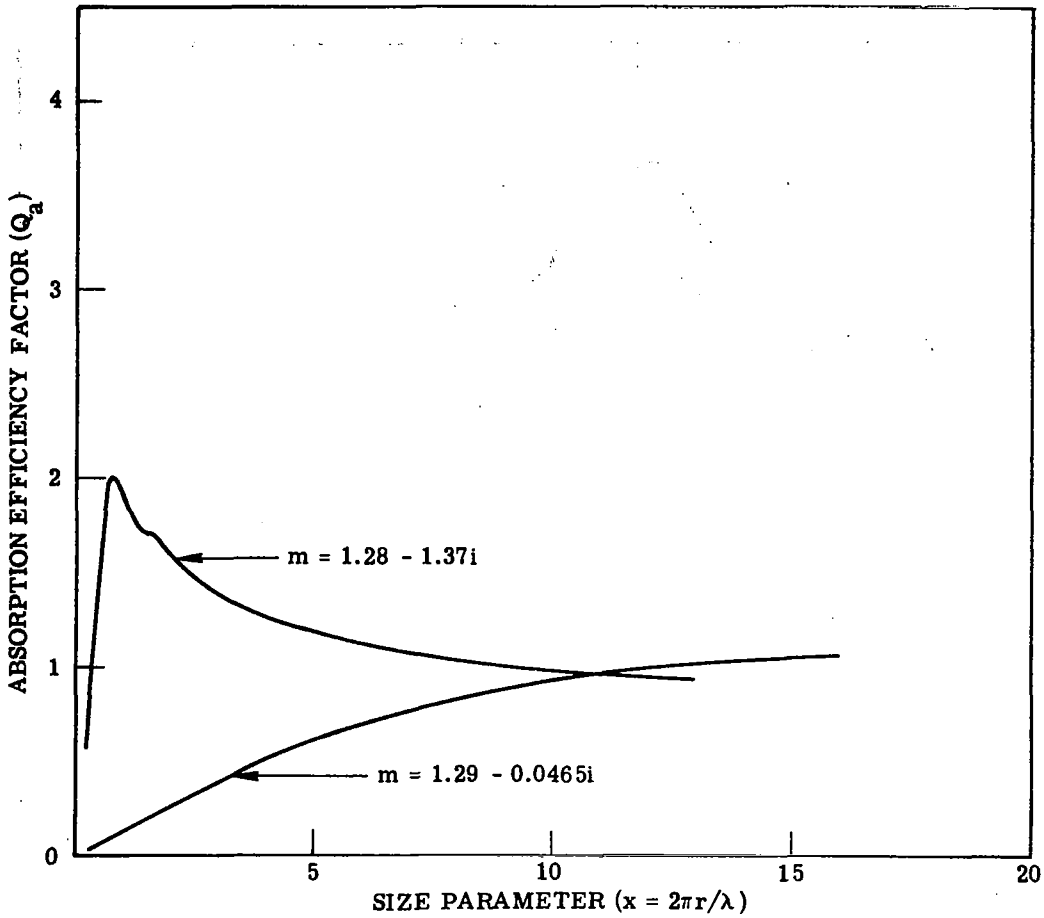

FIGURE 5. ABSORPTION EFFICIENCY FACTOR FOR HOMOGENEOUS SPHERES OF COMPLEX REFRACTIVE INDEX m

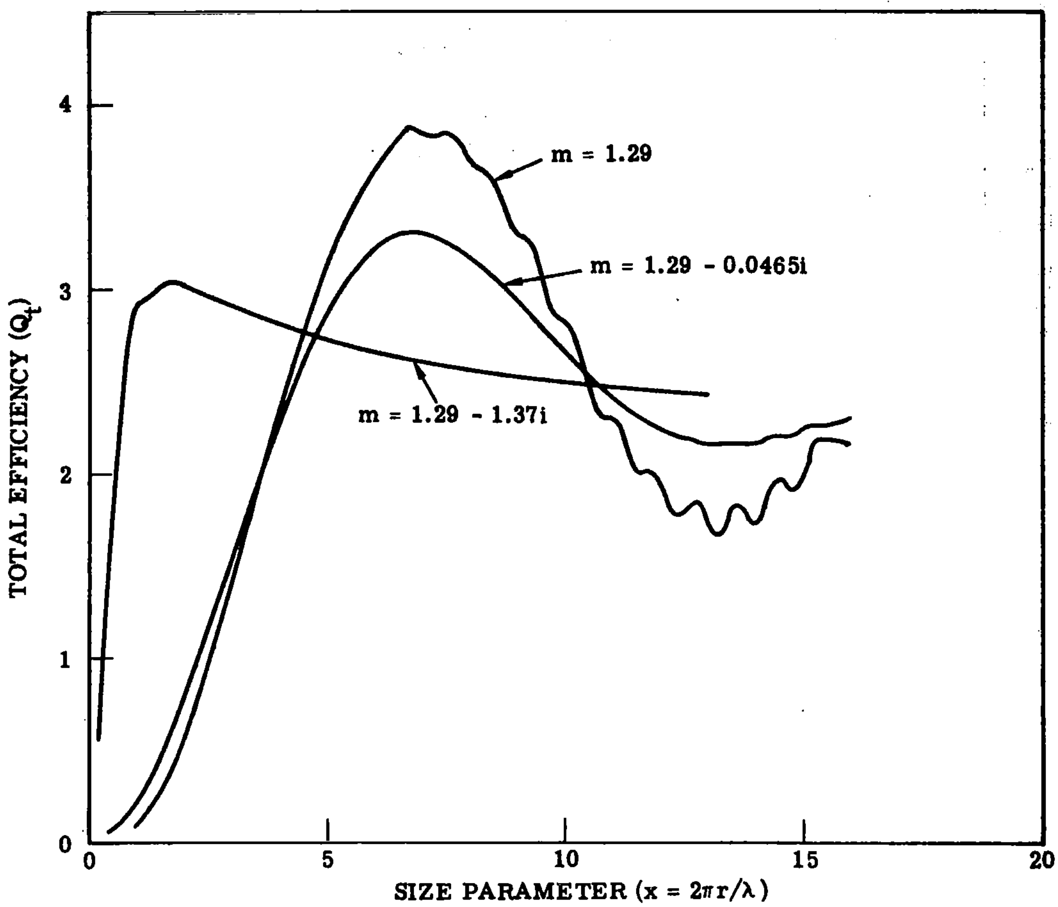

FIGURE 6. TOTAL EFFICIENCY FACTOR FOR HOMOGENEOUS SPHERES OF COMPLEX REFRACTIVE INDEX m

where n(z) is just the total number density. Likewise, the corresponding coefficients for molecular scattering can be found. The scattering cross-section is given by Equation (16), and the absorption cross-section is usually taken to be that for ozone in the visible spectral region. Thus, we have for the complete atmosphere:

$$\alpha(\lambda, m, s, z) = \alpha_R(\lambda, z) + \alpha_A(\lambda, m, s, z) \tag{33}$$

$$\beta(\lambda, m, s, z) = \beta_R(\lambda, z) + \beta_A(\lambda, m, s, z) \tag{34}$$

$$\kappa(\lambda, m, s, z) = \kappa_R(\lambda, z) + \kappa_A(\lambda, m, s, z) \tag{35}$$

where we have shown the explicit dependence on a complex refractive index m and a particular size distribution s.

It is sometimes useful to deal with an average cross-section for aerosols. Assuming that the size distribution is altitude-independent, we can write Equations (29), (30), and (31) as

$$\alpha_A(\lambda, m, z) = N(z)\, \overline{\alpha}_{a,A}(\lambda, m) \tag{36}$$

$$\beta_A(\lambda, m, z) = N(z)\, \overline{\sigma}_{s,A}(\lambda, m) \tag{37}$$

$$\kappa_A(\lambda, m, z) = N(z)\, \overline{\sigma}_{t,A}(\lambda, m) \tag{38}$$

where

$$\overline{\sigma}_{i,A}(\lambda, m) = \int_0^\infty \sigma_{i,A}(\lambda, m, r)\psi(r)dr \tag{39}$$

in which the function $\psi(r)$ is normalized to 1 and the index i can indicate a, s, or t. We have computed many values of the average cross-sections for homogeneous spheres of various refractive indices and size distributions. The results of this analysis will be presented later.

2.2.2 OPTICAL DEPTH

For radiative-transfer calculations it is usually more meaningful to deal with the dimensionless quantity, optical depth in a medium, rather than with actual distances. We define optical depth

$$\tau(\lambda, h) = \int_h^\infty \kappa(\lambda, z)dz \tag{40}$$

and optical thickness as

$$\tau_o(\lambda) = \int_0^\infty \kappa(\lambda, z)dz \tag{41}$$

where h is some definite altitude. Thus, at the top of the atmosphere $\tau(\lambda, h \to \infty) = 0$, while at the bottom $\tau(\lambda, h = 0) = \tau_o(\lambda)$. Optical depth can be thought of as the distance into a medium expressed in units of mean free photon paths. A small τ_o indicates that little attenuation takes place, whereas a large τ_o means that the atmosphere is either strongly absorbing or scatters much of the radiation. Optical depths can easily be obtained for Rayleigh atmospheres. Elterman [27] has tabulated the results for all altitudes from 0 to 50 km and for selected wavelengths from 0.27 μm to 4.00 μm. The optical thickness varies from 1.928 at 0.27 μm to 0.001 at 1.67 μm.

Likewise, if the extinction coefficient for aerosols is available, the corresponding aerosol optical depths can be determined. By analyzing many experimentally determined aerosol profiles, Elterman [28] has calculated the extinction coefficients and optical depths for realistic atmospheric conditions. For a 2 km visual range, the aerosol optical thickness is 2.521 at 0.36 μm and 1.053 at 0.90 μm. These results indicate that multiple scattering occurs in Earth's atmosphere since the mean free photon paths are short compared to the actual distances traveled.

2.2.4 SINGLE-SCATTERING ALBEDO

A very important parameter in radiative-transfer analysis is the single-scattering albedo, defined as

$$\omega_o(\lambda, m, s, z) \equiv \frac{\beta_R(\lambda, z) + \beta_A(\lambda, m, s, z)}{\kappa(\lambda, m, s, z)} \tag{42}$$

where $\kappa(\lambda, m, s, z)$ is the total (Rayleigh plus aerosol) extinction coefficient. The albedo $\omega_o(\lambda, m, s, z)$ is the fraction of scattering which can occur. Thus, if there is neither aerosol absorption nor ozone absorption, then $\omega_o(\lambda, m, s, z) = 1$ and we have a pure scattering atmosphere. For strongly absorbing aerosols, however, $\beta_A(\lambda, m, s, z)$ is small and $\omega_o(\lambda, m, s, z)$ can be as small as 0.09.

2.3 THE RADIATION MODEL

In this section, we shall discuss briefly the radiative transfer equation which is used to determine the radiation field within a plane-parallel, homogeneous atmosphere with aerosol scattering. A more complete discussion and derivation of the equation is given by Turner [29] and Malila et al. [30].

The basic integro-differential equation of radiative transfer for a plane-parallel, homogeneous atmosphere illuminated by solar radiation is given by

$$\mu \frac{dL}{d\tau} = L(\tau, \mu, \phi) - \frac{\omega_0}{4\pi} \int_0^{2\pi} \int_{-1}^{1} p(\mu,\phi,\mu',\phi') L(\tau,\mu',\phi') d\mu' d\phi'$$

$$- \frac{\omega_0}{4\pi} E_s(\tau) p(\mu, \phi, -\mu_0, \phi_0) - (1 - \omega_0) B(\tau) \qquad (43)$$

where

$$E_s(\tau) = E_0 e^{-\tau/\mu_0} \qquad (44)$$

$L(\tau, \mu, \phi)$ is the spectral radiance at optical depth τ, zenith angle θ (of which the cosine is μ), and azimuthal angle ϕ. $E_s(\tau)$ is the solar irradiance at optical depth τ and $p(\mu, \phi, \mu', \phi')$ is the single-scattering phase function which describes the function of energy scattered from the direction μ', ϕ' into the direction μ,ϕ. $B(\tau)$ is the Planck radiation function and ω_0 is called the single scattering albedo defined as

$$\omega_0 = \frac{\beta}{\kappa} \qquad (45)$$

The direct solar radiation enters Earth's atmosphere with a zenith angle the cosine of which is μ_0 and azimuthal angle ϕ_0.

For the visible spectral region, $B(\tau)$ is usually negligible and $\omega_o \approx 1$ since there is very little absorption by either gases or particulate matter. Nevertheless, Equation (43) is quite difficult to solve exactly and has been done only for isotrophic and Rayleigh-type scattering. For realistic atmospheres with an aerosol component, the phase function is highly anisotropic and approximations must be made to solve the transfer equation. One approximation to simplify Equation (43) is the following:

$$p(\mu, \phi, \mu', \phi') = F\,\delta(\mu - \mu')\delta(\phi - \phi') + B\delta(\mu + \mu')\delta(\pi + \phi - \phi') \quad (46)$$

where F is the fraction of energy scattered into the forward direction and B is the fraction scattered into the backward direction. Since scattering by aerosols is trongly peaked in the forward direction, this approximation seems to be a reasonable one. Use of Equation (46) in Equation (43) permits a solution in terms of arbitrary constants which are determined from boundary conditions. The general boundary conditions are,

$$L(0, -\mu, \phi) = 0 \quad (47)$$

$$L(\tau_0,\mu,\phi) = \int_0^{2\pi}\int_0^1 \mu'\rho'(\mu,\phi, -\mu',\phi')[L(\tau_0,-\mu',\phi') + L_s(\tau_0,-\mu',\phi')]d\mu' d\phi' \quad (48)$$

where Equation (47) simply states that there is no diffuse radiation entering the top of Earth's atmosphere and Equation (48) indicates that we must integrate the diffuse and solar radiation with the bidirectional reflectance over the hemisphere of incoming radiation. If we deal with a Lambertian (perfectly diffuse) surface, the boundary conditions reduce to

$$E_-(0) = 0 \quad (49)$$

$$E_+(\tau_0) = \rho\left[E_-(\tau_0) + \mu_0 E_0\, e^{-\tau_0/\mu_0}\right] \quad (50)$$

where $E_-(0)$ is the downward diffuse irradiance at the top of the atmosphere, $E_-(\tau_0)$ is the downward diffuse irradiance at the bottom of the atmosphere, $E_+(\tau_0)$ is the upward diffuse irradiance at the bottom of the atmosphere, E_0 is the direct solar irradiance at the top of the atmosphere, and ρ is the hemispherical reflectance of the surface.

Breaking the radiation fields up into two components, an anisotropic one for $\rho = 0$, and an isotropic one for $\rho \neq 0$, we can solve the irradiances at any point within the atmosphere, i.e.,

$$E_+(\tau) = \frac{\mu_0 E_0}{\mu_0 + (1 - \eta)\tau_0} \left[(1 - \eta)(\tau_0 - \tau) + \rho\mu_0 \frac{1 + 2(1 - \eta)\tau}{1 + 2(1 - \eta)(1 - \rho)\tau_0}\right] \quad (51)$$

$$E_-(\tau) = \frac{\mu_0 E_0}{\mu_0 + (1 - \eta)\tau_0} \left[\mu_0 + (1-\eta)(\tau_0 - \tau) - [\mu_0 + (1-\eta)\tau_0]e^{-\tau/\mu} + \frac{2\rho\mu_0(1-\eta)\tau}{1+2(1-\eta)(1-\rho)\tau_0}\right] \quad (52)$$

$$\tilde{E}_-(\tau) = \frac{\mu_0 E_0}{\mu_0 + (1 - \eta)\tau_0} \left[\mu_0 + (1 - \eta)(\tau_0 - \tau) + \frac{2\mu_0\rho(1 - \eta)\tau}{1 + 2(1 - \eta)(1 - \rho)\tau_0}\right] \quad (53)$$

where η is $F/4\pi$ and $\tilde{E}_-(\tau)$ is the total downward irradiance.

Having determined the irradiances, we can now find the radiances by using the approximation

$$L(\tau, \mu, \phi) = \frac{1}{\mu_0} [E'_+(\tau)\delta(\mu - \mu_0)\delta(\pi + \phi_0 - \phi) + E'_-(\tau)\delta(\mu + \mu_0)\delta(\phi - \phi_0)] \frac{E''_+(\tau) + E''_-(\tau)}{2\pi} \quad (54)$$

where the primed irradiances represent the radiation field with $\rho = 0$ and the double primed irradiances represent the radiation field with $\rho \neq 0$. The complete spectral path radiance in the upward and downward hemispheres are then, respectively

$$L_p(\tau, \mu, \phi) = \frac{E_0}{4\pi[\mu_0 + (1 - \eta)\tau_0]}$$

$$\Bigg(\Big\{(1 - \eta)\tau_0[p(\mu, \phi, \mu_0, \pi + \phi_0) + p(\mu, \phi, -\mu_0, \phi_0)] + \mu_0 p(\mu, \phi, -\mu_0, \phi_0)$$

$$+ \frac{2\mu_0^2\rho}{1 + 2(1-\eta)(1-\rho)\tau_0}\Big\}\left[1 - e^{-(\tau_0-\tau)/\mu}\right] + \Big\{(1-\eta)[p(\mu,\phi, \mu_0, \pi + \phi_0)$$

$$+ p(\mu, \phi, -\mu_0, \phi_0) - \frac{8(1-\eta)\mu_0^2\rho}{1+2(1-\eta)(1-\rho)\tau_0}\Big\}\left[(\tau_0 + \tau)e^{-(\tau_0-\tau)/\mu} - (\tau + \mu)\right]\Bigg) \quad (55)$$

$$L_p(\tau, -\mu, \phi) = \frac{E_0}{4\pi[\mu_0 + (1 - \eta)\tau_0]}$$

$$\Bigg(\Big\{(1 - \eta)\tau_0[p(-\mu, \phi, \mu_0, \pi + \phi_0) + p(-\mu, \phi, -\mu_0, \phi_0) + \mu_0 p(-\mu, \phi, -\mu_0, \phi_0)$$

$$+ \frac{2\mu_0^2\rho}{1 + 2(1 - \eta)(1 - \rho)\tau_0}\Big\}(1 - e^{-\tau/\mu}) - \Big\{(1 - \eta)[p(-\mu, \phi, \mu_0, \pi + \phi_0)$$

$$+ p(-\mu, \phi, -\mu_0, \phi_0)] - \frac{8(1 - \eta)\mu_0^2\rho}{1 + 2(1 -\eta)(1 - \rho)\tau_0}\Big\}(\mu e^{-\tau/\mu} + \tau - \mu)\Bigg) \qquad (56)$$

where the single-scattering phase functions are given by

$$p(\mu, \phi, \mu_0, \pi + \phi_0) = p\left[\mu\mu_0 - \sqrt{(1 - \mu^2)(1 - \mu_0^2)}\cos(\phi - \phi_0)\right] \tag{57}$$

$$p(\mu, \phi, -\mu_0, \phi_0) = p\left[-\mu\mu_0 + \sqrt{(1 - \mu^2)(1 - \mu_0^2)}\cos(\phi - \phi_0)\right] \tag{58}$$

$$p(-\mu, \phi, \mu_0, \pi + \phi_0) = p\left[-\mu\mu_0 - \sqrt{(1 - \mu^2)(1 - \mu_0^2)}\cos(\phi - \phi_0)\right] \tag{59}$$

$$p(-\mu, \phi, -\mu_0, \phi_0) = p\left[\mu\mu_0 + \sqrt{(1 - \mu^2)(1 - \mu_0^2)}\cos(\phi - \phi_0)\right] \tag{60}$$

As an additional illustration of the general validity of our atmospheric radiation model, we can compare our sky radiances with those computed by Coulson et al. [31] using the results of Chandrasekhar's theory [32]. This comparison is shown in Figures 7, 8, and 9 (for a Rayleigh atmosphere). Figures 7 and 8 illustrate the sky radiance in and perpendicular to the solar plane, respectively, for a solar zenith angle of ∿37° and Figure 9 shows the sky radiance for a solar zenith angle of 0°. In all cases, the agreement is excellent although there is some deviation in the case of an extremely large solar zenith angle of ∿84°.

In conclusion, the radiative-transfer model described in this report has been used in analyzing multispectral remote sensing data for a wide range of variations in the model parameters. At the present time the multiple scattered radiation field within Earth's atmosphere can be calculated in terms of sun angle, atmospheric conditions (i.e., visibility), viewing geometry, altitude of observer,

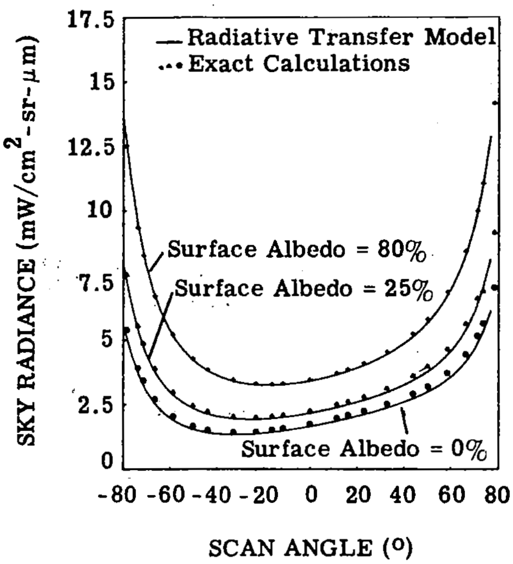

FIGURE 7. DEPENDENCE OF SKY RADIANCE ON SCAN ANGLE (IN THE SOLAR PLANE); SOLAR ZENITH ANGLE = 36.9°. Visual range = 336 km; wavelength = 0.546 μm.

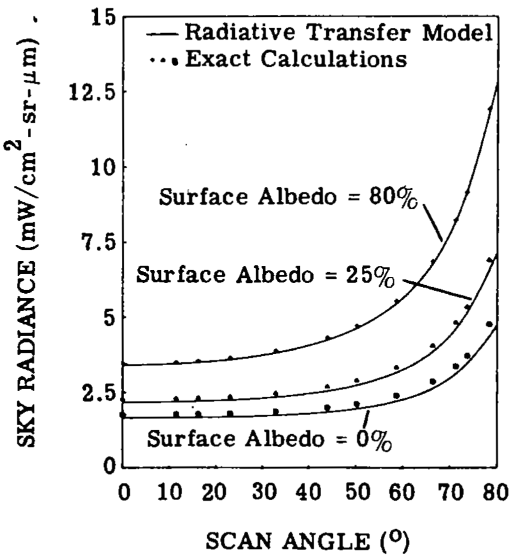

FIGURE 8. DEPENDENCE OF SKY RADIANCE ON SCAN ANGLE (PERPENDICULAR TO THE SOLAR PLANE); SOLAR ZENITH ANGLE = 36.9°. Visual range = 336 km; wavelength = 0.546 μm.

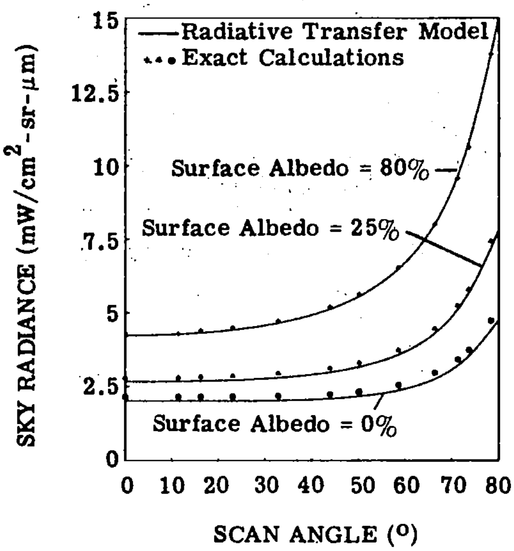

FIGURE 9. DEPENDENCE OF SKY RADIANCE ON SCAN ANGLE (IN THE SOLAR PLANE); SOLAR ZENITH ANGLE = 0°. Visual range = 336 km; wavelength = 0.546 μm.

target reflectance, background reflectance, and wavelength. Additionally the singly-scattered component arising from the surface for <u>any</u> complex pattern can be calculated. The effects of absorption by aerosols are included but gaseous absorption, other than ozone, is not included in this model. As output, spectral sky radiance, spectral path radiance, total spectral radiance, direct (solar) irradiance, diffuse (sky) irradiance, optical thickness of the atmosphere, and transmittance of the atmosphere can be calculated.

2.4 CALCULATION OF RADIANCE DATA

The conditions for which radiance calculations were made are as follows:

1. Satellite altitude = 900 km.
2. Solar zenith angle = 35°, 45°, 55°, 60°
3. Visual range = 15 km, 23 km, 40 km, 60 km
4. Atmospheric conditions = Diemendjian's Haze M
5. Spectral region = 0.4 μm to 1.0 μm
6. Zero scan angle
7. Earth at mean distance from sun
8. Zero background reflectance

The results of the calculations are presented as total radiance (L) at the entrance to the satellite's optics. This includes radiance from the target together with path radiance.

$$L = L_o T + L_p \tag{61}$$

where, L = total radiance

L_o = target radiance at earth surface

T = transmittance of atmosphere

L_p = path radiance

Surfaces were assumed to be Lambertian.

The term, path radiance, is a function of not only atmospheric conditions, and solar irradiance, but is also a function of target reflectance and background reflectance. It must be recognized that materials outside of the instantaneous field of view can affect the target radiance as a result of atmospheric scattering. This issue is discussed in Section 4, RESEARCH NEEDS. A background reflectance of zero was assumed in the radiance calculations which follow. This means that the calculated values shown represent the low radiance values for the target materials under the conditions specified. Background contribution will tend to increase path radiance as shown in Table 1.

TABLE 1

PATH RADIANCE

VISIBILITY: 23 km. ATMOSPHERE: HAZE M SOLAR ZENITH ANGLE = 45°

WAVELENGTH μm	PATH RADIANCE $mw\ cm^{-2}\ sr^{-1}\ \mu m^{-1}$		
	Background Reflectance		
	0	0.05	0.10
0.400	4.1409	4.4497	4.7673
0.500	2.7662	3.1013	3.4413
0.600	1.3827	1.6206	1.8604
0.700	0.7706	0.9428	1.1160
0.800	0.4775	0.6062	0.7355
0.900	0.3199	0.4181	0.5167
1.000	0.2373	0.3171	0.3971

3

SPECTRAL REFLECTANCE AND RADIANCE DATA

3.1 WATER BODIES

Included in this section is data for those surface waters for which physical-chemical-biological data or "pollutants" are unknown or the information is extremely limited. In some cases, the general characteristics are known. The clear oceanic waters are examples of surface waters relatively free of pollutants.

The Tongue-of-the-Ocean area in the Bahamas is a readily identifiable geographic area which has been proposed as one possible "benchmark" for satellite remote sensing. The waters are an excellent example of clear oceanic waters.

The material which follows is subdivided into:

1. Clear Oceanic Waters
2. Coastal Waters - Pacific Off California
3. Oceanic Waters - Atlantic
4. Lakes - Oligotrophic, Eutrophic
5. Salton Sea

Atmospheric corrections have been applied to the data, as required, to reduce data to surface level.

3.1.1 Clear Oceanic Waters

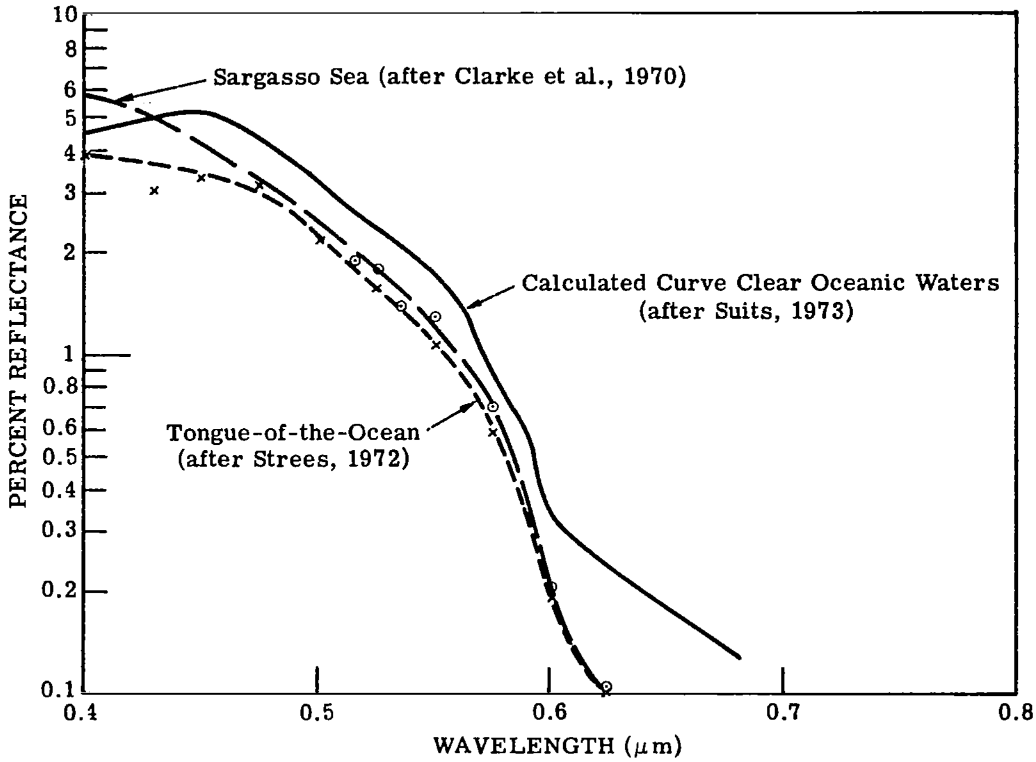

FIGURE 10. CLEAR OCEANIC WATERS

TABLE 2
SARGASSO SEA REFLECTANCE DATA
68°W 38°N

λ (μm)	ρ
0.400	0.058
0.425	0.050
0.450	0.042
0.475	0.033
0.500	0.025
0.525	0.018
0.550	0.013
0.575	0.007
0.600	0.002
0.625	0.001
0.650	0.001

Sea level data

Source: Clarke, G.L., Ewing, G. C., and Lorenzen, C.J. [33] Aircraft data, 305 m. altitude, TRW spectrometer (400 nm to 650 nm) with polarizing filter, instrument tilted at Brewster's angle (53° $\pm$).

TABLE 3

SARGASSO SEA RADIANCE DATA

SATELLITE ALTITUDE VISIBILITY 15 km.

Solar Zenith Angle	Total Radiance (mw cm^{-2} sr^{-1} μm^{-1}) 35°	45°	55°	60°
Wavelength (μm)				
0.400	5.808	4.849	4.160	3.848
0.425	5.881	4.884	4.184	3.866
0.450	5.971	4.932	4.223	3.902
0.475	5.230	4.290	3.674	3.398
0.500	4.239	3.454	2.962	2.746
0.525	3.483	2.813	2.416	2.245
0.550	2.800	2.243	1.931	1.798
0.575	2.392	1.895	1.637	1.532
0.600	1.972	1.542	1.338	1.260
0.625	1.700	1.318	1.144	1.078
0.650	1.486	1.143	0.992	0.936

TABLE 4

SARGASSO SEA RADIANCE DATA

SATELLITE ALTITUDE VISIBILITY 23 km

Solar Zenith Angle	Total Radiance ($mw\ cm^{-2} sr^{-1} \mu m^{-1}$) 35°	45°	55°	60°
Wavelength (μm)				
0.400	5.749	4.872	4.189	3.874
0.425	5.799	4.892	4.198	3.878
0.450	5.857	4.918	4.218	3.894
0.475	5.080	4.242	3.638	3.361
0.500	4.077	3.385	2.908	2.692
0.525	3.304	2.723	2.343	2.174
0.550	2.624	2.147	1.852	1.723
0.575	2.198	1.781	1.542	1.442
0.600	1.775	1.421	1.238	1.164
0.625	1.509	1.198	1.044	0.984
0.650	1.307	1.029	0.897	0.846

TABLE 5

SARGASSO SEA RADIANCE DATA

SATELLITE ALTITUDE VISIBILITY 40 km

Solar Zenith Angle	Total Radiance ($mw\ cm^{-2} sr^{-1} \mu m^{-1}$) 35°	45°	55°	60°
Wavelength (μm)				
0.400	5.701	4.900	4.221	3.903
0.425	5.730	4.907	4.218	3.892
0.450	5.758	4.913	4.218	3.890
0.475	4.946	4.202	3.609	3.330
0.500	3.931	3.326	2.861	2.644
0.525	3.141	2.643	2.278	2.110
0.550	2.463	2.060	1.780	1.653
0.575	2.021	1.677	1.456	1.359
0.600	1.594	1.310	1.145	1.076
0.625	1.334	1.088	0.951	0.896
0.650	1.144	0.926	0.809	0.763

TABLE 6

SARGASSO SEA RADIANCE DATA

SATELLITE ALTITUDE VISIBILITY 60 km

Solar Zenith Angle	Total Radiance (mw cm^{-2} sr^{-1} μm^{-1}) 35°	45°	55°	60°
Wavelength (μm)				
0.400	5.679	4.917	4.240	3.920
0.425	5.698	4.917	4.229	3.902
0.450	5.710	4.913	4.220	3.890
0.475	4.879	4.184	3.595	3.315
0.500	3.857	3.296	2.837	2.620
0.525	3.058	2.602	2.244	2.077
0.550	2.381	2.016	1.743	1.618
0.575	1.929	1.624	1.411	1.317
0.600	1.500	1.253	1.097	1.030
0.625	1.243	1.031	0.904	0.851
0.650	1.059	0.872	0.764	0.720

TABLE 7

TONGUE-OF-THE-OCEAN REFLECTANCE DATA
(BAHAMA ISLANDS)

λ (μm)	ρ
0.400	0.039
0.425	0.030
0.450	0.033
0.475	0.032
0.500	0.022
0.525	0.016
0.550	0.011
0.575	0.006
0.600	0.002
0.625	0.001
0.650	0.001

Sea level data

Source: Strees L.V. [34]
Spectral irradiance curves for upwelling radiation (350-700 nm); Gamma Scientific model 300 spectrometer.

TABLE 8

TONGUE-OF-THE-OCEAN RADIANCE DATA

SATELLITE ALTITUDE VISIBILITY 15 km

Solar Zenith Angle	Total Radiance ($mw\ cm^{-2} sr^{-1} \mu m^{-1}$) 35°	45°	55°	60°
Wavelength (μm)				
0.400	5.556	4.639	3.997	3.711
0.425	5.519	4.579	3.947	3.666
0.450	5.755	4.750	4.080	3.781
0.475	5.204	4.268	3.656	3.383
0.500	4.158	3.385	2.908	2.699
0.525	3.428	2.767	2.379	2.213
0.550	2.747	2.198	1.894	1.767
0.575	2.365	1.872	1.618	1.515
0.600	1.972	1.542	1.338	1.260
0.625	1.700	1.318	1.144	1.078
0.650	1.486	1.143	0.992	0.936

TABLE 9

TONGUE-OF-THE-OCEAN RADIANCE DATA

SATELLITE ALTITUDE **VISIBILITY** 23 km

Solar Zenith Angle	**Total Radiance ($mw\ cm^{-2} sr^{-1} \mu m^{-1}$)** 35°	45°	55°	60°
Wavelength (μm)				
0.400	5.462	4.632	4.003	3.718
0.425	5.389	4.547	3.930	3.650
0.450	5.614	4.713	4.057	3.757
0.475	5.050	4.216	3.618	3.344
0.500	3.987	3.308	2.847	2.640
0.525	3.243	2.672	2.302	2.139
0.550	2.565	2.097	1.812	1.688
0.575	2.168	1.755	1.522	1.424
0.600	1.775	1.421	1.238	1.164
0.625	1.509	1.198	1.044	0.984
0.650	1.307	1.029	0.897	0.846

TABLE 10

TONGUE-OF-THE-OCEAN RADIANCE DATA

SATELLITE ALTITUDE VISIBILITY 40 km

Solar Zenith Angle	Total Radiance ($mw\ cm^{-2} sr^{-1} \mu m^{-1}$) 35°	45°	55°	60°
Wavelength (μm)				
0.400	5.379	4.630	4.013	3.728
0.425	5.273	4.521	3.917	3.638
0.450	5.489	4.685	4.039	3.738
0.475	4.914	4.174	3.587	3.311
0.500	3.832	3.241	2.794	2.587
0.525	3.075	2.586	2.233	2.072
0.550	2.399	2.006	1.736	1.616
0.575	1.988	1.649	1.433	1.340
0.600	1.594	1.310	1.145	1.076
0.625	1.334	1.088	0.951	0.896
0.650	1.144	0.926	0.809	0.763

TABLE 11

TONGUE-OF-THE-OCEAN RADIANCE DATA

SATELLITE ALTITUDE VISIBILITY 60 km

Solar Zenith Angle	Total Radiance ($mw\ cm^{-2} sr^{-1} \mu m^{-1}$) 35°	45°	55°	60°
Wavelength (μm)				
0.400	5.338	4.631	4.019	3.734
0.425	5.214	4.510	3.912	3.633
0.450	5.426	4.673	4.032	3.729
0.475	4.845	4.155	3.572	3.295
0.500	3.753	3.208	2.767	2.560
0.525	2.989	2.543	2.197	2.037
0.550	2.314	1.959	1.698	1.578
0.575	1.895	1.595	1.388	1.296
0.600	1.500	1.253	1.097	1.030
0.625	1.243	1.031	0.904	0.851
0.650	1.059	0.872	0.764	0.720

TABLE 12

CLEAR OCEANIC - CALCULATED REFLECTANCE

$\theta_s = 45°$

$\lambda(\mu m)$	$\dot{\rho}$
0.400	0.045
0.425	0.049
0.450	0.053
0.475	0.044
0.500	0.033
0.525	0.024
0.550	0.018
0.575	0.0087
0.590	0.0059
0.600	0.0034
0.625	0.0023
0.650	0.0018
0.675	0.0013

Sea level data

Source: Suits, G. [unpublished data]. Calculated spectral reflectance (0.4µm-0.7µm) of ocean water containing various concentrations of "yellow substance", phytoplankton, and sand.

TABLE 13

CLEAR OCEANIC RADIANCE DATA

SATELLITE ALTITUDE VISIBILITY 15 km

Solar Zenith Angle	Total Radiance ($mw\ cm^{-2} sr^{-1} \mu m^{-1}$) 35°	45°	55°	60°
Wavelength (μm)				
0.400	5.635	4.705	4.048	3.754
0.425	5.862	4.869	4.172	3.856
0.450	6.234	5.155	4.397	4.050
0.475	5.523	4.539	3.869	3.564
0.500	4.456	3.638	3.108	2.870
0.525	3.646	2.953	2.527	2.339
0.550	2.933	2.356	2.021	1.876
0.560	2.694	2.154	1.850	1.722
0.575	2.439	1.935	1.669	1.559
0.590	2.202	1.735	1.500	1.405
0.600	2.011	1.575	1.365	1.282
0.625	1.735	1.348	1.168	1.099
0.650	1.507	1.160	1.006	0.948
0.675	1.330	1.018	0.882	0.832

TABLE 14

CLEAR OCEANIC RADIANCE DATA

SATELLITE ALTITUDE VISIBILITY 23 km

Solar Zenith Angle	Total Radiance (mw $cm^{-2} sr^{-1} \mu m^{-1}$) 35°	45°	55°	60°
Wavelength (μm)				
0.400	5.552	4.707	4.062	3.768
0.425	5.778	4.875	4.185	3.866
0.450	6.153	5.169	4.414	4.061
0.475	5.407	4.519	3.857	3.548
0.500	4.318	3.590	3.071	2.831
0.525	3.485	2.878	2.466	2.280
0.550	2.771	2.272	1.952	1.809
0.560	2.519	2.058	1.771	1.645
0.575	2.250	1.825	1.578	1.472
0.590	2.010	1.621	1.404	1.315
0.600	1.817	1.457	1.267	1.189
0.625	1.547	1.230	1.070	1.006
0.650	1.330	1.049	0.912	0.859
0.675	1.160	0.909	0.790	0.745

TABLE 15

CLEAR OCEANIC RADIANCE DATA

SATELLITE ALTITUDE **VISIBILITY** 40 km

Solar Zenith Angle	**Total Radiance ($mw\,cm^{-2}sr^{-1}\mu m^{-1}$)** 35°	45°	55°	60°
Wavelength (μm)				
0.400	5.481	4.715	4.079	3.783
0.425	5.708	4.887	4.202	3.880
0.450	6.087	5.191	4.437	4.076
0.475	5.308	4.509	3.851	3.537
0.500	4.197	3.551	3.040	2.797
0.525	3.340	2.812	2.412	2.226
0.550	2.623	2.197	1.889	1.747
0.560	2.360	1.971	1.699	1.575
0.575	2.077	1.725	1.494	1.392
0.590	1.834	1.516	1.317	1.231
0.600	1.640	1.349	1.176	1.103
0.625	1.375	1.123	0.980	0.921
0.650	1.168	0.947	0.826	0.777
0.675	1.005	0.809	0.706	0.665

TABLE 16

CLEAR OCEANIC RADIANCE DATA

SATELLITE ALTITUDE VISIBILITY 60 km

Solar Zenith Angle	Total Radiance ($mw\ cm^{-2} sr^{-1} \mu m^{-1}$) 35°	45°	55°	60°
Wavelength (μm)				
0.400	5.446	4.722	4.089	3.792
0.425	5.673	4.897	4.214	3.888
0.450	6.057	5.206	4.451	4.085
0.475	5.260	4.507	3.850	3.532
0.500	4.136	3.533	3.025	2.781
0.525	3.266	2.780	2.385	2.199
0.550	2.548	2.159	1.857	1.716
0.560	2.279	1.927	1.662	1.539
0.575	1.988	1.674	1.451	1.351
0.590	1.743	1.462	1.272	1.188
0.600	1.548	1.294	1.130	1.059
0.625	1.286	1.068	0.933	0.876
0.650	1.085	0.894	0.782	0.735
0.675	0.925	0.757	0.662	0.623

3.1.2 Coastal Waters, Pacific Off California

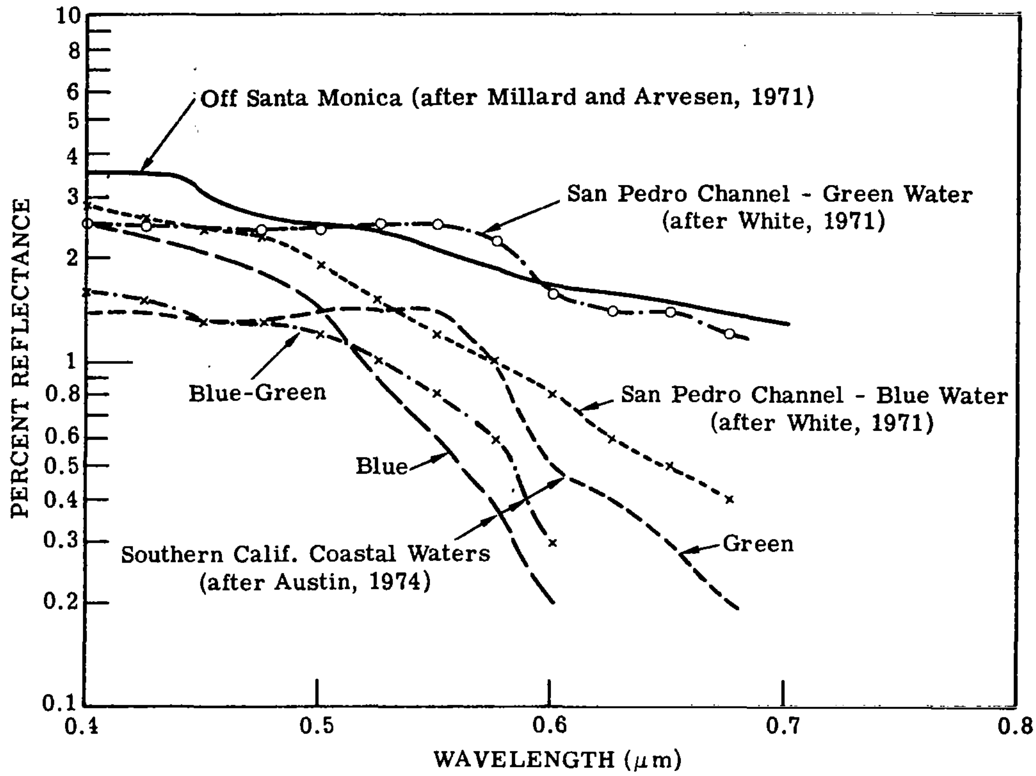

FIGURE 11. COASTAL WATERS - PACIFIC OFF CALIFORNIA. Sea Level Data

TABLE 17

PACIFIC NEAR SANTA MONICA, REFLECTANCE

λ(μm)	ρ
0.400	0.035
0.420	0.035
0.440	0.034
0.460	0.028
0.500	0.025
0.520	0.024
0.550	0.021
0.600	0.017
0.650	0.015
0.700	0.013

Sea level data

Source: Millard, J. P. and Arvesen, J. C. [35]

Pacific, 16 km. West of Santa Monica (Calif).; aircraft data, 152 m. altitude, modified Cary 14; spectral radiance curve (375-1000 nm); water quality characteristics undefined.

TABLE 18

PACIFIC NEAR SANTA MONICA, RADIANCE DATA

SATELLITE ALTITUDE VISIBILITY 15 km

Solar Zenith Angle	Total Radiance (mw cm^{-2}sr^{-1}µm^{-1}) 35°	45°	55°	60°
Wavelength (µm)				
0.400	5.503	4.594	3.963	3.683
0.420	5.958	4.951	4.262	3.955
0.440	5.497	4.548	3.909	3.623
0.460	5.553	4.566	3.922	3.638
0.500	4.239	3.454	2.962	2.746
0.520	3.682	2.985	2.555	2.366
0.550	3.013	2.424	2.075	1.922
0.600	2.384	1.894	1.620	1.502
0.650	1.851	1.455	1.242	1.153
0.700	1.463	1.140	0.972	0.903

TABLE 19

PACIFIC NEAR SANTA MONICA, RADIANCE DATA

SATELLITE ALTITUDE VISIBILITY 23 km

Solar Zenith Angle	Total Radiance ($mw\ cm^{-2} sr^{-1} \mu m^{-1}$) 35°	45°	55°	60°
Wavelength (μm)				
0.400	5.402	4.581	3.964	3.686
0.420	5.836	4.928	4.254	3.948
0.440	5.371	4.518	3.892	3.606
0.460	5.382	4.504	3.879	3.595
0.500	4.077	3.385	2.908	2.692
0.520	3.522	2.911	2.495	2.307
0.550	2.859	2.347	2.011	1.860
0.600	2.226	1.808	1.547	1.431
0.650	1.706	1.371	1.171	1.083
0.700	1.330	1.059	0.903	0.836

TABLE 20

PACIFIC NEAR SANTA MONICA, RADIANCE DATA

SATELLITE ALTITUDE **VISIBILITY** 40 km

Solar Zenith Angle	Total Radiance ($mw\ cm^{-2} sr^{-1} \mu m^{-1}$) 35°	45°	55°	60°
Wavelength (μm)				
0.400	5.311	4.573	3.969	3.691
0.420	5.728	4.914	4.251	3.944
0.440	5.260	4.497	3.881	3.594
0.460	5.228	4.453	3.842	3.558
0.500	3.931	3.326	2.861	2.644
0.520	3.377	2.846	2.443	2.255
0.550	2.720	2.279	1.955	1.804
0.600	2.084	1.730	1.481	1.367
0.650	1.574	1.295	1.106	1.020
0.700	1.209	0.986	0.841	0.775

TABLE 21

PACIFIC NEAR SANTA MONICA, RADIANCE DATA

SATELLITE ALTITUDE **VISIBILITY** 60 km

Solar Zenith Angle	**Total Radiance ($mw\ cm^{-2} sr^{-1} \mu m^{-1}$)** **35°**	**45°**	**55°**	**60°**
Wavelength (μm)				
0.400	5.266	4.571	3.973	3.694
0.420	5.673	4.908	4.251	3.944
0.440	5.204	4.488	3.876	3.588
0.460	5.150	4.428	3.824	3.540
0.500	3.857	3.296	2.837	2.620
0.520	3.303	2.814	2.416	2.228
0.550	2.649	2.245	1.926	1.775
0.600	2.011	1.691	1.448	1.333
0.650	1.507	1.257	1.073	0.987
0.700	1.147	0.949	0.809	0.743

TABLE 22

SAN PEDRO CHANNEL, GREEN WATER, REFLECTANCE

λ(μm)	ρ
0.400	0.025
0.425	0.025
0.450	0.024
0.475	0.024
0.500	0.024
0.525	0.025
0.550	0.025
0.575	0.022
0.600	0.016
0.625	0.014
0.650	0.014
0.675	0.012

Sea level data

Source: White, P. G. [36]

Aircraft data, 152 m. altitude, radiance ratios (400 nm - 700 nm), TRW spectrometer.

TABLE 23

SAN PEDRO CHANNEL, GREEN WATER, RADIANCE

SATELLITE ALTITUDE VISIBILITY 15 km

Solar Zenith Angle	**Total Radiance ($mw\ cm^{-2}\ sr^{-1}\ \mu m^{-1}$)** 35°	45°	55°	60°
Wavelength (μm)				
0.400	5.371	4.483	3.877	3.611
0.425	5.428	4.503	3.887	3.616
0.450	5.540	4.568	3.938	3.660
0.475	4.991	4.087	3.514	3.262
0.500	4.212	3.431	2.944	2.730
0.525	3.674	2.976	2.545	2.355
0.550	3.119	2.515	2.147	1.984
0.575	2.804	2.247	1.918	1.773
0.600	2.356	1.871	1.601	1.486
0.625	2.048	1.616	1.383	1.284
0.650	1.825	1.433	1.225	1.137
0.675	1.600	1.250	1.068	0.993

TABLE 24

SAN PEDRO CHANNEL, GREEN WATER, RADIANCE

SATELLITE ALTITUDE VISIBILITY 23 km

Solar Zenith Angle	Total Radiance ($mw\ cm^{-2} sr^{-1} \mu m^{-1}$) 35°	45°	55°	60°
Wavelength (μm)				
0.400	5.251	4.455	3.867	3.604
0.425	5.286	4.460	3.862	3.594
0.450	5.371	4.508	3.896	3.621
0.475	4.812	4.014	3.459	3.208
0.500	4.047	3.359	2.888	2.675
0.525	3.515	2.904	2.487	2.297
0.550	2.976	2.448	2.091	1.929
0.575	2.652	2.169	1.852	1.709
0.600	2.196	1.782	1.526	1.414
0.625	1.890	1.524	1.305	1.210
0.650	1.677	1.347	1.151	1.066
0.675	1.455	1.162	0.994	0.921

TABLE 25

SAN PEDRO CHANNEL, GREEN WATER, RADIANCE

SATELLITE ALTITUDE VISIBILITY 40 km

Solar Zenith Angle	Total Radiance ($mw\ cm^{-2}sr^{-1}\mu m^{-1}$) 35°	45°	55°	60°
Wavelength (μm)				
0.400	5.142	4.431	3.859	3.599
0.425	5.159	4.425	3.842	3.575
0.450	5.220	4.457	3.861	3.586
0.475	4.651	3.951	3.410	3.161
0.500	3.898	3.297	2.838	2.625
0.525	3.373	2.841	2.435	2.245
0.550	2.848	2.389	2.042	1.879
0.575	2.514	2.100	1.794	1.650
0.600	2.051	1.702	1.459	1.347
0.625	1.746	1.442	1.235	1.141
0.650	1.543	1.269	1.085	1.001
0.675	1.323	1.082	0.926	0.855

TABLE 26

SAN PEDRO CHANNEL, GREEN WATER, RADIANCE

SATELLITE ALTITUDE VISIBILITY 60 km

Solar Zenith Angle	Total Radiance (mw $cm^{-2}sr^{-1}\mu m^{-1}$) 35°	45°	55°	60°
Wavelength (μm)				
0.400	5.087	4.421	3.856	3.597
0.425	5.094	4.408	3.833	3.566
0.450	5.143	4.433	3.844	3.569
0.475	4.568	3.920	3.386	3.137
0.500	3.823	3.267	2.814	2.600
0.525	3.301	2.809	2.409	2.219
0.550	2.783	2.360	2.017	1.854
0.575	2.444	2.065	1.764	1.621
0.600	1.977	1.662	1.424	1.313
0.625	1.673	1.400	1.199	1.106
0.650	1.475	1.229	1.051	0.968
0.675	1.255	1.042	0.891	0.821

TABLE 27

SAN PEDRO CHANNEL, BLUE WATER, REFLECTANCE

λ (μm)	ρ
0.400	0.028
0.425	0.026
0.450	0.024
0.475	0.023
0.500	0.019
0.525	0.015
0.550	0.012
0.575	0.010
0.600	0.008
0.625	0.006
0.650	0.005
0.675	0.004

Sea level data

Source: White, P.G. [36]

Aircraft data, 152 m. altitude, radiance ratios (400 nm - 700 nm), TRW spectrometer

TABLE 28

SAN PEDRO CHANNEL, BLUE WATER, RADIANCE

SATELLITE ALTITUDE **VISIBILITY** 15 km

Solar Zenith Angle	**Total Radiance ($mw\ cm^{-2} sr^{-1} \mu m^{-1}$)** 35°	45°	55°	60°
Wavelength (μm)				
0.400	5.410	4.517	3.903	3.632
0.425	5.446	4.519	3.899	3.626
0.450	5.540	4.568	3.938	3.660
0.475	4.964	4.065	3.496	3.246
0.500	4.077	3.316	2.853	2.652
0.525	3.401	2.744	2.361	2.197
0.550	2.774	2.220	1.912	1.783
0.575	2.475	1.966	1.693	1.580
0.600	2.137	1.683	1.451	1.357
0.625	1.834	1.433	1.236	1.158
0.650	1.590	1.232	1.063	0.998
0.675	1.398	1.076	0.929	0.873

TABLE 29

SAN PEDRO CHANNEL, BLUE WATER, RADIANCE

SATELLITE ALTITUDE VISIBILITY 23 km

Solar Zenith Angle	Total Radiance (mw $cm^{-2} sr^{-1} \mu m^{-1}$) 35°	45°	55°	60°
Wavelength (μm)				
0.400	5.296	4.492	3.896	3.628
0.425	5.307	4.478	3.876	3.605
0.450	5.371	4.508	3.896	3.621
0.475	4.782	3.989	3.439	3.191
0.500	3.896	3.231	2.786	2.588
0.525	3.213	2.646	2.282	2.121
0.550	2.595	2.122	1.832	1.706
0.575	2.289	1.859	1.604	1.495
0.600	1.955	1.576	1.361	1.271
0.625	1.655	1.323	1.144	1.071
0.650	1.421	1.127	0.975	0.914
0.675	1.234	0.972	0.842	0.790

TABLE 30

SAN PEDRO CHANNEL, BLUE WATER, RADIANCE

SATELLITE ALTITUDE VISIBILITY 40 km

Solar Zenith Angle	Total Radiance (mw $cm^{-2}sr^{-1}\mu m^{-1}$) 35°	45°	55°	60°
Wavelength (μm)				
0.400	5.193	4.474	3.892	3.626
0.425	5.182	4.444	3.857	3.588
0.450	5.220	4.457	3.861	3.586
0.475	4.618	3.923	3.388	3.142
0.500	3.733	3.156	2.726	2.529
0.525	3.042	2.558	2.210	2.052
0.550	2.431	2.033	1.758	1.635
0.575	2.119	1.762	1.524	1.418
0.600	1.790	1.478	1.279	1.192
0.625	1.492	1.224	1.061	0.990
0.650	1.267	1.031	0.894	0.836
0.675	1.085	0.878	0.761	0.713

TABLE 31

SAN PEDRO CHANNEL, BLUE WATER, RADIANCE

SATELLITE ALTITUDE **VISIBILITY** 60 km

Solar Zenith Angle	**Total Radiance ($mw\ cm^{-2} sr^{-1} \mu m^{-1}$)** 35°	45°	55°	60°
Wavelength (µm)				
0.400	5.141	4.466	3.891	3.626
0.425	5.118	4.429	3.848	3.579
0.450	5.143	4.433	3.844	3.569
0.475	4.534	3.890	3.363	3.117
0.500	3.649	3.119	2.696	2.499
0.525	2.954	2.513	2.174	2.017
0.550	2.347	1.988	1.720	1.598
0.575	2.032	1.712	1.482	1.377
0.600	1.705	1.428	1.237	1.152
0.625	1.409	1.173	1.017	0.949
0.650	1.187	0.982	0.852	0.796
0.675	1.008	0.829	0.720	0.673

TABLE 32

S. CALIFORNIA, GREEN COASTAL WATER, REFLECTANCE

λ (μm)	ρ
0.400	0.014
0.425	0.014
0.450	0.013
0.475	0.013
0.500	0.014
0.525	0.014
0.550	0.014
0.575	0.010
0.600	0.005
0.625	0.004
0.650	0.003
0.675	0.002

Sea level data

Source: Austin, R. W. [37]

Underwater spectral radiance data and total spectral irradiance (400 nm–700 nm) given for three ocean waters of distinctly different color; green, blue-green, and blue. Available data was used to calculate reflectance at a point above water surface.

TABLE 33

S. CALIFORNIA, GREEN COASTAL WATER, RADIANCE

SATELLITE ALTITUDE **VISIBILITY** 15 km

Solar Zenith Angle	Total Radiance ($mw\ cm^{-2} sr^{-1} \mu m^{-1}$) 35°	45°	55°	60°
Wavelength (μm)				
0.400	5.225	4.361	3.783	3.532
0.425	5.229	4.336	3.757	3.506
0.450	5.276	4.345	3.763	3.512
0.475	4.698	3.839	3.318	3.095
0.500	3.942	3.201	2.762	2.574
0.525	3.374	2.721	2.342	2.181
0.550	2.827	2.266	1.949	1.814
0.575	2.475	1.966	1.693	1.580
0.600	2.054	1.613	1.395	1.308
0.625	1.780	1.387	1.199	1.126
0.650	1.538	1.187	1.028	0.967
0.675	1.347	1.033	0.894	0.843

TABLE 34

S. CALIFORNIA, GREEN COASTAL WATER, RADIANCE

SATELLITE ALTITUDE VISIBILITY 23 km

Solar Zenith Angle	Total Radiance (mw cm^{-2} sr^{-1} μm^{-1}) 35°	45°	55°	60°
Wavelength (μm)				
0.400	5.085	4.316	3.759	3.513
0.425	5.061	4.271	3.715	3.469
0.450	5.075	4.257	3.700	3.454
0.475	4.484	3.736	3.239	3.021
0.500	3.746	3.103	2.685	2.501
0.525	3.183	2.620	2.261	2.104
0.550	2.653	2.172	1.872	1.740
0.575	2.289	1.859	1.604	1.495
0.600	1.865	1.498	1.300	1.218
0.625	1.597	1.273	1.104	1.036
0.650	1.364	1.078	0.936	0.880
0.675	1.179	0.925	0.804	0.757

TABLE 35

S. CALIFORNIA, GREEN COASTAL WATER, RADIANCE

SATELLITE ALTITUDE VISIBILITY 40 km

Solar Zenith Angle	Total Radiance ($mw\ cm^{-2} sr^{-1} \mu m^{-1}$) 35°	45°	55°	60°
Wavelength (μm)				
0.400	4.956	4.275	3.739	3.497
0.425	4.907	4.213	3.677	3.435
0.450	4.891	4.179	3.642	3.400
0.475	4.289	3.644	3.168	2.954
0.500	3.567	3.015	2.615	2.433
0.525	3.009	2.530	2.188	2.033
0.550	2.495	2.088	1.802	1.672
0.575	2.119	1.762	1.524	1.418
0.600	1.692	1.394	1.212	1.134
0.625	1.429	1.169	1.017	0.953
0.650	1.205	0.978	0.852	0.799
0.675	1.026	0.827	0.720	0.677

TABLE 36

S. CALIFORNIA, GREEN COASTAL WATER, RADIANCE

SATELLITE ALTITUDE VISIBILITY 60 km

Solar Zenith Angle	Total Radiance ($mw\ cm^{-2} sr^{-1} \mu m^{-1}$) 35°	45°	55°	60°
Wavelength (μm)				
0.400	4.889	4.255	3.728	3.489
0.425	4.828	4.184	3.658	3.418
0.450	4.796	4.139	3.613	3.373
0.475	4.188	3.597	3.132	2.919
0.500	3.475	2.971	2.579	2.399
0.525	2.919	2.484	2.150	1.996
0.550	2.414	2.045	1.766	1.637
0.575	2.032	1.712	1.482	1.377
0.600	1.603	1.340	1.167	1.091
0.625	1.342	1.116	0.972	0.910
0.650	1.123	0.927	0.808	0.758
0.675	0.946	0.776	0.677	0.636

3.1.3 Oceanic Waters, Atlantic

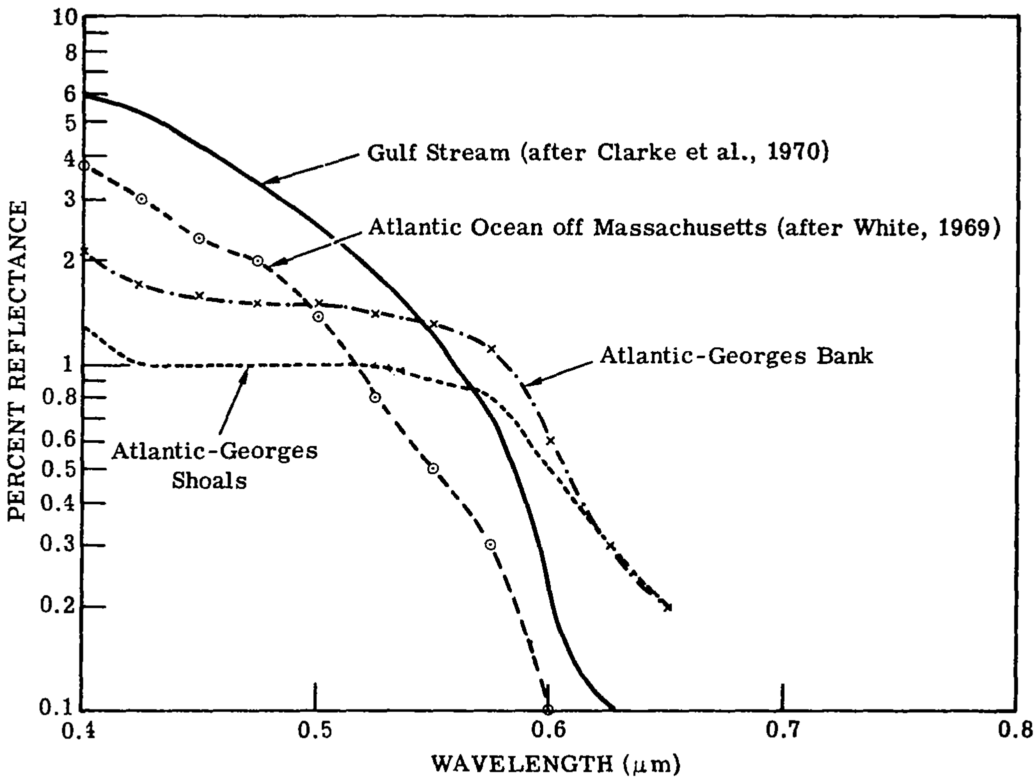

FIGURE 12. OCEANIC WATERS - ATLANTIC. Sea Level Data

TABLE 37

ATLANTIC OCEAN NEAR MASSACHUSETTS, REFLECTANCE

λ (μm)	ρ
0.400	0.037
0.425	0.030
0.450	0.023
0.475	0.020
0.500	0.014
0.525	0.008
0.550	0.005
0.575	0.003
0.600	0.001

Sea level data

Source: White, P. G. [38]

Aircraft data, 305 m. altitude, water color spectrometer (WCS), reflectance data (400 nm-700 nm).

TABLE 38

ATLANTIC OCEAN NEAR MASSACHUSETTS, RADIANCE

SATELLITE ALTITUDE VISIBILITY 15 km

Solar Zenith Angle	Total Radiance ($mw\ cm^{-2} sr^{-1} \mu m^{-1}$) 35°	45°	55°	60°
Wavelength (μm)				
0.400	5.530	4.616	3.980	3.697
0.425	5.519	4.579	3.947	3.666
0.450	5.516	4.547	3.922	3.647
0.475	4.884	3.997	3.443	3.201
0.500	3.942	3.201	2.762	2.574
0.525	3.210	2.581	2.232	2.086
0.550	2.588	2.061	1.786	1.674
0.575	2.282	1.801	1.562	1.467
0.600	1.945	1.519	1.320	1.244

TABLE 39

ATLANTIC OCEAN NEAR MASSACHUSETTS, RADIANCE

SATELLITE ALTITUDE VISIBILITY 23 km

Solar Zenith Angle	Total Radiance ($mw\ cm^{-2} sr^{-1} \mu m^{-1}$) 35°	45°	55°	60°
Wavelength (μm)				
0.400	5.432	4.606	3.984	3.702
0.425	5.389	4.547	3.930	3.650
0.450	5.344	4.485	3.878	3.605
0.475	4.693	3.913	3.379	3.140
0.500	3.746	3.103	2.685	2.501
0.525	3.001	2.465	2.138	1.998
0.550	2.389	1.946	1.692	1.585
0.575	2.077	1.678	1.460	1.371
0.600	1.745	1.395	1.217	1.147

TABLE 40

ATLANTIC OCEAN NEAR MASSACHUSETTS, RADIANCE

SATELLITE ALTITUDE VISIBILITY 40 km

Solar Zenith Angle	Total Radiance (mw cm^{-2} sr^{-1} μm^{-1}) 35°	45°	55°	60°
Wavelength (μm)				
0.400	5.345	4.602	3.991	3.709
0.425	5.273	4.521	3.917	3.638
0.450	5.190	4.432	3.841	3.569
0.475	4.519	3.829	3.322	3.085
0.500	3.567	3.015	2.615	2.433
0.525	2.810	2.360	2.053	1.917
0.550	2.207	1.841	1.605	1.503
0.575	1.889	1.565	1.366	1.282
0.600	1.561	1.282	1.122	1.057

TABLE 41

ATLANTIC OCEAN NEAR MASSACHUSETTS, RADIANCE

SATELLITE ALTITUDE VISIBILITY 60 km

Solar Zenith Angle	Total Radiance (mw $cm^{-2} sr^{-1} \mu m^{-1}$) 35°	45°	55°	60°
Wavelength (μm)				
0.400	5.302	4.601	3.996	3.714
0.425	5.214	4.510	3.912	3.633
0.450	5.111	4.406	3.823	3.551
0.475	4.430	3.802	3.294	3.057
0.500	3.475	2.971	2.579	2.399
0.525	2.711	2.306	2.009	1.875
0.550	2.113	1.787	1.561	1.461
0.575	1.792	1.507	1.317	1.236
0.600	1.466	1.224	1.073	1.010

TABLE 42

ATLANTIC, GEORGES BANK, REFLECTANCE

λ (μm)	ρ
0.400	0.021
0.425	0.017
0.450	0.016
0.475	0.015
0.500	0.015
0.525	0.014
0.550	0.013
0.575	0.011
0.600	0.006
0.625	0.003
0.650	0.002

Sea level data

Source: Clarke, G. L., Ewing, G.C., and Lorenzen, C.J. [33].

Aircraft data, 305 m. altitude, TRW spectrometer (400 nm to 650 nm) with polarizing filter, instrument tilted at Brewster's angle (53° ±).

TABLE 43

ATLANTIC, GEORGES BANK, RADIANCE

SATELLITE ALTITUDE VISIBILITY 15 km

Solar Zenith Angle	Total Radiance ($mw\ cm^{-2} sr^{-1} \mu m^{-1}$) 35°	45°	55°	60°
Wavelength (μm)				
0.400	5.318	4.439	3.843	3.582
0.425	5.283	4.381	3.793	3.536
0.450	5.348	4.406	3.811	3.553
0.475	4.751	3.884	3.354	3.125
0.500	3.969	3.224	2.780	2.590
0.525	3.374	2.721	2.342	2.181
0.550	2.800	2.243	1.931	1.798
0.575	2.502	1.989	1.712	1.596
0.600	2.082	1.636	1.413	1.324
0.625	1.753	1.364	1.181	1.110
0.650	1.512	1.165	1.010	0.951

TABLE 44

ATLANTIC, GEORGES BANK, RADIANCE

SATELLITE ALTITUDE VISIBILITY 23 km

Solar Zenith Angle	Total Radiance ($mw\ cm^{-2} sr^{-1} \mu m^{-1}$) 35°	45°	55°	60°
Wavelength (μm)				
0.400	5.190	4.404	3.828	3.571
0.425	5.122	4.322	3.755	3.503
0.450	5.156	4.326	3.753	3.499
0.475	4.544	3.787	3.279	3.055
0.500	3.776	3.128	2.705	2.518
0.525	3.183	2.620	2.261	2.104
0.550	2.624	2.147	1.852	1.723
0.575	2.319	1.885	1.625	1.513
0.600	1.895	1.524	1.320	1.236
0.625	1.567	1.248	1.084	1.018
0.650	1.336	1.054	0.916	0.863

TABLE 45

ATLANTIC, GEORGES BANK, RADIANCE

SATELLITE ALTITUDE VISIBILITY 40 km

Solar Zenith Angle	Total Radiance (mw cm^{-2} sr^{-1} μm^{-1}) 35°	45°	55°	60°
Wavelength (μm)				
0.400	5.074	4.375	3.815	3.562
0.425	4.976	4.271	3.722	3.473
0.450	4.981	4.255	3.702	3.451
0.475	4.355	3.700	3.212	2.991
0.500	3.600	3.043	2.637	2.453
0.525	3.009	2.530	2.188	2.033
0.550	2.463	2.060	1.780	1.653
0.575	2.152	1.790	1.546	1.437
0.600	1.724	1.422	1.235	1.154
0.625	1.397	1.142	0.995	0.934
0.650	1.174	0.952	0.830	0.781

TABLE 46

ATLANTIC, GEORGES BANK, RADIANCE

SATELLITE ALTITUDE VISIBILITY 60 km

Solar Zenith Angle	Total Radiance (mw $cm^{-2} sr^{-1} \mu m^{-1}$) 35°	45°	55°	60°
Wavelength (μm)				
0.400	5.015	4.361	3.810	3.557
0.425	4.900	4.245	3.705	3.458
0.450	4.891	4.219	3.676	3.426
0.475	4.257	3.656	3.178	2.959
0.500	3.510	3.000	2.602	2.419
0.525	2.919	2.484	2.150	1.996
0.550	2.381	2.016	1.743	1.618
0.575	2.067	1.742	1.505	1.398
0.600	1.637	1.370	1.190	1.111
0.625	1.309	1.088	0.949	0.890
0.650	1.091	0.900	0.786	0.739

TABLE 47

ATLANTIC, GEORGES SHOALS, REFLECTANCE

λ (μm)	ρ
0.400	0.013
0.425	0.010
0.450	0.010
0.475	0.010
0.500	0.010
0.525	0.010
0.550	0.009
0.575	0.008
0.600	0.005
0.625	0.003
0.650	0.002

Sea level data

Source: Clarke, G. L., Ewing, G. C., and Lorenzen, C.J. [33]

Aircraft data, 305 m. altitude, TRW spectrometer (400 nm to 650 nm) with polarizing filter, instrument tilted at Brewster's angle (53° $\pm$).

TABLE 48

ATLANTIC, GEORGES SHOALS, RADIANCE

SATELLITE ALTITUDE VISIBILITY 15 km

Solar Zenith Angle	Total Radiance ($mw\ cm^{-2} sr^{-1} \mu m^{-1}$) 35°	45°	55°	60°
Wavelength (μm)				
0.400	5.212	4.350	3.775	3.525
0.425	5.156	4.275	3.710	3.466
0.450	5.204	4.284	3.716	3.472
0.475	4.618	3.772	3.265	3.050
0.500	3.833	3.109	2.689	2.512
0.525	3.264	2.628	2.269	2.118
0.550	2.694	2.152	1.858	1.736
0.575	2.420	1.919	1.655	1.548
0.600	2.054	1.613	1.395	1.308
0.625	1.753	1.364	1.181	1.110
0.650	1.512	1.165	1.010	0.951

TABLE 49

ATLANTIC, GEORGES SHOALS, RADIANCE

SATELLITE ALTITUDE VISIBILITY 23 km

Solar Zenith Angle	Total Radiance ($mw\ cm^{-2} sr^{-1} \mu m^{-1}$) 35°	45°	55°	60°
Wavelength (μm)				
0.400	5.070	4.303	3.750	3.505
0.425	4.979	4.202	3.661	3.423
0.450	4.994	4.189	3.646	3.408
0.475	4.395	3.661	3.180	2.970
0.500	3.625	3.000	2.604	2.431
0.525	3.062	2.517	2.179	2.034
0.550	2.507	2.047	1.772	1.654
0.575	2.229	1.807	1.563	1.460
0.600	1.865	1.498	1.300	1.218
0.625	1.567	1.248	1.084	1.018
0.650	1.336	1.054	0.916	0.863

TABLE 50
ATLANTIC, GEORGES SHOALS, RADIANCE

SATELLITE ALTITUDE VISIBILITY 40 km

Solar Zenith Angle	Total Radiance (mw $cm^{-2} sr^{-1} \mu m^{-1}$) 35°	45°	55°	60°
Wavelength (μm)				
0.400	4.939	4.261	3.728	3.488
0.425	4.816	4.136	3.617	3.384
0.450	4.801	4.103	3.583	3.350
0.475	4.190	3.560	3.102	2.897
0.500	3.434	2.902	2.525	2.357
0.525	2.876	2.417	2.098	1.956
0.550	2.335	1.951	1.693	1.578
0.575	2.054	1.706	1.478	1.379
0.600	1.692	1.394	1.212	1.134
0.625	1.397	1.142	0.995	0.934
0.650	1.174	0.952	0.830	0.781

TABLE 51

ATLANTIC, GEORGES SHOALS, RADIANCE

SATELLITE ALTITUDE VISIBILITY 60 km

Solar Zenith Angle	Total Radiance ($mw\ cm^{-2} sr^{-1} \mu m^{-1}$) 35°	45°	55°	60°
Wavelength (μm)				
0.400	4.871	4.240	3.717	3.479
0.425	4.731	4.103	3.594	3.364
0.450	4.702	4.059	3.550	3.320
0.475	4.084	3.509	3.062	2.860
0.500	3.336	2.852	2.485	2.318
0.525	2.780	2.365	2.056	1.916
0.550	2.247	1.902	1.652	1.539
0.575	1.964	1.653	1.435	1.337
0.600	1.603	1.340	1.167	1.091
0.625	1.309	1.088	0.949	0.890
0.650	1.091	0.900	0.786	0.739

3.1.4 Lakes - Oligotrophic, Eutrophic

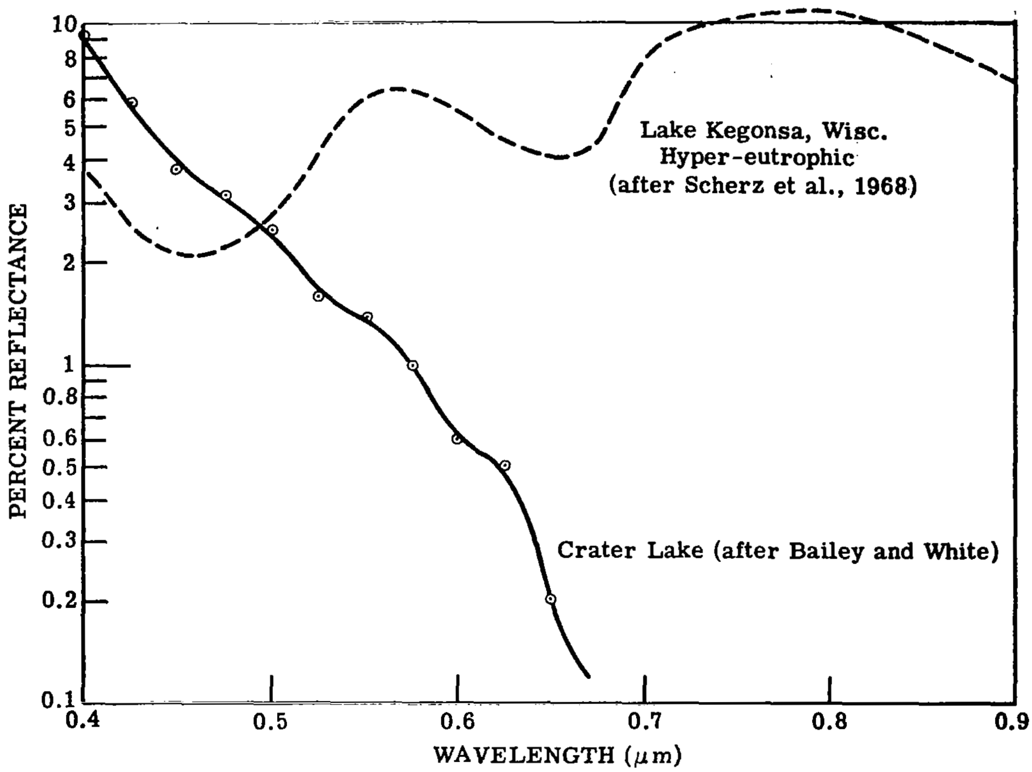

FIGURE 13. LAKES OLIGOTROPHIC-EUTROPHIC

TABLE 52

CRATER LAKE, REFLECTANCE
(OLIGOTROPHIC)

$\lambda (\mu m)$	ρ
0.400	0.094
0.425	0.057
0.450	0.037
0.475	0.031
0.500	0.024
0.525	0.016
0.550	0.014
0.575	0.010
0.600	0.006
0.625	0.005
0.650	0.002

Lake level data

Source: Bailey, J. S. and White, P. G. [39]

Aircraft data, 762 m. altitude above lake, water color spectrometer (400 nm to 700 nm).

TABLE 53

CRATER LAKE, RADIANCE

SATELLITE ALTITUDE VISIBILITY 15 km

Solar Zenith Angle	Total Radiance ($mw\ cm^{-2} sr^{-1} \mu m^{-1}$) 35°	45°	55°	60°
Wavelength (μm)				
0.400	6.284	5.248	4.467	4.106
0.425	6.007	4.991	4.267	3.937
0.450	5.851	4.831	4.144	3.835
0.475	5.177	4.245	3.638	3.368
0.500	4.212	3.431	2.944	2.730
0.525	3.428	2.767	2.379	2.213
0.550	2.827	2.266	1.949	1.814
0.575	2.475	1.966	1.693	1.580
0.600	2.082	1.636	1.413	1.324
0.625	1.807	1.410	1.217	1.142
0.650	1.512	1.165	1.010	0.951

TABLE 54

CRATER LAKE, RADIANCE

SATELLITE ALTITUDE VISIBILITY 23 km

Solar Zenith Angle	Total Radiance (mw $cm^{-2} sr^{-1} \mu m^{-1}$) 35°	45°	55°	60°
Wavelength (μm)				
0.400	6.292	5.327	4.540	4.170
0.425	5.942	5.013	4.292	3.957
0.450	5.722	4.804	4.128	3.818
0.475	5.020	4.191	3.598	3.327
0.500	4.047	3.359	2.888	2.675
0.525	3.243	2.672	2.302	2.139
0.550	2.653	2.172	1.872	1.740
0.575	2.289	1.859	1.604	1.495
0.600	1.895	1.524	1.320	1.236
0.625	1.626	1.298	1.124	1.053
0.650	1.336	1.054	0.916	0.863

TABLE 55

CRATER LAKE, RADIANCE

SATELLITE ALTITUDE VISIBILITY 40 km

Solar Zenith Angle	Total Radiance ($mw\ cm^{-2} sr^{-1} \mu m^{-1}$) 35°	45°	55°	60°
Wavelength (μm)				
0.400	6.311	5.411	4.616	4.235
0.425	5.890	5.042	4.323	3.981
0.450	5.609	4.786	4.119	3.806
0.475	4.881	4.146	3.565	3.292
0.500	3.898	3.297	2.838	2.625
0.525	3.075	2.586	2.233	2.072
0.550	2.495	2.088	1.802	1.672
0.575	2.119	1.762	1.524	1.418
0.600	1.724	1.422	1.235	1.154
0.625	1.461	1.197	1.039	0.972
0.650	1.174	0.952	0.830	0.781

TABLE 56

CRATER LAKE, RADIANCE

SATELLITE ALTITUDE VISIBILITY 60 km

Solar Zenith Angle	Total Radiance ($mw\ cm^{-2} sr^{-1} \mu m^{-1}$) 35°	45°	55°	60°
Wavelength (μm)				
0.400	6.325	5.459	4.659	4.272
0.425	5.867	5.060	4.341	3.996
0.450	5.552	4.780	4.116	3.800
0.475	4.810	4.125	3.549	3.275
0.500	3.823	3.267	2.814	2.600
0.525	2.989	2.543	2.197	2.037
0.550	2.414	2.045	1.766	1.637
0.575	2.032	1.712	1.482	1.377
0.600	1.637	1.370	1.190	1.111
0.625	1.376	1.144	0.995	0.929
0.650	1.091	0.900	0.786	0.739

TABLE 57

LAKE KEGONSA, REFLECTANCE

(EUTROPHIC)

λ(μm)	ρ
0.400	0.037
0.425	0.025
0.450	0.021
0.475	0.022
0.500	0.027
0.525	0.042
0.550	0.060
0.575	0.063
0.600	0.055
0.625	0.045
0.650	0.041
0.675	0.045
0.700	0.080
0.800	0.110
0.900	0.066

Sea level data

Source: Scherz, J.P., Boyle, W.C., and Graff, D.R. [40]

Laboratory reflectance measurements; Beckman DU-2 spectrophotometer with special attachment; illumination provided by a Sylvania Quartz-Iodine Sun Gun (0.2 μm-1.2 μm).

TABLE 58

LAKE KEGONSA, RADIANCE

SATELLITE ALTITUDE VISIBILITY 15 km

Solar Zenith Angle	Total Radiance (mw $cm^{-2} sr^{-1} \mu m^{-1}$) 35°	45°	55°	60°
Wavelength (μm)				
0.400	5.530	4.616	3.980	3.697
0.425	5.428	4.503	3.887	3.616
0.450	5.468	4.507	3.890	3.620
0.475	4.938	4.042	3.478	3.231
0.500	4.294	3.500	2.999	2.777
0.525	4.137	3.371	2.859	2.624
0.550	4.049	3.308	2.779	2.527
0.575	3.930	3.210	2.685	2.434
0.600	3.426	2.786	2.333	2.117
0.625	2.878	2.327	1.952	1.776
0.650	2.528	2.036	1.708	1.555
0.675	2.435	1.966	1.643	1.490
0.700	3.097	2.542	2.099	1.877
0.800	3.011	2.498	2.046	1.814
0.900	1.641	1.343	1.107	0.988

TABLE 59

LAKE KEGONSA, RADIANCE

SATELLITE ALTITUDE VISIBILITY 23 km

Solar Zenith Angle	Total Radiance ($mw\ cm^{-2} sr^{-1} \mu m^{-1}$) 35°	45°	55°	60°
Wavelength (μm)				
0.400	5.432	4.606	3.984	3.702
0.425	5.286	4.460	3.862	3.594
0.450	5.291	4.440	3.843	3.575
0.475	4.752	3.964	3.419	3.174
0.500	4.138	3.436	2.949	2.727
0.525	4.029	3.342	2.835	2.596
0.550	4.003	3.325	2.790	2.530
0.575	3.891	3.229	2.699	2.438
0.600	3.371	2.787	2.331	2.108
0.625	2.799	2.303	1.930	1.749
0.650	2.446	2.006	1.680	1.523
0.675	2.365	1.943	1.621	1.464
0.700	3.108	2.586	2.131	1.899
0.800	3.072	2.576	2.107	1.861
0.900	1.629	1.352	1.112	0.988

TABLE 60

LAKE KEGONSA, RADIANCE

SATELLITE ALTITUDE VISIBILITY 40 km

Solar Zenith Angle	Total Radiance ($mw\ cm^{-2} sr^{-1} \mu m^{-1}$) 35°	45°	55°	60°
Wavelength (μm)				
0.400	5.345	4.602	3.991	3.709
0.425	5.159	4.425	3.842	3.575
0.450	5.130	4.381	3.801	3.535
0.475	4.585	3.895	3.366	3.123
0.500	3.998	3.382	2.905	2.682
0.525	3.936	3.321	2.817	2.573
0.550	3.969	3.347	2.806	2.536
0.575	3.863	3.254	2.716	2.446
0.600	3.326	2.794	2.333	2.102
0.625	2.731	2.286	1.912	1.727
0.650	2.374	1.981	1.657	1.496
0.675	2.305	1.925	1.604	1.442
0.700	3.124	2.632	2.165	1.922
0.800	3.135	2.653	2.167	1.909
0.900	1.623	1.363	1.118	0.990

TABLE 61

LAKE KEGONSA, RADIANCE

SATELLITE ALTITUDE VISIBILITY 60 km

Solar Zenith Angle	Total Radiance ($mw\ cm^{-2} sr^{-1} \mu m^{-1}$) 35°	45°	55°	60°
Wavelength (μm)				
0.400	5.302	4.601	3.996	3.714
0.425	5.094	4.408	3.833	3.566
0.450	5.048	4.353	3.781	3.516
0.475	4.499	3.861	3.340	3.097
0.500	3.927	3.356	2.884	2.660
0.525	3.890	3.312	2.809	2.563
0.550	3.954	3.361	2.816	2.541
0.575	3.852	3.270	2.728	2.452
0.600	3.305	2.800	2.336	2.101
0.625	2.697	2.278	1.905	1.716
0.650	2.338	1.970	1.647	1.483
0.675	2.275	1.918	1.596	1.432
0.700	3.135	2.657	2.184	1.936
0.800	3.170	2.695	2.200	1.935
0.900	1.620	1.370	1.122	0.991

3.1.5 Salton Sea

TABLE 62

SALTON SEA, REFLECTANCE

ERTS-1 BAND (μm)	ρ
0.5-0.6	0.083
0.6-0.7	0.078
0.7-0.8	0.006

Sea level data

Source: Griggs, M. [41]

ERTS-1 data, radiance vs wavelength for several sun angles and aerosol content

TABLE 63

SALTON SEA, RADIANCE

SATELLITE ALTITUDE VISIBILITY 15 km

Solar Zenith Angle	Total Radiance ($mw\ cm^{-2} sr^{-1} \mu m^{-1}$) 35°	45°	55°	60°
ERTS-1 band (μm)				
0.5-0.6	4.660	3.830	3.194	2.884
0.6-0.7	3.492	2.863	2.371	2.127
0.7-0.8	1.056	0.805	0.692	0.648

TABLE 64

SALTON SEA, RADIANCE

SATELLITE ALTITUDE VISIBILITY 23 km

Solar Zenith Angle	Total Radiance ($mw\ cm^{-2} sr^{-1} \mu m^{-1}$) 35°	45°	55°	60°
ERTS-1 band (μm)				
0.5-0.6	4.678	3.901	3.249	2.924
0.6-0.7	3.498	2.909	2.405	2.150
0.7-0.8	0.924	0.720	0.619	0.579

TABLE 65

SALTON SEA, RADIANCE

SATELLITE ALTITUDE VISIBILITY 40 km

Solar Zenith Angle	Total Radiance ($mw\ cm^{-2} sr^{-1} \mu m^{-1}$) 35°	45°	55°	60°
ERTS-1 band (μm)				
0.5-0.6	4.706	3.977	3.308	2.968
0.6-0.7	3.512	2.958	2.442	2.175
0.7-0.8	0.803	0.643	0.553	0.515

TABLE 66

SALTON SEA, RADIANCE

SATELLITE ALTITUDE VISIBILITY 60 km

Solar Zenith Angle	Total Radiance ($mw\ cm^{-2} sr^{-1} \mu m^{-1}$) 35°	45°	55°	60°
ERTS-1 band (μm)				
0.5-0.6	4.724	4.019	3.341	2.993
0.6-0.7	3.522	2.986	2.463	2.190
0.7-0.8	0.742	0.603	0.519	0.482

3.2 PHYTOPLANKTON - CHLOROPHYLL

Eutrophication of surface waters is a major contemporary water quality management problem. Although phytoplankton are not "pollutants" in the usual sense, they are included in this analysis because: (1) of their effect on the optical properties of surface waters, and (2) because phytoplankton, or the chlorophyll content of the photic zone, are important indicators of primary productivity. From the water pollution control viewpoint, chlorophyll is one indicator of trophic state and one manifestation of nutrient loading, or "enrichment", of surface waters.

The substances responsible for the absorption of light are the chlorophyll pigments, carotenoids, and special accessory pigments. Chlorophyll a is found in all green plants and is the predominant pigment in planktonic algae. Chlorophyll b appears to be present only in the Chlorophyceae, whereas chlorophyll c is found in several algae including all of the diatoms [42,43]. Other major pigments are fucoxanthin found in the diatoms, phycoerythrin found in red algae, and phycocyanin found in red and blue-green algae. Spectral information of relevance to the problem under consideration is presented in Table 67. A major characteristic common to all species is absorbance in the blue and red regions of the spectrum. In the case of phytoplankton blooms an increase reflectance in the near-IR is expected.

As in the case of all substances introduced into the aquatic environment, the optical properties of the base water will affect the composite reflectance properties.

TABLE 67

SPECTRAL CHARACTERISTICS OF PIGMENTS

In vivo

Wavelength (Peak Absorption)	Pigment
6750 - 6950 Å ca. 4400 Å	Chlorophyll _a_
ca. 6500 Å ca. 4650 Å	Chlorophyll _b_
ca. 6400 Å ca. 5850 Å	Chlorophyll _c_
ca. 4700 Å	Fucoxanthin
ca. 5650 Å	Phycoerythrin
ca. 6200 Å	Phycocyanin

Source: Strickland [42] Seliger and McElroy [43]

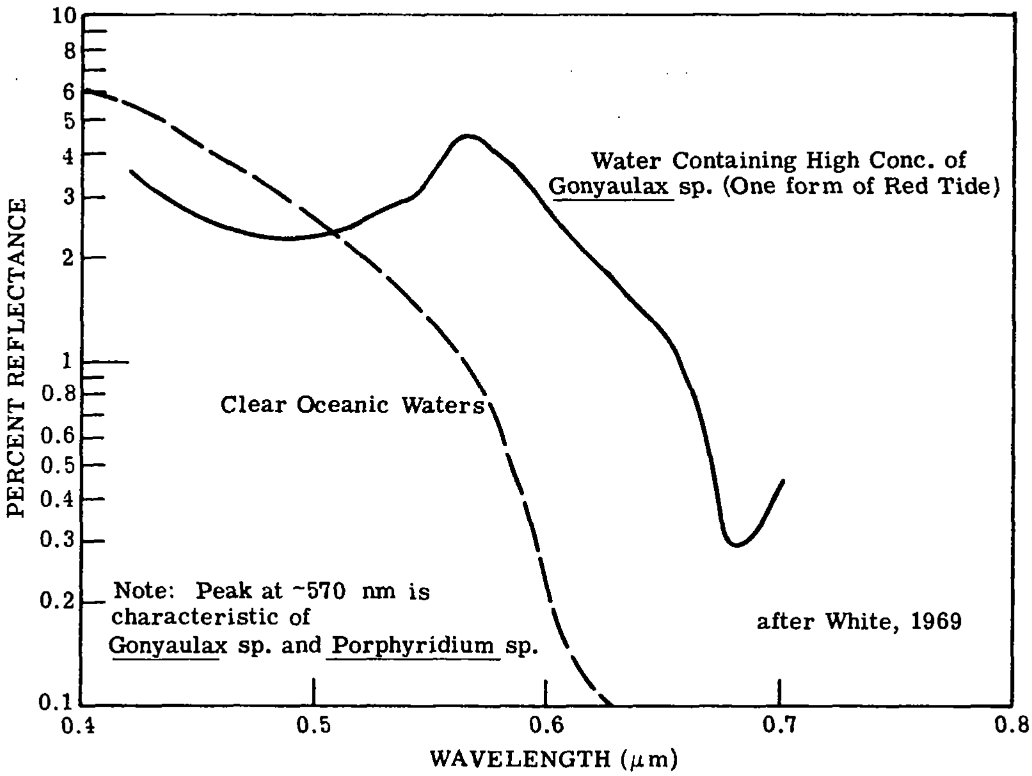

FIGURE 14. GONYAULAX sp. Pacific Coastal Waters

TABLE 68

GONYAULAX SP., PACIFIC COASTAL WATERS, REFLECTANCE

λ (μm)	ρ
0.400	0.065
0.425	0.033
0.450	0.026
0.475	0.023
0.500	0.023
0.525	0.027
0.540	0.029
0.550	0.035
0.565	0.044
0.575	0.040
0.590	0.034
0.600	0.026
0.625	0.018
0.650	0.012
0.675	0.003

Sea level data

Source: White, P. G. [38]
Bailey, J. S. and White, P. G. [39]

Aircraft data, 914 m. altitude, TRW spectrometer, reflectance (400 nm-700 nm), S. California coast, one of several plankton which are commonly referred to as "red tide".

TABLE 69

GONYAULAX SP., PACIFIC COASTAL WATERS, RADIANCE

SATELLITE ALTITUDE VISIBILITY 15 km

Solar Zenith Angle	Total Radiance ($mw\ cm^{-2} sr^{-1} \mu m^{-1}$) 35°	45°	55°	60°
Wavelength (μm)				
0.400	5.900	4.927	4.219	3.898
0.425	5.573	4.625	3.982	3.696
0.450	5.587	4.608	3.969	3.687
0.475	4.964	4.065	3.496	3.246
0.500	4.185	3.408	2.926	2.715
0.525	3.728	3.023	2.582	2.387
0.540	3.449	2.791	2.379	2.195
0.550	3.385	2.742	2.328	2.140
0.565	3.465	2.813	2.373	2.169
0.575	3.298	2.670	2.255	2.063
0.590	2.980	2.401	2.031	1.863
0.600	2.631	2.106	1.789	1.648
0.625	2.155	1.708	1.456	1.348
0.650	1.773	1.388	1.189	1.106
0.675	1.373	1.055	0.912	0.858

TABLE 70

GONYAULAX SP., PACIFIC COASTAL WATERS, RADIANCE

SATELLITE ALTITUDE VISIBILITY 23 km

Solar Zenith Angle	Total Radiance (mw $cm^{-2} sr^{-1} \mu m^{-1}$) 35°	45°	55°	60°
Wavelength (μm)				
0.400	5.854	4.960	4.257	3.932
0.425	5.450	4.599	3.970	3.685
0.450	5.425	4.553	3.932	3.651
0.475	4.782	3.989	3.439	3.191
0.500	4.017	3.334	2.868	2.657
0.525	3.576	2.955	2.528	2.332
0.540	3.311	2.731	2.330	2.145
0.550	3.270	2.698	2.291	2.100
0.565	3.373	2.787	2.350	2.141
0.575	3.196	2.635	2.224	2.029
0.590	2.864	2.352	1.989	1.819
0.600	2.497	2.040	1.733	1.591
0.625	2.007	1.625	1.386	1.279
0.650	1.620	1.298	1.112	1.032
0.675	1.207	0.949	0.823	0.773

TABLE 71

GONYAULAX SP., PACIFIC COASTAL WATERS, RADIANCE

SATELLITE ALTITUDE VISIBILITY 40 km

Solar Zenith Angle	Total Radiance (mw cm^{-2} sr^{-1} μm^{-1}) 35°	45°	55°	60°
Wavelength (μm)				
0.400	5.820	4.999	4.298	3.968
0.425	5.342	4.579	3.962	3.676
0.450	5.280	4.508	3.900	3.620
0.475	4.618	3.923	3.388	3.142
0.500	3.865	3.269	2.816	2.606
0.525	3.439	2.897	2.480	2.284
0.540	3.188	2.680	2.287	2.100
0.550	3.168	2.663	2.260	2.067
0.565	3.293	2.768	2.332	2.119
0.575	3.107	2.607	2.199	2.000
0.590	2.762	2.311	1.953	1.780
0.600	2.378	1.982	1.683	1.541
0.625	1.873	1.551	1.323	1.217
0.650	1.482	1.216	1.043	0.964
0.675	1.055	0.852	0.741	0.695

TABLE 72

GONYAULAX SP., PACIFIC COASTAL WATERS, RADIANCE

SATELLITE ALTITUDE VISIBILITY 60 km

Solar Zenith Angle	Total Radiance ($mw\ cm^{-2} sr^{-1} \mu m^{-1}$) 35°	45°	55°	60°
Wavelength (μm)				
0.400	5.805	5.023	4.322	3.988
0.425	5.287	4.571	3.960	3.673
0.450	5.206	4.486	3.885	3.605
0.475	4.534	3.890	3.363	3.117
0.500	3.788	3.237	2.790	2.580
0.525	3.370	2.868	2.456	2.259
0.540	3.125	2.655	2.266	2.078
0.550	3.117	2.646	2.246	2.050
0.565	3.254	2.760	2.325	2.108
0.575	3.062	2.594	2.187	1.985
0.590	2.711	2.291	1.936	1.761
0.600	2.318	1.953	1.658	1.515
0.625	1.805	1.513	1.290	1.185
0.650	1.411	1.174	1.007	0.930
0.675	0.977	0.803	0.699	0.655

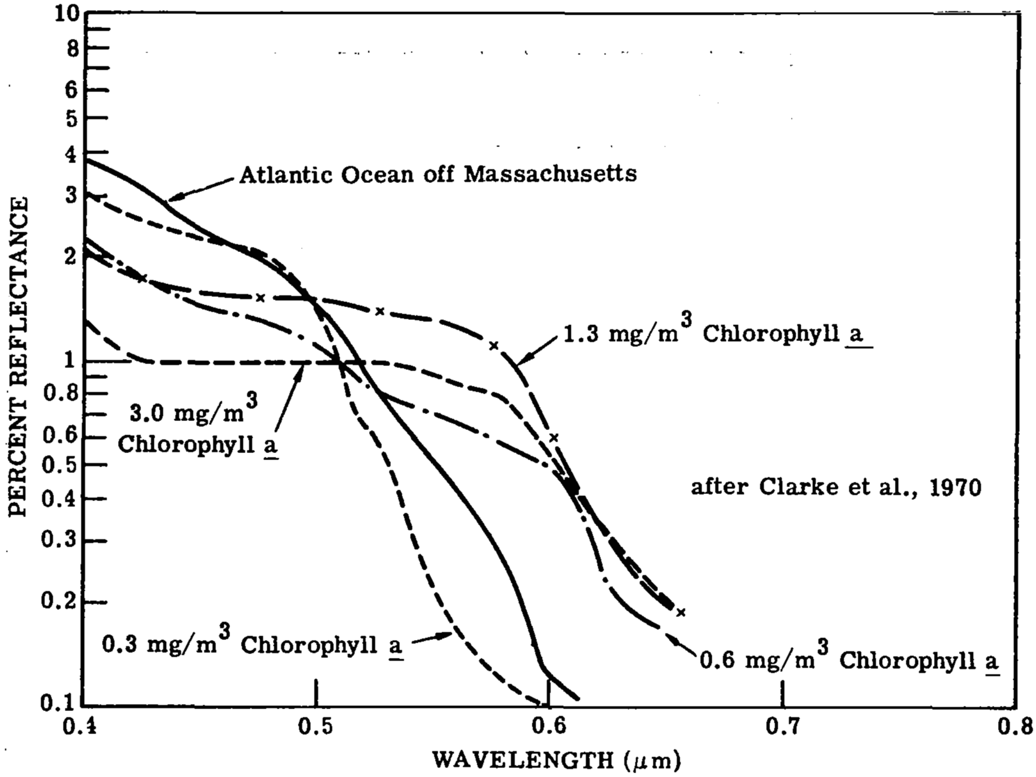

FIGURE 15. LOW CHLOROPHYLL LEVELS - ATLANTIC OCEAN

TABLE 73

CHLOROPHYLL a 0.3 mg/m^3, ATLANTIC, REFLECTANCE

λ (μm)	ρ
0.400	0.030
0.425	0.025
0.450	0.022
0.475	0.021
0.500	0.014
0.515	0.007
0.525	0.006
0.535	0.004
0.550	0.002
0.575	0.001

Sea level data

Source: Clarke, G. L., Ewing, G. C., and Lorenzen, C. J. [33]

Aircraft data, 305 m. altitude, TRW spectrometer (400 nm to 650 nm) with polarizing filter, instrument tilted at Brewster's angle (53° ±).

TABLE 74

CHLOROPHYLL a, 0.3 mg/m^3, ATLANTIC, RADIANCE

SATELLITE ALTITUDE VISIBILITY 15 km

Solar Zenith Angle	Total Radiance (mw cm^{-2} sr^{-1} μm^{-1}) 35°	45°	55°	60°
Wavelength (μm)				
0.400	5.437	4.539	3.920	3.647
0.425	5.428	4.503	3.887	3.616
0.450	5.492	4.527	3.906	3.633
0.475	4.911	4.020	3.460	3.216
0.500	3.942	3.201	2.762	2.574
0.515	3.309	2.668	2.309	2.159
0.525	3.155	2.535	2.195	2.055
0.535	2.897	2.317	2.010	1.885
0.550	2.508	1.993	1.732	1.628
0.575	2.227	1.755	1.524	1.435

TABLE 75

CHLOROPHYLL a, 0.3 mg/m^3, ATLANTIC, RADIANCE

SATELLITE ALTITUDE VISIBILITY 23 km

Solar Zenith Angle	Total Radiance ($mw\ cm^{-2} sr^{-1} \mu m^{-1}$) 35°	45°	55°	60°
Wavelength (μm)				
0.400	5.326	4.518	3.915	3.645
0.425	5.286	4.460	3.862	3.594
0.450	5.318	4.462	3.860	3.590
0.475	4.723	3.938	3.399	3.157
0.500	3.746	3.103	2.685	2.501
0.515	3.098	2.551	2.215	2.072
0.525	2.941	2.414	2.097	1.963
0.535	2.682	2.194	1.909	1.791
0.550	2.301	1.871	1.632	1.534
0.575	2.017	1.626	1.419	1.335

TABLE 76

CHLOROPHYLL a, 0.3 mg/m^3, ATLANTIC, RADIANCE

SATELLITE ALTITUDE VISIBILITY 40 km

Solar Zenith Angle	Total Radiance (mw cm^{-2} sr^{-1} µm^{-1}) 35°	45°	55°	60°
Wavelength (µm)				
0.400	5.227	4.502	3.914	3.645
0.425	5.519	4.425	3.842	3.575
0.450	5.160	4.407	3.821	3.552
0.475	4.552	3.867	3.344	3.104
0.500	3.567	3.015	2.615	2.433
0.515	2.904	2.444	2.129	1.991
0.525	2.743	2.304	2.008	1.879
0.535	2.485	2.080	1.817	1.703
0.550	2.111	1.759	1.540	1.447
0.575	1.823	1.508	1.321	1.243

TABLE 77

CHLOROPHYLL a, 0.3 mg/m^3, ATLANTIC, RADIANCE

SATELLITE ALTITUDE VISIBILITY 60 km

Solar Zenith Angle	Total Radiance ($mw\ cm^{-2} sr^{-1} \mu m^{-1}$) 35°	45°	55°	60°
Wavelength (μm)				
0.400	5.176	4.496	3.914	3.646
0.425	5.094	4.408	3.833	3.566
0.450	5.080	4.379	3.802	3.533
0.475	4.465	3.832	3.317	3.077
0.500	3.475	2.971	2.579	2.399
0.515	2.804	2.390	2.085	1.949
0.525	2.642	2.247	1.962	1.835
0.535	2.383	2.022	1.769	1.658
0.550	2.013	1.702	1.492	1.402
0.575	1.723	1.448	1.270	1.195

TABLE 78

CHLOROPHYLL a, 0.6 mg/m^3, ATLANTIC, REFLECTANCE

λ(μm)	ρ
0.400	0.022
0.425	0.017
0.450	0.014
0.475	0.013
0.500	0.011
0.515	0.009
0.525	0.008
0.550	0.007
0.575	0.006
0.600	0.005
0.625	0.002
0.650	0.002

Sea level data

Source: Clarke, G. L., Ewing, G. C., and Lorenzen, C. J. [33]

Aircraft data, 305 m. altitude, TRW spectrometer (400 nm to 650 nm) with polarizing filter, instrument tilted at Brewster's angle (53° ±)

TABLE 79

CHLOROPHYLL A, 0.6 mg/m^3, ATLANTIC, RADIANCE

SATELLITE ALTITUDE VISIBILITY 15 km

Solar Zenith Angle	Total Radiance ($mw\ cm^{-2} sr^{-1} \mu m^{-1}$) 35°	45°	55°	60°
Wavelength (μm)				
0.400	5.331	4.450	3.852	3.589
0.425	5.283	4.381	3.793	3.536
0.450	5.300	4.365	3.779	3.526
0.475	4.698	3.839	3.318	3.095
0.500	3.861	3.132	2.708	2.528
0.515	3.362	2.713	2.344	2.190
0.525	3.210	2.581	2.232	2.086
0.550	2.641	2.107	1.822	1.705
0.575	2.365	1.872	1.618	1.515
0.600	2.054	1.613	1.395	1.308
0.625	1.726	1.341	1.162	1.094
0.650	1.512	1.165	1.010	0.951

TABLE 80

CHLOROPHYLL a, 0.6 mg/m^3, ATLANTIC, RADIANCE

SATELLITE ALTITUDE VISIBILITY 23 km

Solar Zenith Angle	Total Radiance (mw cm^{-2} sr^{-1} μm^{-1}) 35°	45°	55°	60°
Wavelength (μm)				
0.400	5.205	4.417	3.837	3.579
0.425	5.122	4.322	3.755	3.503
0.450	5.102	4.280	3.717	3.469
0.475	4.484	3.736	3.239	3.021
0.500	3.655	3.026	2.624	2.449
0.515	3.157	2.601	2.255	2.106
0.525	3.001	2.465	2.138	1.998
0.550	2.448	1.997	1.732	1.620
0.575	2.168	1.755	1.522	1.424
0.600	1.865	1.498	1.300	1.218
0.625	1.538	1.223	1.064	1.001
0.650	1.336	1.054	0.916	0.863

TABLE 81

CHLOROPHYLL a, 0.6 mg/m^3, ATLANTIC, RADIANCE

SATELLITE ALTITUDE VISIBILITY 40 km

Solar Zenith Angle	Total Radiance ($mw\ cm^{-2}\ sr^{-1}\ \mu m^{-1}$) 35°	45°	55°	60°
Wavelength (μm)				
0.400	5.091	4.389	3.826	3.571
0.425	4.976	4.271	3.722	3.473
0.450	4.921	4.204	3.662	3.417
0.475	4.289	3.644	3.168	2.954
0.500	3.467	2.931	2.548	2.376
0.515	2.968	2.499	2.173	2.028
0.525	2.810	2.360	2.053	1.917
0.550	2.271	1.896	1.649	1.541
0.575	1.988	1.649	1.433	1.340
0.600	1.692	1.394	1.212	1.134
0.625	1.365	1.115	0.973	0.915
0.650	1.174	0.952	0.830	0.781

TABLE 82

CHLOROPHYLL a, 0.6 mg/m^3, ATLANTIC, RADIANCE

SATELLITE ALTITUDE VISIBILITY 60 km

Solar Zenith Angle	Total Radiance ($mw\ cm^{-2} sr^{-1} \mu m^{-1}$) 35°	45°	55°	60°
Wavelength (μm)				
0.400	5.033	4.376	3.821	3.567
0.425	4.900	4.245	3.705	3.458
0.450	4.828	4.166	3.634	3.391
0.475	4.188	3.597	3.132	2.919
0.500	3.371	2.882	2.508	2.338
0.515	2.871	2.447	2.131	1.988
0.525	2.711	2.306	2.009	1.875
0.550	2.180	1.845	1.606	1.500
0.575	1.895	1.595	1.388	1.296
0.600	1.603	1.340	1.167	1.091
0.625	1.276	1.059	0.926	0.870
0.650	1.091	0.900	0.786	0.739

TABLE 83

CHLOROPHYLL a, 1.3 mg/m^3, ATLANTIC REFLECTANCE

λ(μm)	ρ
0.400	0.021
0.425	0.017
0.450	0.016
0.475	0.015
0.500	0.015
0.525	0.014
0.550	0.013
0.575	0.011
0.600	0.006
0.625	0.003
0.650	0.002

Sea level data

Source: Clarke, G. L., Ewing, G. C., and Lorenzen, C. J. [33]

Aircraft data, 305 m. altitude, TRW spectrometer (400 nm to 650 nm) with polarizing filter, instrument tilted at Brewster's angle (53° ±).

TABLE 84

CHLOROPHYLL a, 1.3 mg/m^3, ATLANTIC, RADIANCE

SATELLITE ALTITUDE VISIBILITY 15 km

Solar Zenith Angle	Total Radiance ($mw\ cm^{-2} sr^{-1} \mu m^{-1}$) 35°	45°	55°	60°
Wavelength (μm)				
0.400	5.318	4.439	3.843	3.582
0.425	5.283	4.381	3.793	3.536
0.450	5.348	4.406	3.811	3.553
0.475	4.751	3.884	3.354	3.125
0.500	3.969	3.224	2.780	2.590
0.525	3.374	2.721	2.342	2.181
0.550	2.800	2.243	1.931	1.798
0.575	2.502	1.989	1.712	1.596
0.600	2.082	1.636	1.413	1.324
0.625	1.753	1.364	1.181	1.110
0.650	1.512	1.165	1.010	0.951

TABLE 85

CHLOROPHYLL a, 1.3 mg/m^3, ATLANTIC, RADIANCE

SATELLITE ALTITUDE VISIBILITY 23 km

Solar Zenith Angle	Total Radiance (mw cm^{-2}sr^{-1}µm^{-1}) 35°	45°	55°	60°
Wavelength (µm)				
0.400	5.190	4.404	3.828	3.571
0.425	5.122	4.322	3.755	3.503
0.450	5.156	4.326	3.753	3.499
0.475	4.544	3.787	3.279	3.055
0.500	3.776	3.128	2.705	2.518
0.525	3.183	2.620	2.261	2.104
0.550	2.624	2.147	1.852	1.723
0.575	2.319	1.885	1.625	1.513
0.600	1.895	1.524	1.320	1.236
0.625	1.567	1.248	1.084	1.018
0.650	1.336	1.054	0.916	0.863

TABLE 86

CHLOROPHYLL a, 1.3 mg/m^3, ATLANTIC, RADIANCE

SATELLITE ALTITUDE VISIBILITY 40 km

Solar Zenith Angle	Total Radiance ($mw\ cm^{-2} sr^{-1} \mu m^{-1}$) 35°	45°	55°	60°
Wavelength (μm)				
0.400	5.074	4.375	3.815	3.562
0.425	4.976	4.271	3.722	3.473
0.450	4.981	4.255	3.702	3.451
0.475	4.355	3.700	3.212	2.991
0.500	3.600	3.043	2.637	2.453
0.525	3.009	2.530	2.188	2.033
0.550	2.463	2.060	1.780	1.653
0.575	2.152	1.790	1.546	1.437
0.600	1.724	1.422	1.235	1.154
0.625	1.397	1.142	0.995	0.934
0.650	1.174	0.952	0.830	0.781

TABLE 87

CHLOROPHYLL a, 1.3 mg/m^3, ATLANTIC, RADIANCE

SATELLITE ALTITUDE VISIBILITY 60 km

Solar Zenith Angle	Total Radiance ($mw\ cm^{-2} sr^{-1} \mu m^{-1}$) 35°	45°	55°	60°
Wavelength (μm)				
0.400	5.015	4.361	3.810	3.557
0.425	4.900	4.245	3.705	3.458
0.450	4.891	4.219	3.676	3.426
0.475	4.257	3.656	3.178	2.959
0.500	3.510	3.000	2.602	2.419
0.525	2.919	2.484	2.150	1.996
0.550	2.381	2.016	1.743	1.618
0.575	2.067	1.742	1.505	1.398
0.600	1.637	1.370	1.190	1.111
0.625	1.309	1.088	0.949	0.890
0.650	1.091	0.900	0.786	0.739

TABLE 88

CHLOROPHYLL a, 3.0 mg/m^3, ATLANTIC, REFLECTANCE

$\lambda(\mu m)$	ρ
0.400	0.013
0.425	0.010
0.450	0.010
0.475	0.010
0.500	0.010
0.525	0.010
0.550	0.009
0.575	0.008
0.600	0.005
0.625	0.003
0.650	0.002

Sea level data

Source: Clarke, G. L., Ewing, G. C., and Lorenzen, C.J. [33]

Aircraft data, 305 m. altitude, TRW spectrometer (400 nm to 650 nm) with polarizing filter, instrument tilted at Brewster's angle (53° $\pm$).

TABLE 89

CHLOROPHYLL a, 3.0 mg/m^3, ATLANTIC, RADIANCE

SATELLITE ALTITUDE VISIBILITY 15 km

Solar Zenith Angle	Total Radiance (mw cm^{-2} sr^{-1} µm^{-1}) 35°	45°	55°	60°
Wavelength (µm)				
0.400	5.212	4.350	3.775	3.525
0.425	5.156	4.275	3.710	3.466
0.450	5.204	4.284	3.716	3.472
0.475	4.618	3.772	3.265	3.050
0.500	3.833	3.109	2.689	2.512
0.525	3.264	2.628	2.269	2.118
0.550	2.694	2.152	1.858	1.736
0.575	2.420	1.919	1.655	1.548
0.600	2.054	1.613	1.395	1.308
0.625	1.753	1.364	1.181	1.110
0.650	1.512	1.165	1.010	0.951

TABLE 90

CHLOROPHYLL a, 3.0 mg/m^3, ATLANTIC, RADIANCE

SATELLITE ALTITUDE VISIBILITY 23 km

Solar Zenith Angle	Total Radiance (mw cm^{-2}sr^{-1}µm^{-1}) 35°	45°	55°	60°
Wavelength (µm)				
0.400	5.070	4.303	3.750	3.505
0.425	4.979	4.202	3.661	3.423
0.450	4.994	4.189	3.646	3.408
0.475	4.395	3.661	3.180	2.970
0.500	3.625	3.000	2.604	2.431
0.525	3.062	2.517	2.179	2.034
0.550	2.507	2.047	1.772	1.654
0.575	2.229	1.807	1.563	1.460
0.600	1.865	1.498	1.300	1.218
0.625	1.567	1.248	1.084	1.018
0.650	1.336	1.054	0.916	0.863

TABLE 91

CHLOROPHYLL a, 3.0 mg/m^3, ATLANTIC, RADIANCE

SATELLITE ALTITUDE VISIBILITY 40 km

Solar Zenith Angle	Total Radiance ($mw\ cm^{-2} sr^{-1} \mu m^{-1}$) 35°	45°	55°	60°
Wavelength (μm)				
0.400	4.939	4.261	3.728	3.488
0.425	4.816	4.136	3.617	3.384
0.450	4.801	4.103	3.583	3.350
0.475	4.190	3.560	3.102	2.897
0.500	3.434	2.902	2.525	2.357
0.525	2.876	2.417	2.098	1.956
0.550	2.335	1.951	1.693	1.578
0.575	2.054	1.706	1.478	1.379
0.600	1.692	1.394	1.212	1.134
0.625	1.397	1.142	0.995	0.934
0.650	1.174	0.952	0.830	0.781

TABLE 92

CHLOROPHYLL a, 3.0 mg/m^3, ATLANTIC, RADIANCE

SATELLITE ALTITUDE VISIBILITY 60 km

Solar Zenith Angle	Total Radiance ($mw\ cm^{-2} sr^{-1} \mu m^{-1}$) 35°	45°	55°	60°
Wavelength (μm)				
0.400	4.871	4.240	3.717	3.479
0.425	4.731	4.103	3.594	3.364
0.450	4.702	4.059	3.550	3.320
0.475	4.084	3.509	3.062	2.860
0.500	3.336	2.852	2.485	2.318
0.525	2.780	2.365	2.056	1.916
0.550	2.247	1.902	1.652	1.539
0.575	1.964	1.653	1.435	1.337
0.600	1.603	1.340	1.167	1.091
0.625	1.309	1.088	0.949	0.890
0.650	1.091	0.900	0.786	0.739

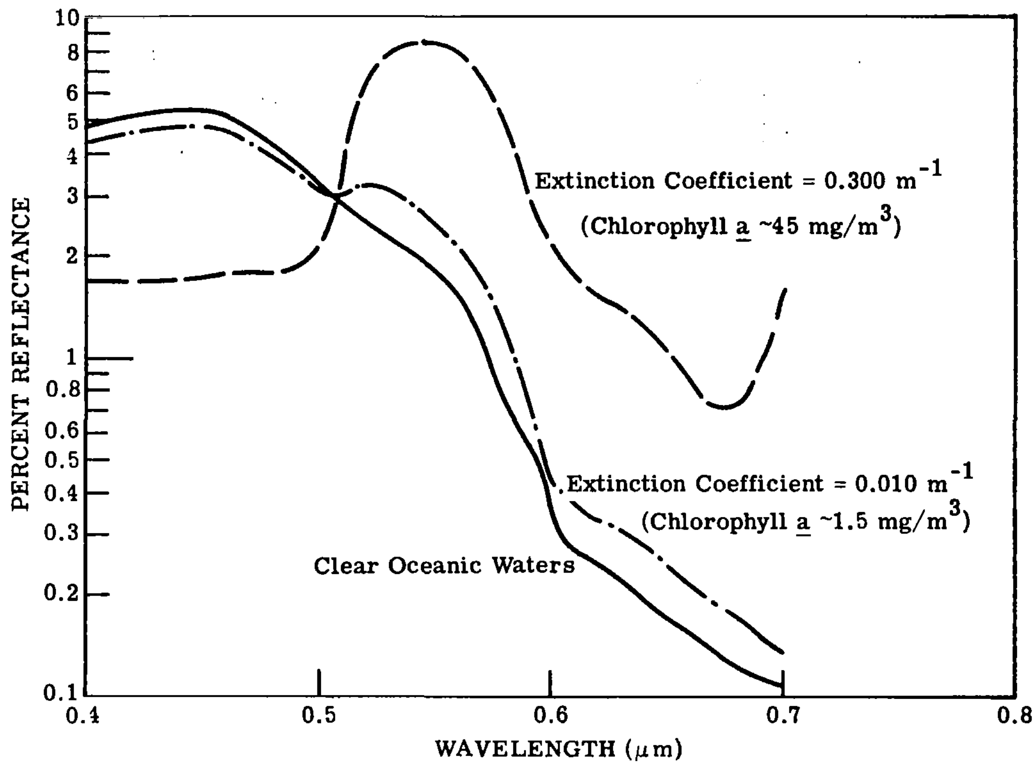

FIGURE 16. PHYTOPLANKTON. Calculated Data - Low Concentration of Non-Chlorophyll Particulates in Base Water (after Suits, 1973).

TABLE 93

PHYTOPLANKTON-CHLOROPHYLL, LOW TURBIDITY, REFLECTANCE
(Low conc. in chlor. bearing particulates)
Extinction Coef. = 0.300 m^{-1}

λ (µm)	ρ
0.400	0.017
0.425	0.017
0.450	0.018
0.475	0.018
0.500	0.022
0.508	0.029
0.525	0.070
0.550	0.080
0.575	0.055
0.600	0.022
0.675	0.007
0.700	0.018

Sea level data

Source: Suits, G. [unpublished data]. Calculated spectral reflectance (0.4µm-0.7µm) of ocean water containing various concentrations of "yellow substance", phytoplankton, and sand.

TABLE 94
PHYTOPLANKTON-CHLOROPHYLL, LOW TURBIDITY, RADIANCE
EXTINCTION COEF. = 0.300 m^{-1}
SATELLITE ALTITUDE VISIBILITY 15 km

Solar Zenith Angle	Total Radiance ($mw\ cm^{-2} sr^{-1} \mu m^{-1}$) 35°	45°	55°	60°
Wavelength (μm)				
0.400	5.265	4.395	3.809	3.553
0.425	5.283	4.381	3.793	3.536
0.450	5.396	4.446	3.843	3.579
0.475	4.831	3.952	3.407	3.171
0.500	4.158	3.385	2.908	2.699
0.508	4.142	3.371	2.881	2.663
0.525	4.901	4.022	3.375	3.067
0.550	4.580	3.762	3.140	2.837
0.575	3.710	3.022	2.536	2.305
0.600	2.521	2.012	1.714	1.583
0.675	1.474	1.141	0.981	0.918
0.700	1.585	1.244	1.056	0.975

TABLE 95

PHYTOPLANKTON-CHLOROPHYLL, LOW TURBIDITY, RADIANCE
EXTINCTION COEF. = 0.300 m^{-1}
SATELLITE ALTITUDE VISIBILITY 23 km

Solar Zenith Angle	Total Radiance ($mw\ cm^{-2} sr^{-1} \mu m^{-1}$) 35°	45°	55°	60°
Wavelength (μm)				
0.400	5.130	4.353	3.789	3.538
0.425	5.122	4.322	3.755	3.503
0.450	5.210	4.371	3.789	3.530
0.475	4.633	3.863	3.339	3.106
0.500	3.987	3.308	2.847	2.640
0.508	3.989	3.308	2.830	2.612
0.525	4.876	4.064	3.409	3.088
0.550	4.590	3.826	3.189	2.873
0.575	3.649	3.022	2.534	2.296
0.600	2.377	1.937	1.650	1.520
0.675	1.317	1.044	0.899	0.839
0.700	1.462	1.173	0.995	0.915

TABLE 96

PHYTOPLANKTON-CHLOROPHYLL, LOW TURBIDITY, RADIANCE
EXTINCTION COEF. = 0.300 m^{-1}

SATELLITE ALTITUDE VISIBILITY 40 km

Solar Zenith Angle	Total Radiance ($mw \cdot cm^{-2} sr^{-1} \mu m^{-1}$) 35°	45°	55°	60°
Wavelength (μm)				
0.400	5.007	4.318	3.771	3.525
0.425	4.976	4.271	3.722	3.473
0.450	5.040	4.305	3.742	3.485
0.475	4.453	3.783	3.278	3.048
0.500	3.832	3.241	2.794	2.587
0.508	3.851	3.253	2.787	2.568
0.525	4.864	4.112	3.446	3.114
0.550	4.610	3.894	3.243	2.912
0.575	3.600	3.029	2.536	2.291
0.600	2.247	1.870	1.593	1.463
0.675	1.174	0.954	0.823	0.766
0.700	1.352	1.109	0.939	0.860

TABLE 97
PHYTOPLANKTON-CHLOROPHYLL, LOW TURBIDITY, RADIANCE
EXTINCTION COEF. = 0.300 m^{-1}
SATELLITE ALTITUDE VISIBILITY 60 km

Solar Zenith Angle	Total Radiance ($mw\ cm^{-2} sr^{-1} \mu m^{-1}$) 35°	45°	55°	60°
Wavelength (μm)				
0.400	4.943	4.300	3.763	3.518
0.425	4.900	4.245	3.705	3.458
0.450	4.954	4.273	3.718	3.462
0.475	4.361	3.744	3.247	3.018
0.500	3.753	3.208	2.767	2.560
0.508	3.782	3.227	2.765	2.545
0.525	4.861	4.141	3.469	3.129
0.550	4.624	3.934	3.273	2.934
0.575	3.577	3.035	2.540	2.289
0.600	2.182	1.837	1.565	1.434
0.675	1.101	0.909	0.784	0.729
0.700	1.295	1.076	0.911	0.832

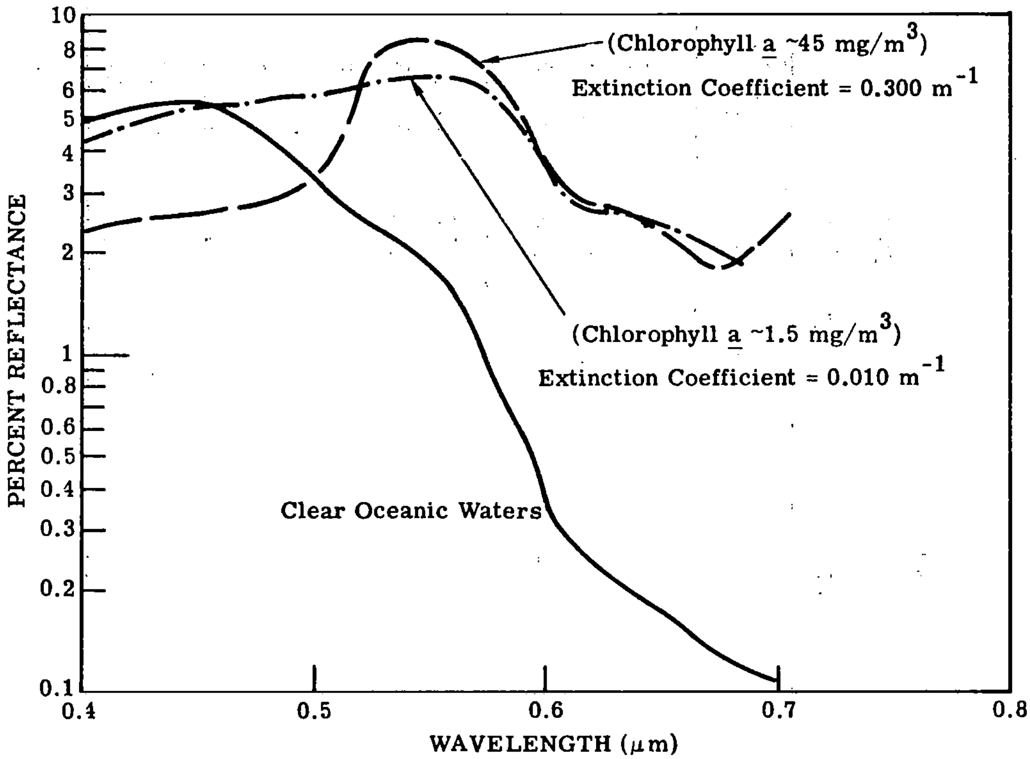

FIGURE 17. PHYTOPLANKTON. Calculated Data - High Turbidity. High Concentration of Non-Chlorophyll Bearing Particulates (after Suits, 1973).

TABLE 98

PHYTOPLANKTON-CHLOROPHYLL, HIGH TURBIDITY, REFLECTANCE
(High con. non-chlor. bearing particulates)
EXTINCTION COEF. = 0.300 m^{-1}

λ (μm)	ρ
0.400	0.023
0.425	0.025
0.450	0.025
0.475	0.027
0.500	0.033
0.520	0.060
0.550	0.080
0.575	0.065
0.600	0.033
0.650	0.022
0.675	0.017
0.700	0.026

Sea level data

Source: Suits, G. [unpublished data]

Calculated spectral reflectance (0.4μm-0.7μm) of ocean water containing various concentrations of "yellow substance", phytoplankton, and sand.

TABLE 99

PHYTOPLANKTON-CHLOROPHYLL, HIGH TURBIDITY, RADIANCE

EXTINCTION COEF. = 0.300 m^{-1}

SATELLITE ALTITUDE VISIBILITY 15 km

Solar Zenith Angle	Total Radiance ($mw\ cm^{-2} sr^{-1} \mu m^{-1}$) 35°	45°	55°	60°
Wavelength (μm)				
0.400	5.344	4.461	3.860	3.596
0.425	5.428	4.503	3.887	3.616
0.450	5.563	4.588	3.954	3.674
0.475	5.071	4.155	3.567	3.307
0.500	4.456	3.638	3.108	2.870
0.520	4.644	3.804	3.205	2.923
0.550	4.580	3.762	3.140	2.837
0.575	3.985	3.257	2.723	2.466
0.600	2.823	2.270	1.920	1.761
0.650	2.033	1.612	1.368	1.261
0.675	1.727	1.358	1.155	1.069
0.700	1.780	1.412	1.191	1.092

TABLE 100
PHYTOPLANKTON-CHLOROPHYLL, HIGH TURBIDITY, RADIANCE
EXTINCTION COEF. = 0.300 m^{-1}
SATELLITE ALTITUDE VISIBILITY 23 km

Solar Zenith Angle	Total Radiance (mw $cm^{-2}sr^{-1}\mu m^{-1}$) 35°	45°	55°	60°
Wavelength (μm)				
0.400	5.221	4.429	3.847	3.587
0.425	5.286	4.460	3.862	3.594
0.450	5.398	4.531	3.914	3.636
0.475	4.901	4.090	3.518	3.259
0.500	4.318	3.590	3.071	2.831
0.520	4.589	3.821	3.218	2.927
0.550	4.590	3.826	3.189	2.873
0.575	3.952	3.281	2.740	2.474
0.600	2.708	2.220	1.877	1.716
0.650	1.905	1.542	1.308	1.202
0.675	1.593	1.280	1.089	1.004
0.700	1.675	1.355	1.142	1.042

TABLE 101

PHYTOPLANKTON-CHLOROPHYLL, HIGH TURBIDITY, RADIANCE
EXTINCTION COEF. = 0.300 m^{-1}

SATELLITE ALTITUDE VISIBILITY 40 km

Solar Zenith Angle	Total Radiance ($mw\ cm^{-2} sr^{-1} \mu m^{-1}$) 35°	45°	55°	60°
Wavelength (μm)				
0.400	5.108	4.403	3.837	3.580
0.425	5.159	4.425	3.842	3.575
0.450	5.250	4.483	3.881	3.603
0.475	4.749	4.035	3.476	3.217
0.500	4.197	3.551	3.040	2.797
0.520	4.548	3.844	3.236	2.935
0.550	4.610	3.894	3.243	2.912
0.575	3.929	3.311	2.762	2.485
0.600	2.607	2.178	1.840	1.676
0.650	1.790	1.480	1.255	1.148
0.675	1.472	1.210	1.028	0.944
0.700	1.580	1.305	1.098	0.997

TABLE 102
PHYTOPLANKTON-CHLOROPHYLL, HIGH TURBIDITY, RADIANCE
EXTINCTION COEF. = 0.300 m^{-1}
SATELLITE ALTITUDE VISIBILITY 60 km

Solar Zenith Angle	Total Radiance (mw $cm^{-2}sr^{-1}\mu m^{-1}$) 35°	45°	55°	60°
Wavelength (μm)				
0.400	5.051	4.391	3.833	3.577
0.425	5.094	4.408	3.833	3.566
0.450	5.174	4.459	3.864	3.587
0.475	4.672	4.008	3.456	3.196
0.500	4.136	3.533	3.025	2.781
0.520	4.529	3.859	3.247	2.942
0.550	4.624	3.934	3.273	2.934
0.575	3.921	3.329	2.775	2.492
0.600	2.556	2.158	1.822	1.657
0.650	1.731	1.449	1.227	1.121
0.675	1.410	1.174	0.998	0.914
0.700	1.532	1.280	1.075	0.975

3.3 SUSPENDED SOLIDS

Both pure and polluted waters will absorb and scatter light. In the general case, scattering and absorption is caused by water molecules and by any suspended particulate materials present. The relative importance of scattering and absorption as mechanisms of attenuation is wavelength dependent.

The introduction of particulates (non-chlorophyll) into a body of water will scatter light increasingly (relative to pure water) with increased wavelength in the visible portion of the spectrum. This is particularly true in the red region of the spectrum. Beyond 0.7 μm the high attenuation coefficient of water limits observations to essentially the water surface. In the region 0.4μm to 0.5μm, increases in the concentration of suspended solids (non-chlorophyll bearing) have little effect on the reflectance spectrum. On the other hand, "gelbstoff" (yellow substance) will absorb in the blue region of the spectrum and have virtually no effect in the red. For these reasons, suspended solids measurements are generally made using a red spectral band.

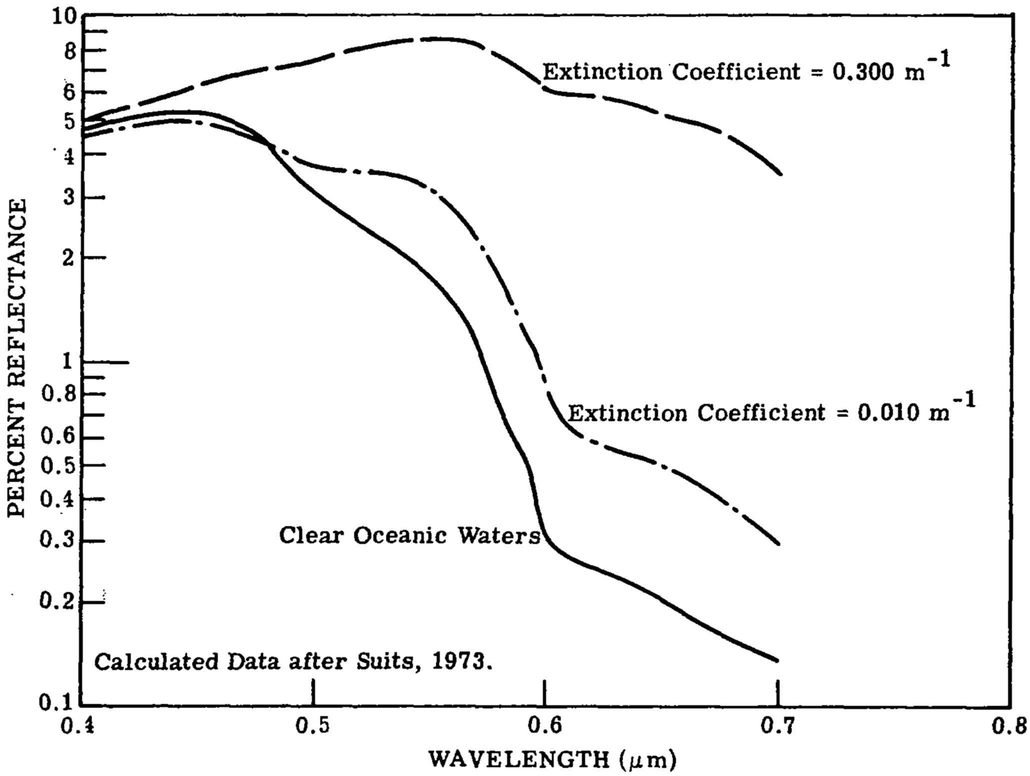

FIGURE 18. SUSPENDED SOLIDS. Sand Suspension - Low Concentration Yellow Substance.

TABLE 103

SUSPENDED SOLIDS, LOW YELLOW SUBSTANCE,
REFLECTANCE

λ (µm)	ρ
0.400	0.050
0.425	0.055
0.450	0.060
0.475	0.067
0.500	0.072
0.525	0.080
0.550	0.083
0.575	0.076
0.600	0.060
0.625	0.055
0.650	0.050
0.675	0.045
0.700	0.035
EXTINCTION COEF. = $0.300 m^{-1}$	

Sea level data

Source: Suits, G. [unpublished data]
Calculated spectral reflectance (0.4µm-0.7µm) of ocean water.

TABLE 104

SUSPENDED SOLIDS, LOW YELLOW SUBSTANCE, RADIANCE

EXTINCTION COEF. = 0.300 m^{-1}

SATELLITE ALTITUDE VISIBILITY 15 km

Solar Zenith Angle	Total Radiance ($mw\ cm^{-2} sr^{-1} \mu m^{-1}$) 35°	45°	55°	60°
Wavelength (μm)				
0.400	5.702	4.760	4.091	3.790
0.425	5.971	4.960	4.243	3.917
0.450	6.402	5.296	4.508	4.145
0.475	6.135	5.057	4.277	3.912
0.500	5.512	4.535	3.818	3.477
0.525	5.174	4.254	3.560	3.225
0.550	4.660	3.830	3.194	2.884
0.575	4.287	3.515	2.929	2.644
0.600	3.563	2.904	2.427	2.198
0.625	3.146	2.557	2.136	1.934
0.650	2.763	2.237	1.869	1.694
0.675	2.435	1.966	1.643	1.490
0.700	2.000	1.600	1.342	1.223

TABLE 105

SUSPENDED SOLIDS, LOW YELLOW SUBSTANCE, RADIANCE

EXTINCTION COEF. = 0.300 m^{-1}

SATELLITE ALTITUDE VISIBILITY 23 km

Solar Zenith Angle	Total Radiance ($mw\ cm^{-2} sr^{-1} \mu m^{-1}$) 35°	45°	55°	60°
Wavelength (μm)				
0.400	5.628	4.771	4.111	3.809
0.425	5.901	4.978	4.266	3.935
0.450	6.342	5.328	4.539	4.167
0.475	6.092	5.100	4.315	3.938
0.500	5.494	4.590	3.862	3.508
0.525	5.179	4.322	3.613	3.264
0.550	4.678	3.901	3.249	2.925
0.575	4.284	3.565	2.967	2.669
0.600	3.521	2.916	2.434	2.197
0.625	3.092	2.555	2.131	1.923
0.650	2.702	2.225	1.857	1.676
0.675	2.365	1.943	1.621	1.464
0.700	1.914	1.560	1.306	1.185

TABLE 106

SUSPENDED SOLIDS, LOW YELLOW SUBSTANCE, RADIANCE

EXTINCTION COEF. = 0.300 m^{-1}

SATELLITE ALTITUDE VISIBILITY 40 km

Solar Zenith Angle	Total Radiance ($mw\ cm^{-2} sr^{-1} \mu m^{-1}$) 35°	45°	55°	60°
Wavelength (μm)				
0.400	5.566	4.786	4.134	3.829
0.425	5.845	5.003	4.293	3.956
0.450	6.297	5.368	4.576	4.194
0.475	6.065	5.151	4.357	3.969
0.500	5.490	4.652	3.912	3.544
0.525	5.195	4.395	3.671	3.307
0.550	4.706	3.977	3.308	2.968
0.575	4.291	3.620	3.009	2.698
0.600	3.489	2.934	2.446	2.199
0.625	3.048	2.558	2.131	1.915
0.650	2.651	2.219	1.848	1.662
0.675	2.305	1.925	1.604	1.442
0.700	1.838	1.526	1.276	1.152

TABLE 107

SUSPENDED SOLIDS, LOW YELLOW SUBSTANCE, RADIANCE

EXTINCTION COEF. = 0.300 m^{-1}

SATELLITE ALTITUDE **VISIBILITY** 60 km

Solar Zenith Angle	Total Radiance ($mw\ cm^{-2} sr^{-1} \mu m^{-1}$) 35°	45°	55°	60°
Wavelength (μm)				
0.400	5.535	4.797	4.147	3.841
0.425	5.818	5.019	4.309	3.969
0.450	6.277	5.393	4.597	4.210
0.475	6.055	5.182	4.383	3.987
0.500	5.492	4.688	3.940	3.565
0.525	5.208	4.437	3.704	3.331
0.550	4.724	4.019	3.342	2.993
0.575	4.298	3.652	3.033	2.715
0.600	3.476	2.946	2.453	2.202
0.625	3.028	2.562	2.132	1.913
0.650	2.626	2.217	1.845	1.655
0.675	2.275	1.918	1.596	1.432
0.700	1.800	1.510	1.260	1.135

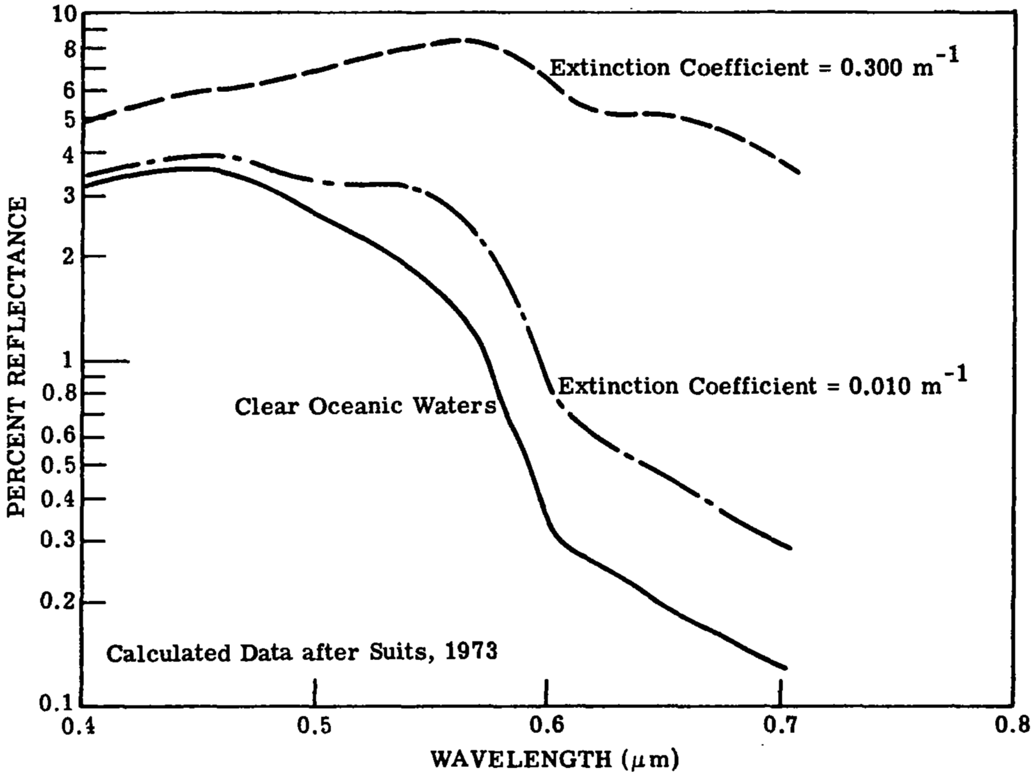

FIGURE 19. SUSPENDED SOLIDS. Sand Suspension - Medium Conc. Yellow Substance.

TABLE 108

SUSPENDED SOLIDS, MED. YELLOW SUBSTANCE, REFLECTANCE

λ (µm)	ρ
0.400	0.048
0.425	0.054
0.450	0.060
0.475	0.062
0.500	0.067
0.525	0.072
0.550	0.078
0.575	0.078
0.600	0.060
0.625	0.052
0.650	0.050
0.675	0.045
0.700	0.035

EXTINCTION COEF. = 0.300 m^{-1}

Sea level data

Source: Suits, G. [unpublished data]
Calculated spectral reflectance (0.4µm-0.7µm) of ocean water.

TABLE 109
SUSPENDED SOLIDS, MED. YELLOW SUBSTANCE, RADIANCE
EXTINCTION COEF. = 0.300 m^{-1}
SATELLITE ALTITUDE VISIBILITY 15 km

Solar Zenith Angle	Total Radiance ($mw\ cm^{-2} sr^{-1} \mu m^{-1}$) 35°	45°	55°	60°
Wavelength (μm)				
0.400	5.675	4.738	4.074	3.776
0.425	5.953	4.945	4.231	3.907
0.450	6.402	5.296	4.508	4.145
0.475	6.002	4.945	4.189	3.837
0.500	5.376	4.420	3.727	3.399
0.525	4.956	4.068	3.412	3.098
0.550	4.527	3.717	3.104	2.806
0.575	4.342	4.562	2.966	2.676
0.600	3.563	2.904	2.427	2.198
0.625	3.066	2.488	2.081	1.887
0.650	2.763	2.237	1.869	1.694
0.675	2.435	1.966	1.643	1.490
0.700	2.000	1.600	1.342	1.223

TABLE 110

SUSPENDED SOLIDS, MED. YELLOW SUBSTANCE, RADIANCE

EXTINCTION COEF. = 0.300 m^{-1}

SATELLITE ALTITUDE VISIBILITY 23 km

Solar Zenith Angle	Total Radiance ($mw\ cm^{-2} sr^{-1} \mu m^{-1}$) 35°	45°	55°	60°
Wavelength (μm)				
0.400	5.598	4.745	4.091	3.792
0.425	5.881	4.961	4.252	3.923
0.450	6.342	5.328	4.539	4.167
0.475	5.943	4.974	4.215	3.853
0.500	5.343	4.462	3.761	3.422
0.525	4.937	4.116	3.449	3.123
0.550	4.531	3.776	3.150	2.839
0.575	4.345	3.617	3.009	2.705
0.600	3.521	2.916	2.434	2.197
0.625	3.004	2.479	2.071	1.871
0.650	2.702	2.225	1.857	1.676
0.675	2.365	1.943	1.621	1.464
0.700	1.914	1.560	1.306	1.185

TABLE 111

SUSPENDED SOLIDS, MED. YELLOW SUBSTANCE, RADIANCE
EXTINCTION COEF. = 0.300 m^{-1}
SATELLITE ALTITUDE VISIBILITY 40 km

Solar Zenith Angle	Total Radiance ($mw\ cm^{-2} sr^{-1} \mu m^{-1}$) 35°	45°	55°	60°
Wavelength (μm)				
0.400	5.532	4.758	4.112	3.811
0.425	5.822	4.984	4.278	3.943
0.450	6.297	5.368	4.576	4.194
0.475	5.900	5.012	4.247	3.875
0.500	5.324	4.511	3.800	3.448
0.525	4.930	4.169	3.491	3.152
0.550	4.546	3.840	3.199	2.874
0.575	4.357	3.677	3.054	2.737
0.600	3.489	2.934	2.446	2.199
0.625	2.953	2.476	2.065	1.859
0.650	2.651	2.219	1.848	1.662
0.675	2.305	1.925	1.604	1.442
0.700	1.838	1.526	1.276	1.152

TABLE 112

SUSPENDED SOLIDS, MED. YELLOW SUBSTANCE, RADIANCE

EXTINCTION COEF. = 0.300 m^{-1}

SATELLITE ALTITUDE VISIBILITY 60 km

Solar Zenith Angle	Total Radiance ($mw\ cm^{-2} sr^{-1} \mu m^{-1}$) 35°	45°	55°	60°
Wavelength (μm)				
0.400	5.499	4.767	4.124	3.822
0.425	5.794	4.999	4.293	3.955
0.450	6.277	5.393	4.597	4.210
0.475	5.882	5.035	4.267	3.888
0.500	5.318	4.540	3.823	3.464
0.525	4.931	4.200	3.516	3.169
0.550	4.557	3.876	3.227	2.895
0.575	4.367	3.711	3.080	2.756
0.600	3.476	2.946	2.453	2.202
0.625	2.929	2.477	2.064	1.854
0.650	2.626	2.217	1.845	1.655
0.675	2.275	1.918	1.596	1.432
0.700	1.800	1.510	1.260	1.135

TABLE 113

SUSPENDED SOLIDS, ERTS-1 DATA, REFLECTANCE

ERTS-1 BAND (μm)	ρ
20 MG/L	SUSPENDED SOLIDS
0.5-0.6	0.126
0.6-0.7	0.065
0.7-0.8	0.025
0.8-1.1	0.004
25 MG/L	SUSPENDED SOLIDS
0.5-0.6	0.131
0.6-0.7	0.070
0.7-0.8	0.034
0.8-1.1	0.016
40 MG/L	SUSPENDED SOLIDS
0.5-0.6	0.146
0.6-0.7	0.088
0.7-0.8	0.052
0.8-1.1	0.024
70 MG/L	SUSPENDED SOLIDS
0.5-0.6	0.171
0.6-0.7	0.114
0.7-0.8	0.063
0.8-1.1	0.028

Source: Klemas, V. et al. [44]

Delaware Bay, ERTS-1 data (1349-15134), radiance data measured suspended solids concentrations.

TABLE 114

SUSPENDED SOLIDS, 20 mg/1, RADIANCE
SATELLITE ALTITUDE

Solar Zenith Angle / Wavelength (μm)*	Total Radiance (mw $cm^{-2}sr^{-1}\mu m^{-1}$) 35°	45°	55°	60°
	VISIBILITY 15 km			
0.550	5.802	4.805	3.970	3.551
0.650	3.154	2.572	2.138	1.926
0.750	1.484	1.173	0.987	0.904
0.950	0.533	0.399	0.343	0.323
	VISIBILITY 23 km			
0.550	5.940	4.979	4.108	3.663
0.650	3.129	2.591	2.150	1.930
0.750	1.388	1.119	0.941	0.857
0.950	0.445	0.339	0.291	0.274
	VISIBILITY 40 km			
0.550	6.083	5.154	4.247	3.776
0.650	3.112	2.615	2.166	1.937
0.750	1.302	1.072	0.899	0.815
0.950	0.365	0.284	0.244	0.228
	VISIBILITY 60 km			
0.550	6.164	5.250	4.323	3.838
0.650	3.106	2.629	2.176	1.942
0.750	1.259	1.048	0.878	0.794
0.950	0.324	0.256	0.220	0.205

*Mid-wavelength ERTS-1 Band

TABLE 115

SUSPENDED SOLIDS, 25 mg/1, RADIANCE
SATELLITE ALTITUDE

Solar Zenith Angle Wavelength (μm)*	Total Radiance ($mw\ cm^{-2}\ sr^{-1}\ \mu m^{-1}$) 35°	45°	55°	60°
	VISIBILITY 15 km			
0.550	5.935	4.918	4.060	3.628
0.650	3.284	2.684	2.227	2.003
0.750	1.687	1.347	1.127	1.026
0.950	0.725	0.564	0.476	0.439
	VISIBILITY 23 km			
0.550	6.087	5.104	4.208	3.749
0.650	3.271	2.713	2.248	2.014
0.750	1.608	1.308	1.093	0.989
0.950	0.652	0.517	0.435	0.399
	VISIBILITY 40 km			
0.550	6.244	5.291	4.356	3.870
0.650	3.266	2.747	2.272	2.028
0.750	1.539	1.275	1.063	0.957
0.950	0.586	0.475	0.398	0.362
	VISIBILITY 60 km			
0.550	6.331	5.393	4.437	3.937
0.650	3.266	2.766	2.286	2.037
0.750	1.504	1.259	1.048	0.941
0.950	0.553	0.453	0.379	0.344

*Mid-wavelength ERTS-1 Band

TABLE 116

SUSPENDED SOLIDS, 40 mg/1, RADIANCE
SATELLITE ALTITUDE

Solar Zenith Angle Wavelength (μm)*	Total Radiance (mw cm^{-2} sr^{-1} μm^{-1}) 35°	45°	55°	60°
	VISIBILITY 15 km			
0.550	6.334	5.259	4.331	3.861
0.650	3.753	3.086	2.550	2.282
0.750	2.092	1.695	1.407	1.268
0.950	0.853	0.674	0.565	0.516
	VISIBILITY 23 km			
0.550	6.527	5.480	4.507	4.006
0.650	3.783	3.153	2.601	2.319
0.750	2.048	1.686	1.397	1.253
0.950	0.790	0.636	0.531	0.482
	VISIBILITY 40 km			
0.550	6.724	5.701	4.684	4.152
0.650	3.820	3.222	2.654	2.359
0.750	2.011	1.682	1.390	1.241
0.950	0.734	0.602	0.501	0.452
	VISIBILITY 60 km			
0.550	6.833	5.822	4.780	4.232
0.650	3.842	3.261	2.683	2.381
0.750	1.994	1.680	1.388	1.236
0.950	0.705	0.585	0.486	0.436

*Mid-wavelength, ERTS-1 Band

TABLE 117

SUSPENDED SOLIDS, 70 mg/1, RADIANCE
SATELLITE ALTITUDE

Solar Zenith Angle Wavelength (μm)*	Total Radiance (mw cm^{-2} sr^{-1} μm^{-1}) 35°	45°	55°	60°
	VISIBILITY 15 km			
0.550	6.998	5.825	4.782	4.248
0.650	4.430	3.667	3.015	2.684
0.750	2.340	1.908	1.579	1.416
0.950	0.917	0.730	0.610	0.554
	VISIBILITY 23 km			
0.550	7.260	6.107	5.007	4.436
0.650	4.523	3.787	3.110	2.760
0.750	2.316	1.917	1.583	1.414
0.950	0.859	0.696	0.579	0.524
	VISIBILITY 40 km			
0.550	7.525	6.386	5.230	4.622
0.650	4.619	3.908	3.205	2.835
0.750	2.300	1.930	1.591	1.415
0.950	0.807	0.666	0.552	0.496
	VISIBILITY 60 km			
0.550	7.670	6.538	5.351	4.723
0.650	4.673	3.974	3.257	2.877
0.750	2.293	1.938	1.595	1.416
0.950	0.782	0.651	0.539	0.482

*Mid-Wavelength, ERTS-1 Band

3.4 OIL

The reflectance of oil on water is made up of two types of components: specular and diffuse. Because the index of oil refraction is higher than that of water, the specular reflectance of oil exceeds that of water. The reverse is true in terms of the diffuse component. Because of multiple scattering in water, the diffuse reflectance of natural waters exceeds that of an oil slick. The net result is that in the near UV, the visible regions of the spectrum, an oil slick may appear lighter or darker than water, depending on the relative contribution of these two components. The radiance differences between an oil slick and water, may be written as follows [45]:

$$\Delta L = (\rho_0^s - \rho_w^s)\, L^{sky} + (\rho_0^d - \rho_w^d)\, \frac{E^{total}}{\pi} \tag{62}$$

where ΔL = radiance difference

ρ_0^s = specular reflectance, oil

ρ_w^s = specular reflectance, water

L^{sky} = radiance of the sky at the specular angle

ρ_0^d = diffuse reflectance, oil

ρ_w^d = diffuse reflectance, water

E^{total} = irradiance onto the surface (sun plus sky)

Since the specular reflectance of oil is greater than water, the term $(\rho_0^s - \rho_w^s)$ will always be positive. Furthermore, in the near UV and the visible ranges, the diffuse reflectance of natural water exceeds that of an oil slick, making the term $(\rho_0^d - \rho_w^d)$ negative. The observed radiance difference, both magnitude and sign, will depend on oil type, thickness, meteorological conditions, water quality, and wavelength of operation. Water quality can have a great influence on the relative radiance and, hence the appearance relative to water.

Presented in this section is data collected during a controlled oil spill investigation off the coast of Southern California. Thickness of the oil is undefined except in general terms, thin or thick. Thin, appears to refer to an oil film less than 10μ in thickness.

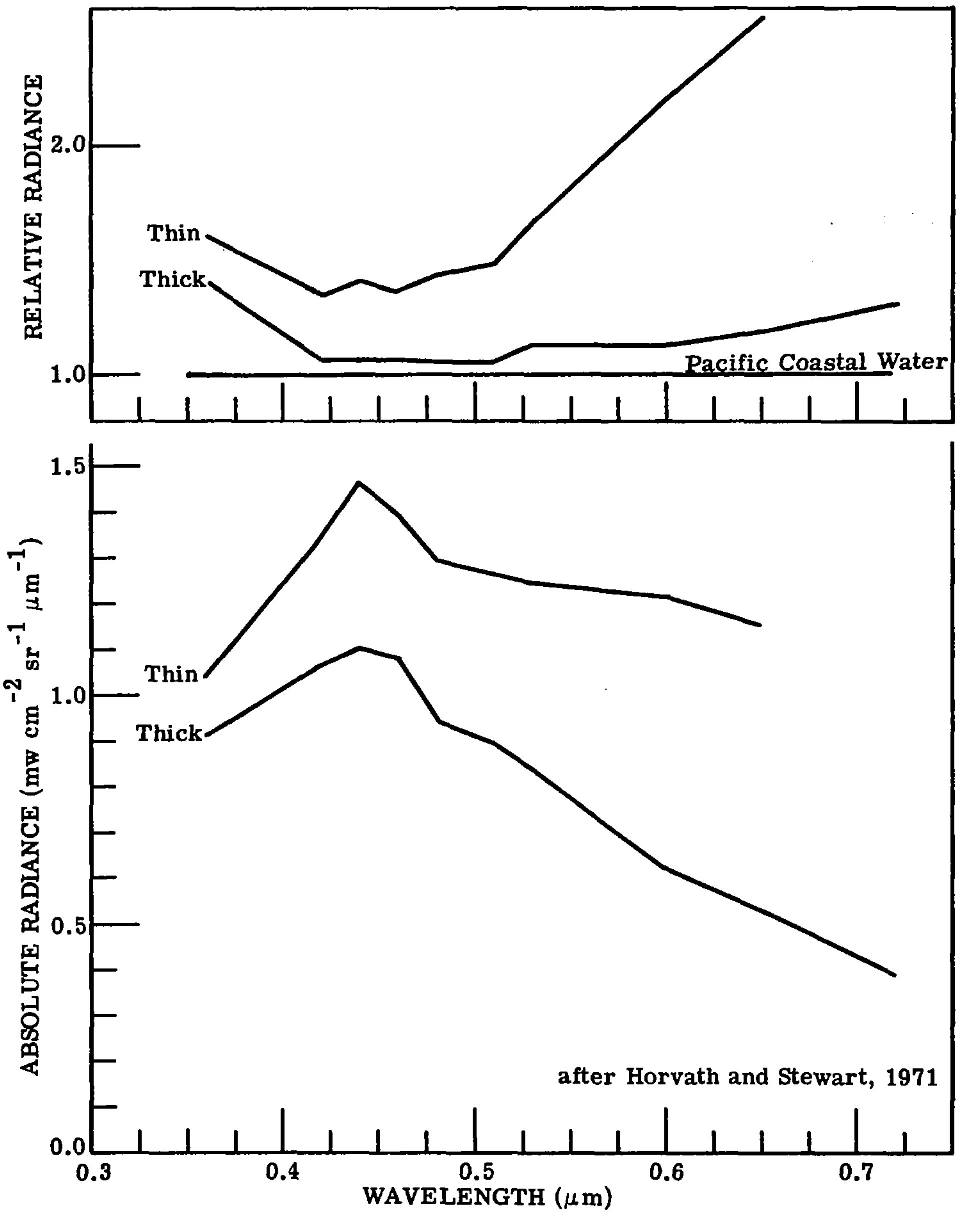

FIGURE 20. 9.7° API FUEL OIL

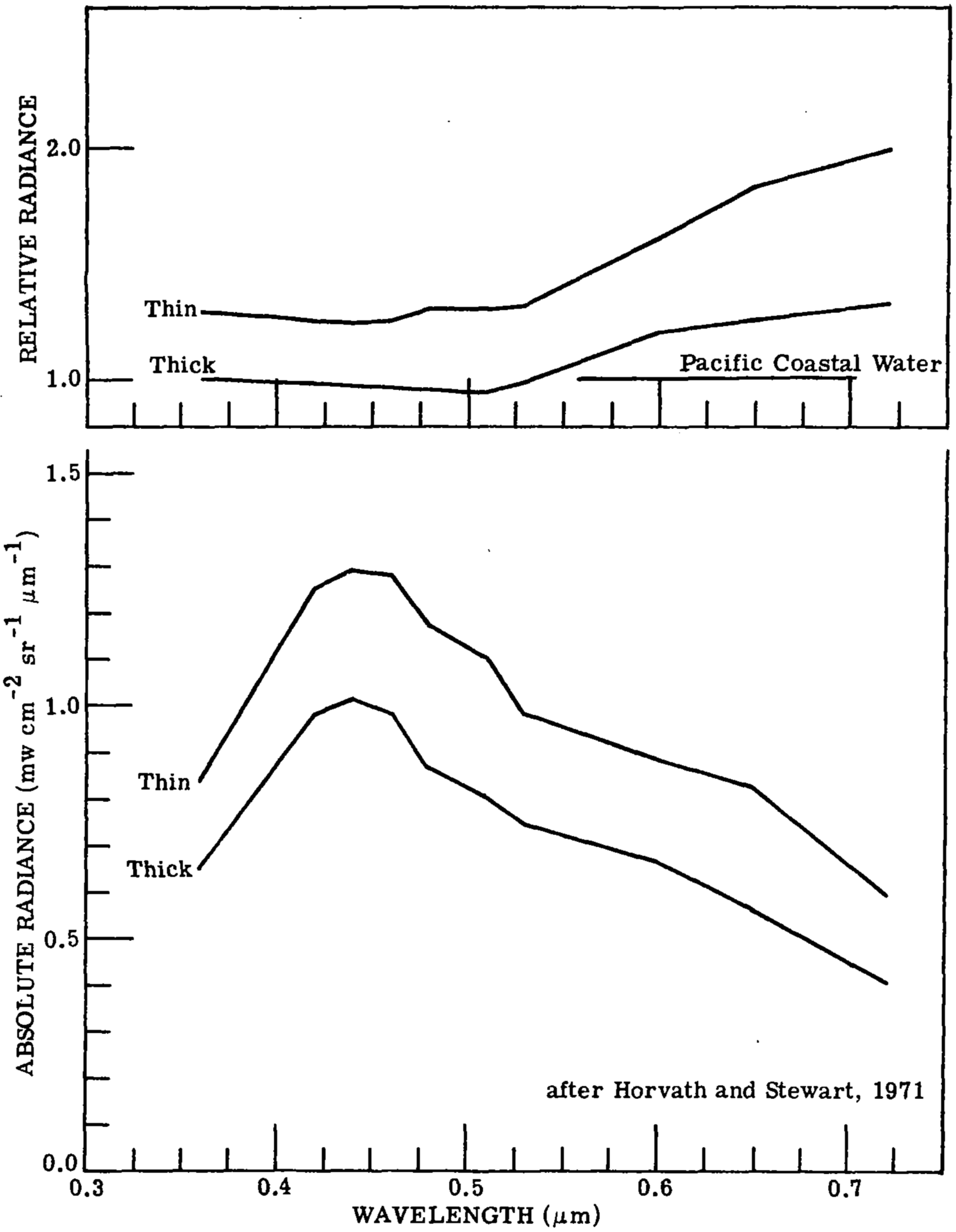

FIGURE 21. 21.6° API CRUDE OIL

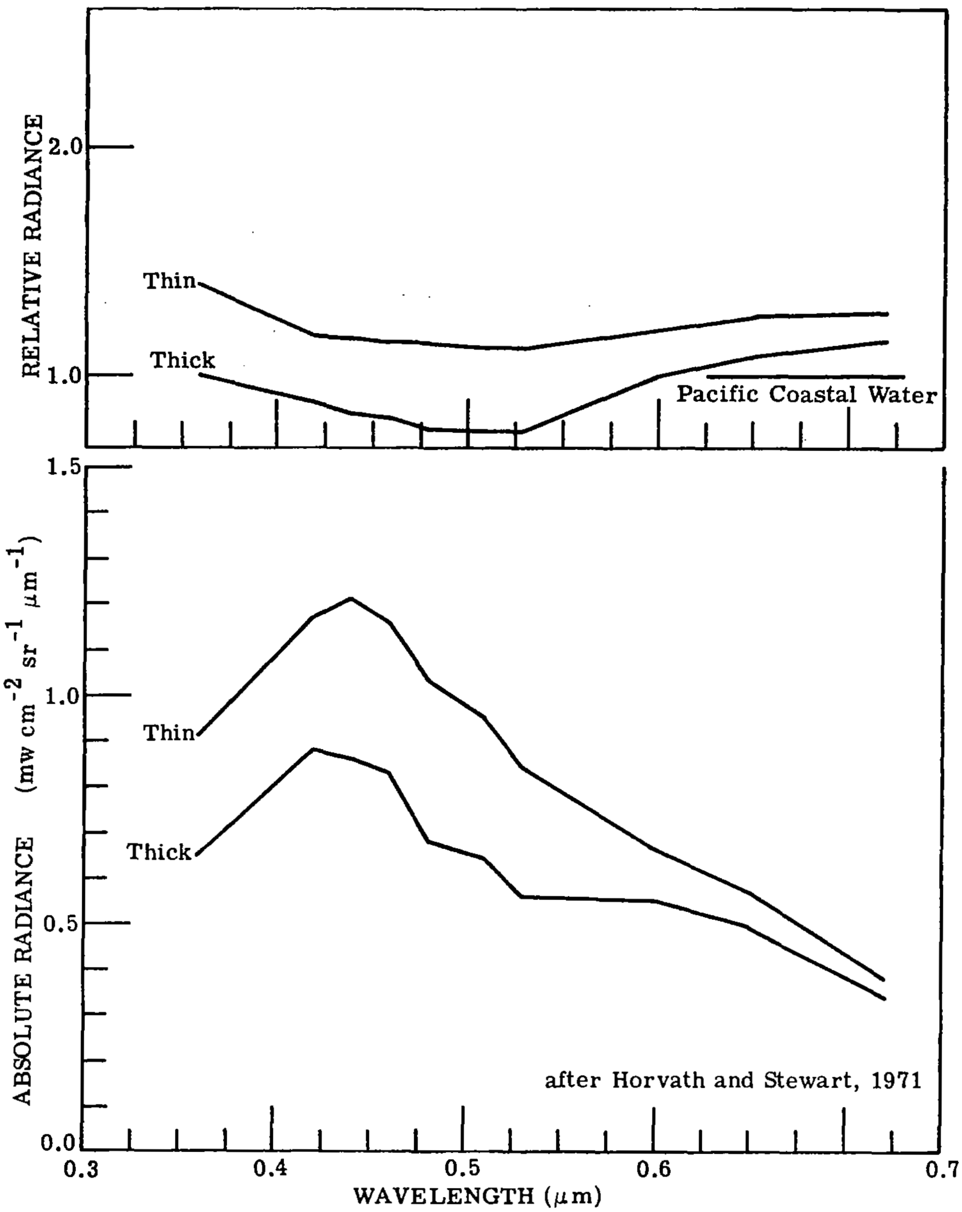

FIGURE 22. 26.1° API CRUDE OIL

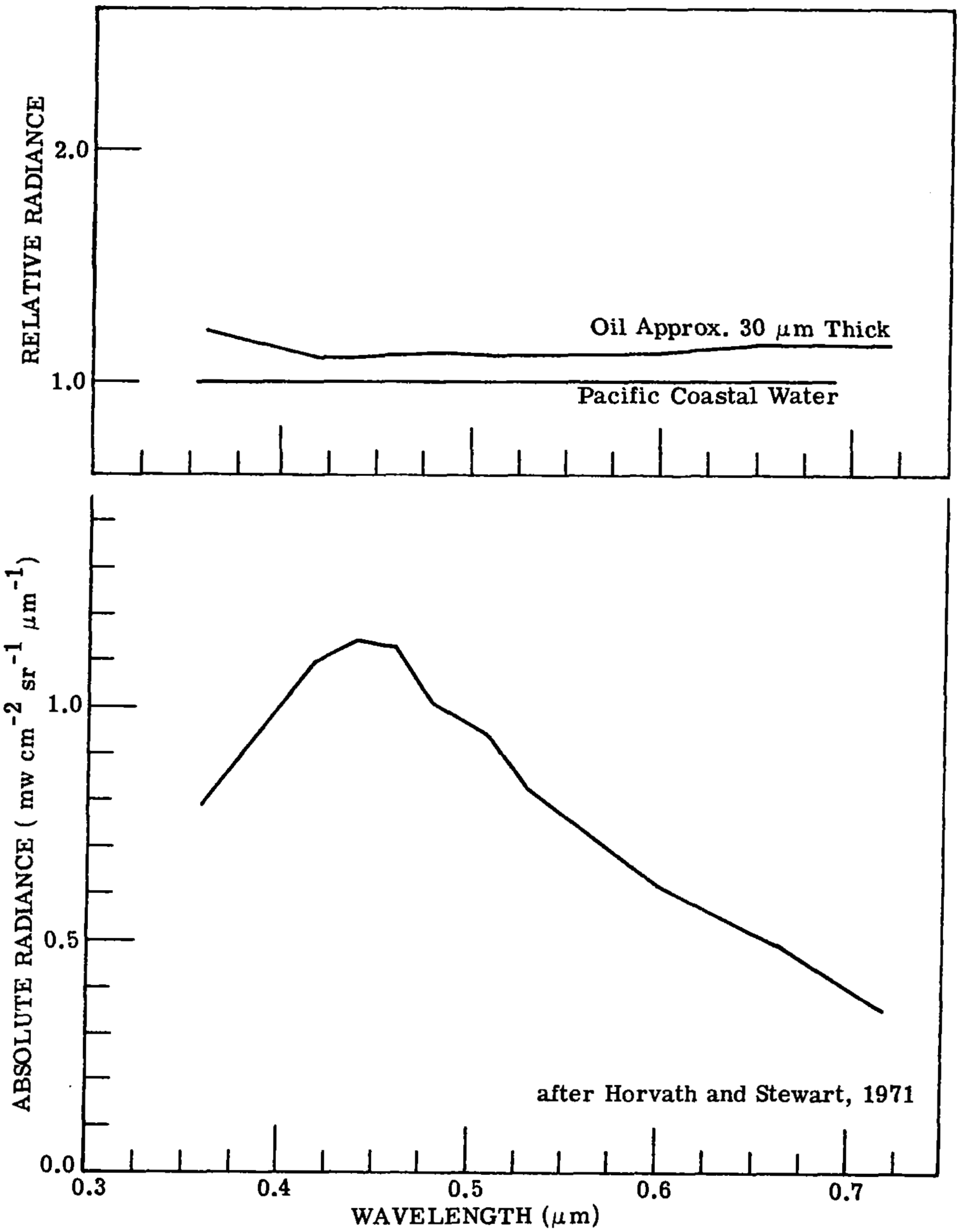

FIGURE 23. #2 DIESEL OIL

TABLE 118
OIL, REFLECTANCE

9.7° API (thin)

λ(µm)	ρ
0.360	0.069
0.420	0.046
0.440	0.047
0.460	0.038
0.480	0.035
0.510	0.036
0.530	0.036
0.600	0.037
0.650	0.039

9.7° API (thick)

λ(µm)	ρ
0.360	0.060
0.420	0.037
0.440	0.035
0.460	0.030
0.480	0.025
0.510	0.026
0.530	0.024
0.600	0.019
0.650	0.018
0.720	0.015

21.6° API (thin)

λ(µm)	ρ
0.360	0.055
0.420	0.043
0.440	0.042
0.460	0.035
0.480	0.031
0.510	0.032
0.530	0.028
0.600	0.027
0.650	0.027
0.720	0.022

21.6° API (thick)

λ(µm)	ρ
0.360	0.043
0.420	0.034
0.440	0.033
0.460	0.027
0.480	0.023
0.510	0.023
0.530	0.021
0.600	0.020
0.650	0.019
0.720	0.015

26.1° API (thin)

λ(µm)	ρ
0.360	0.060
0.420	0.041
0.440	0.039
0.460	0.032
0.480	0.028
0.510	0.027
0.530	0.024
0.600	0.020
0.650	0.019
0.720	0.014

26.1° API (thick)

λ(µm)	ρ
0.360	0.043
0.420	0.030
0.440	0.028
0.460	0.023
0.480	0.018
0.510	0.018
0.530	0.016
0.600	0.017
0.650	0.016
0.720	0.013

NO 2 DIESEL OIL

0.360	0.052
0.420	0.038
0.440	0.037
0.460	0.031
0.480	0.027
0.510	0.027
0.530	0.024
0.600	0.019
0.650	0.017
0.720	0.013

Source: Horvath, R. and Stewart, S.R. [46].

Pacific coastal water, ERIM multispectral scanner, 610 m. altitude, solar zenith angle 47°.

TABLE 119
9.7° API FUEL OIL, RADIANCE
THIN OIL SLICK
SATELLITE ALTITUDE VISIBILITY 15 km

Solar Zenith Angle	Total Radiance ($mw\ cm^{-2} sr^{-1} \mu m^{-1}$) 35°	45°	55°	60°
Wavelength (μm)				
0.420	6.158	5.119	4.393	4.065
0.440	5.767	4.775	4.086	3.774
0.460	5.809	4.782	4.092	3.782
0.480	5.242	4.297	3.675	3.395
0.510	4.264	3.476	2.960	2.727
0.530	3.885	3.157	2.683	2.469
0.600	2.932	2.364	1.995	1.826
0.650	2.476	1.991	1.672	1.524

TABLE 120
9.7° API FUEL OIL, RADIANCE
THIN OIL SLICK
SATELLITE ALTITUDE VISIBILITY 23 km

Solar Zenith Angle	Total Radiance ($mw\ cm^{-2} sr^{-1} \mu m^{-1}$) 35°	45°	55°	60°
Wavelength (μm)				
0.420	6.063	5.120	4.403	4.073
0.440	5.675	4.775	4.093	3.777
0.460	5.669	4.748	4.070	3.758
0.480	5.097	4.253	3.642	3.360
0.510	4.133	3.431	2.924	2.689
0.530	3.761	3.113	2.647	2.430
0.600	2.829	2.323	1.960	1.787
0.650	2.389	1.957	1.641	1.489

TABLE 121
9.7° API FUEL OIL, RADIANCE
THIN OIL SLICK
SATELLITE ALTITUDE VISIBILITY 40 km

Solar Zenith Angle	Total Radiance ($mw\ cm^{-2} sr^{-1} \mu m^{-1}$) 35°	45°	55°	60°
Wavelength (μm)				
0.420	5.981	5.127	4.417	4.085
0.440	5.598	4.783	4.105	3.784
0.460	5.546	4.723	4.054	3.739
0.480	4.969	4.218	3.616	3.331
0.510	4.018	3.394	2.895	2.656
0.530	3.652	3.077	2.617	2.397
0.600	2.738	2.290	1.930	1.754
0.650	2.312	1.929	1.615	1.460

TABLE 122
9.7° API FUEL OIL, RADIANCE
THIN OIL SLICK
SATELLITE ALTITUDE VISIBILITY 60 km

Solar Zenith Angle	Total Radiance ($mw\ cm^{-2} sr^{-1} \mu m^{-1}$) 35°	45°	55°	60°
Wavelength (μm)				
0.420	5.942	5.134	4.427	4.092
0.440	5.561	4.789	4.113	3.789
0.460	5.485	4.712	4.047	3.730
0.480	4.905	4.202	3.604	3.318
0.510	3.960	3.378	2.881	2.641
0.530	3.597	3.061	2.603	2.381
0.600	2.692	2.274	1.915	1.737
0.650	2.275	1.915	1.602	1.445

TABLE 123
21.6° API CRUDE OIL, RADIANCE
THIN OIL SLICK
SATELLITE ALTITUDE VISIBILITY 15 km

Solar Zenith Angle	Total Radiance ($mw\ cm^{-2} sr^{-1} \mu m^{-1}$) 35°	45°	55°	60°
Wavelength (μm)				
0.420	6.103	5.073	4.357	4.035
0.440	5.663	4.688	4.018	3.716
0.460	5.732	4.717	4.041	3.739
0.480	5.132	4.204	3.601	3.333
0.510	4.156	3.385	2.887	2.665
0.530	3.666	2.970	2.535	2.342
0.600	2.658	2.129	1.808	1.664
0.650	2.163	1.723	1.457	1.338
0.720	1.572	1.241	1.048	0.963

TABLE 124
21.6° API CRUDE OIL, RADIANCE
THIN OIL SLICK
SATELLITE ALTITUDE VISIBILITY 23 km

Solar Zenith Angle	Total Radiance ($mw\ cm^{-2} sr^{-1} \mu m^{-1}$) 35°	45°	55°	60°
Wavelength (μm)				
0.420	6.001	5.067	4.362	4.039
0.440	5.558	4.676	4.016	3.711
0.460	5.583	4.675	4.012	3.709
0.480	4.974	4.149	3.560	3.290
0.510	4.014	3.329	2.843	2.620
0.530	3.518	2.906	2.483	2.289
0.600	2.528	2.065	1.753	1.609
0.650	2.047	1.664	1.406	1.286
0.720	1.462	1.177	0.994	0.909

TABLE 125
21.6° API CRUDE OIL, RADIANCE
THIN OIL SLICK
SATELLITE ALTITUDE VISIBILITY 40 km

Solar Zenith Angle	Total Radiance ($mw\ cm^{-2}sr^{-1}\mu m^{-1}$) 35°	45°	55°	60°
Wavelength (μm)				
0.420	5.912	5.069	4.372	4.046
0.440	5.468	4.673	4.018	3.711
0.460	5.451	4.642	3.990	3.685
0.480	4.834	4.103	3.525	3.254
0.510	3.886	3.283	2.806	2.580
0.530	3.386	2.851	2.437	2.242
0.600	2.411	2.010	1.706	1.560
0.650	1.943	1.612	1.361	1.240
0.720	1.363	1.121	0.945	0.860

TABLE 126
21.6° API CRUDE OIL, RADIANCE
THIN OIL SLICK
SATELLITE ALTITUDE VISIBILITY 60 km

Solar Zenith Angle	Total Radiance ($mw\ cm^{-2}sr^{-1}\mu m^{-1}$) 35°	45°	55°	60°
Wavelength (μm)				
0.420	5.868	5.072	4.379	4.052
0.440	5.423	4.673	4.022	3.712
0.460	5.385	4.627	3.980	3.673
0.480	4.763	4.081	3.508	3.236
0.510	3.822	3.260	2.788	2.561
0.530	3.319	2.823	2.414	2.218
0.600	2.352	1.983	1.682	1.535
0.650	1.891	1.586	1.338	1.216
0.720	1.313	1.093	0.920	0.835

TABLE 127
26.1° API CRUDE OIL, RADIANCE
THIN OIL SLICK
SATELLITE ALTITUDE VISIBILITY 15 km

Solar Zenith Angle	Total Radiance ($mw\ cm^{-2} sr^{-1} \mu m^{-1}$) 35°	45°	55°	60°
Wavelength (μm)				
0.420	6.067	5.042	4.333	4.015
0.440	5.601	4.635	3.977	3.681
0.460	5.655	4.652	3.990	3.696
0.480	5.050	4.135	3.546	3.286
0.510	4.022	3.270	2.797	2.587
0.530	3.556	2.877	2.461	2.278
0.600	2.466	1.965	1.676	1.551
0.650	1.955	1.545	1.314	1.214
0.720	1.383	1.078	0.917	0.850

TABLE 128
26.1° API CRUDE OIL, RADIANCE
THIN OIL SLICK
SATELLITE ALTITUDE VISIBILITY 23 km

Solar Zenith Angle	Total Radiance ($mw\ cm^{-2} sr^{-1} \mu m^{-1}$) 35°	45°	55°	60°
Wavelength (μm)				
0.420	5.959	5.033	4.335	4.016
0.440	5.488	4.617	3.969	3.672
0.460	5.497	4.602	3.955	3.660
0.480	4.882	4.071	3.498	3.238
0.510	3.864	3.202	2.743	2.533
0.530	3.397	2.802	2.400	2.218
0.600	2.317	1.885	1.609	1.485
0.650	1.820	1.469	1.249	1.151
0.720	1.256	1.001	0.851	0.786

TABLE 129
26.1° API CRUDE OIL, RADIANCE
THIN OIL SLICK
SATELLITE ALTITUDE VISIBILITY 40 km

Solar Zenith Angle	Total Radiance ($mw\ cm^{-2} sr^{-1} \mu m^{-1}$) 35°	45°	55°	60°
Wavelength (μm)				
0.420	5.866	5.030	4.342	4.021
0.440	5.390	4.607	3.967	3.667
0.460	5.355	4.561	3.927	3.631
0.480	4.732	4.017	3.457	3.196
0.510	3.723	3.143	2.695	2.485
0.530	3.253	2.737	2.347	2.164
0.600	2.182	1.814	1.549	1.425
0.650	1.697	1.401	1.191	1.093
0.720	1.141	0.931	0.791	0.728

TABLE 130
26.1° API CRUDE OIL, RADIANCE
THIN OIL SLICK
SATELLITE ALTITUDE VISIBILITY 60 km

Solar Zenith Angle	Total Radiance ($mw\ cm^{-2} sr^{-1} \mu m^{-1}$) 35°	45°	55°	60°
Wavelength (μm)				
0.420	5.820	5.031	4.347	4.025
0.440	5.341	4.604	3.967	3.665
0.460	5.284	4.542	3.913	3.616
0.480	4.656	3.991	3.437	3.175
0.510	3.651	3.114	2.672	2.461
0.530	3.180	2.705	2.320	2.137
0.600	2.113	1.778	1.518	1.394
0.650	1.635	1.366	1.161	1.063
0.720	1.083	0.896	0.761	0.698

TABLE 131

NO. 2 DIESEL, RADIANCE

SATELLITE ALTITUDE VISIBILITY 15 km

Solar Zenith Angle	Total Radiance ($mw\ cm^{-2} sr^{-1} \mu m^{-1}$) 35°	45°	55°	60°
Wavelength (μm)				
0.420	6.012	4.997	4.298	3.985
0.440	5.560	4.600	3.950	3.658
0.460	5.629	4.631	3.973	3.681
0.480	5.023	4.111	3.528	3.270
0.510	4.022	3.270	2.797	2.587
0.530	3.556	2.877	2.461	2.278
0.600	2.438	1.941	1.657	1.535
0.650	1.903	1.500	1.278	1.183
0.720	1.359	1.058	0.901	0.836

TABLE 132

NO. 2 DIESEL, RADIANCE

SATELLITE ALTITUDE VISIBILITY 23 km

Solar Zenith Angle	Total Radiance ($mw\ cm^{-2} sr^{-1} \mu m^{-1}$) 35°	45°	55°	60°
Wavelength (μm)				
0.420	5.898	4.981	4.295	3.982
0.440	5.441	4.577	3.938	3.646
0.460	5.468	4.577	3.936	3.644
0.480	4.852	4.045	3.478	3.220
0.510	3.864	3.202	2.743	2.533
0.530	3.397	2.802	2.400	2.218
0.600	2.287	1.859	1.588	1.467
0.650	1.763	1.420	1.210	1.117
0.720	1.230	0.979	0.834	0.771

TABLE 133

NO. 2 DIESEL, RADIANCE

SATELLITE ALTITUDE VISIBILITY 40 km

Solar Zenith Angle	Total Radiance ($mw\ cm^{-2} sr^{-1} \mu m^{-1}$) 35°	45°	55°	60°
Wavelength (μm)				
0.420	5.797	4.972	4.297	3.983
0.440	5.338	4.563	3.932	3.638
0.460	5.324	4.534	3.905	3.612
0.480	4.698	3.988	3.434	3.177
0.510	3.723	3.143	2.695	2.485
0.530	3.253	2.737	2.347	2.164
0.600	2.149	1.786	1.526	1.405
0.650	1.636	1.348	1.149	1.056
0.720	1.114	0.907	0.772	0.711

TABLE 134

NO. 2 DIESEL, RADIANCE

SATELLITE ALTITUDE VISIBILITY 60 km

Solar Zenith Angle	Total Radiance ($mw\ cm^{-2} sr^{-1} \mu m^{-1}$) 35°	45°	55°	60°
Wavelength (μm)				
0.420	5.747	4.970	4.299	3.984
0.440	5.286	4.557	3.931	3.634
0.460	5.251	4.513	3.891	3.597
0.480	4.621	3.961	3.413	3.155
0.510	3.651	3.114	2.672	2.461
0.530	3.180	2.705	2.320	2.137
0.600	2.079	1.749	1.494	1.374
0.650	1.571	1.311	1.117	1.025
0.720	1.054	0.871	0.741	0.680

3.5 MUNICIPAL EFFLUENT

Municipal effluent is a very complex mixture of organics and inorganics. The nature of the effluent will reflect the various domestic and industrial uses within a community and the degree of treatment provided. Shown in Table 135 is the typical chemical composition of municipal effluent after secondary treatment. The nature of the receiving waters will also have an important bearing on the composite optical properties of the mixture.

Presented in this section is data for municipal effluent after primary treatment.

TABLE 135
MUNICIPAL EFFLUENT AFTER SECONDARY TREATMENT

COMPONENT	CONCENTRATION (mg/1)
Gross organics	55
Biodegradable organics (as biochemical oxygen demand)	25
Sodium	135
Potassium	15
Ammonium	20
Calcium	60
Magnesium	25
Chloride	130
Nitrate	15
Nitrite	1
Bicarbonate	300
Sulfate	100
Silica	50
Phosphate	25
Hardness (as calcium carbonate)	270
Alkalinity (as calcium carbonate)	250
Total dissolved solids	730

Source: American Chemical Society [48]

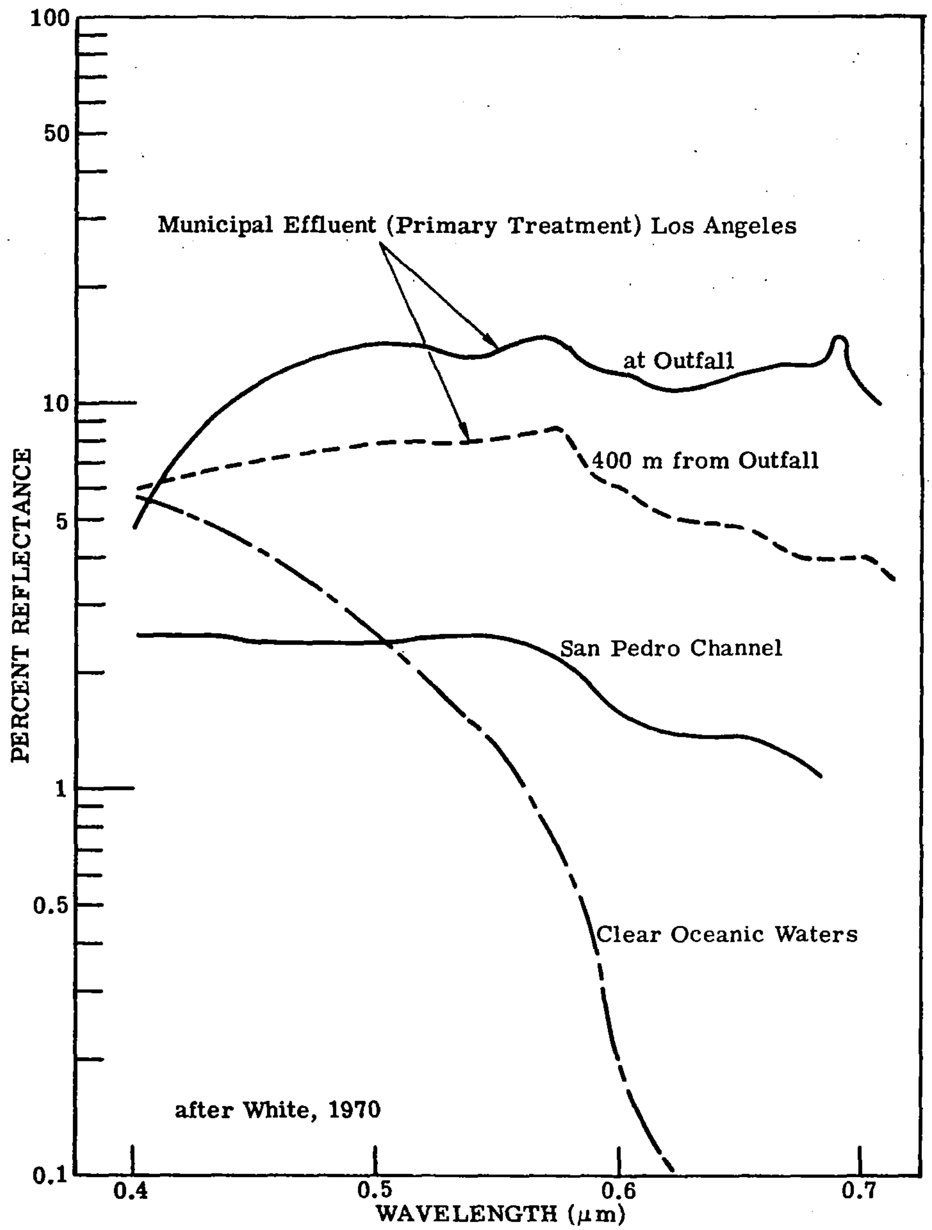

FIGURE 24. MUNICIPAL EFFLUENT

TABLE 136

MUNICIPAL EFFLUENT, REFLECTANCE

$\lambda(\mu m)$	REFLECTANCE at outfall	REFLECTANCE 400 m. from outfall
0.400	0.048	0.060
0.425	0.082	0.066
0.450	0.110	0.070
0.475	0.131	0.075
0.500	0.142	0.079
0.525	0.138	0.079
0.550	0.138	0.082
0.575	0.142	0.085
0.600	0.120	0.060
0.625	0.110	0.050
0.650	0.120	0.048
0.675	0.128	0.040
0.690	0.150	---
0.700	0.115	0.040

Source: White, P. G. 1970 [47].

Aircraft data, 305 m. altitude, Los Angeles Harbor, municipal effluent (primary treatment), quantitative data lacking.

TABLE 137

MUNICIPAL EFFLUENT, RADIANCE (AT OUTFALL)

SATELLITE ALTITUDE VISIBILITY 15 km

Solar Zenith Angle	Total Radiance ($mw\ cm^{-2} sr^{-1} \mu m^{-1}$) 35°	45°	55°	60°
Wavelength (μm)				
0.400	5.675	4.738	4.074	3.776
0.425	6.460	5.372	4.563	4.187
0.450	7.599	6.308	5.301	4.817
0.475	7.837	6.501	5.414	4.881
0.500	7.406	6.146	5.092	4.566
0.525	6.756	5.602	4.629	4.142
0.550	6.121	5.077	4.186	3.736
0.575	6.100	5.064	4.165	3.708
0.600	5.209	4.312	3.553	3.168
0.625	4.619	3.818	3.146	2.806
0.650	4.587	3.801	3.123	2.777
0.675	4.535	3.767	3.089	2.740
0.690	4.932	4.113	3.363	2.974
0.700	3.951	3.275	2.687	2.387

TABLE 138

MUNICIPAL EFFLUENT, RADIANCE (AT OUTFALL)

SATELLITE ALTITUDE VISIBILITY 23 km

Solar Zenith Angle	Total Radiance ($mw\ cm^{-2} sr^{-1} \mu m^{-1}$) 35°	45°	55°	60°
Wavelength (μm)				
0.400	5.598	4.745	4.091	3.792
0.425	6.455	5.444	4.629	4.241
0.450	7.689	6.468	5.433	4.926
0.475	7.998	6.717	5.589	5.025
0.500	7.604	6.386	5.284	4.725
0.525	6.933	5.817	4.802	4.283
0.550	6.292	5.279	4.347	3.869
0.575	6.280	5.272	4.330	3.843
0.600	5.328	4.463	3.672	3.264
0.625	4.704	3.936	3.239	2.879
0.650	4.694	3.934	3.228	2.861
0.675	4.654	3.907	3.199	2.830
0.690	5.097	4.291	3.505	3.090
0.700	4.036	3.383	2.772	2.454

TABLE 139
MUNICIPAL EFFLUENT, RADIANCE (AT OUTFALL)

SATELLITE ALTITUDE VISIBILITY 40 km

Solar Zenith Angle	Total Radiance ($mw\ cm^{-2} sr^{-1} \mu m^{-1}$) 35°	45°	55°	60°
Wavelength (μm)				
0.400	5.532	4.758	4.112	3.811
0.425	6.462	5.523	4.698	4.299
0.450	7.792	6.634	5.569	5.038
0.475	8.169	6.938	5.767	5.172
0.500	7.810	6.627	5.477	4.885
0.525	7.117	6.034	4.975	4.426
0.550	6.468	5.482	4.509	4.002
0.575	6.463	5.479	4.495	3.979
0.600	5.451	4.614	3.791	3.361
0.625	4.794	4.055	3.332	2.954
0.650	4.804	4.067	3.332	2.946
0.675	4.774	4.046	3.309	2.919
0.690	5.261	4.466	3.643	3.205
0.700	4.125	3.491	2.857	2.522

TABLE 140
MUNICIPAL EFFLUENT, RADIANCE (AT OUTFALL)

SATELLITE ALTITUDE VISIBILITY 60 km

Solar Zenith Angle	Total Radiance ($mw\ cm^{-2} sr^{-1} \mu m^{-1}$) 35°	45°	55°	60°
Wavelength (μm)				
0.400	5.499	4.767	4.124	3.822
0.425	6.471	5.569	4.738	4.332
0.450	7.853	6.727	5.644	5.101
0.475	8.267	7.060	5.866	5.253
0.500	7.925	6.760	5.583	4.972
0.525	7.220	6.153	5.070	4.504
0.550	6.565	5.593	4.597	4.074
0.575	6.564	5.592	4.584	4.053
0.600	5.519	4.697	3.856	3.414
0.625	4.845	4.121	3.383	2.994
0.650	4.865	4.139	3.389	2.992
0.675	4.841	4.121	3.368	2.967
0.690	5.350	4.560	3.718	3.267
0.700	4.174	3.550	2.903	2.559

3.6 INDUSTRIAL EFFLUENTS

The concentration of a particular industrial waste, the oxidation state, degree of bio-degradation, and the properties of the receiving waters, are all important factors in determining the reflectance characteristics of industrial process effluents.

Presented in this section is data for the following wastes:

1. Steel mill effluent: oxidized acid-iron waste
2. Paper mill sulfite liquor
3. Chemical: chlor-alkali
4. Tannery effluent
5. Milk waste

The last item "milk waste" is not considered a major target substance and, therefore, radiance calculations are not included.

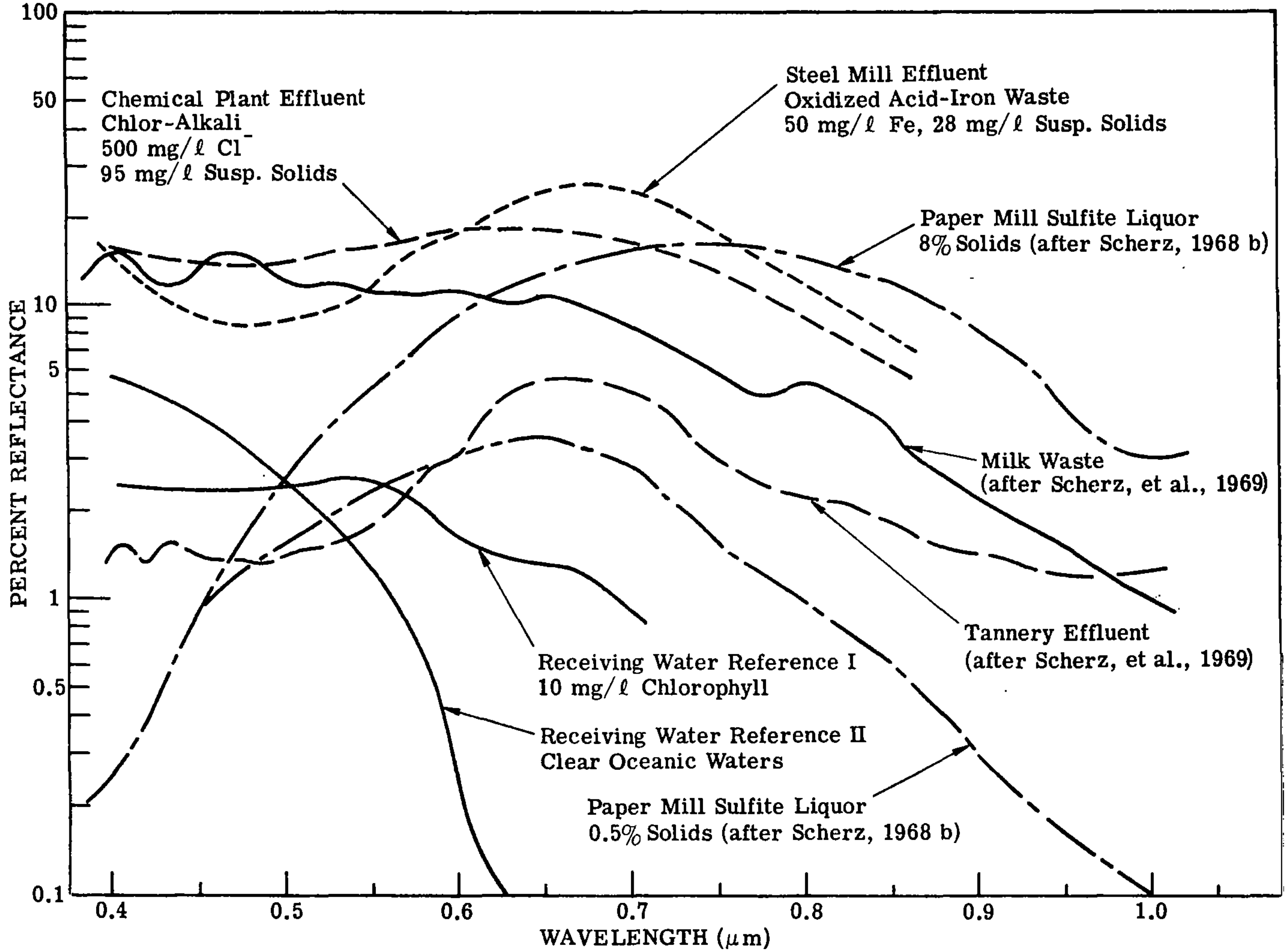

FIGURE 25. INDUSTRIAL EFFLUENTS

TABLE 141

STEEL MILL EFFLUENT, REFLECTANCE

λ(μm)	ρ
0.400	0.150
0.450	0.090
0.500	0.088
0.550	0.110
0.600	0.170
0.650	0.240
0.675	0.260
0.700	0.240
0.750	0.180
0.800	0.120
0.850	0.078

Oxidized acid-iron waste
50 mg/l Fe, 28 mg/l Suspended Solids

Source: Wezernak, C. T., and Polcyn, F. C. [49]

Aircraft data, 305 m. altitude, ERIM multispectral scanner

TABLE 142

STEEL MILL EFFLUENCE, RADIANCE

SATELLITE ALTITUDE VISIBILITY 15 km

Solar Zenith Angle	**Total Radiance ($mw\ cm^{-2} sr^{-1} \mu m^{-1}$)** 35°	45°	55°	60°
Wavelength (μm)				
0.400	7.026	5.869	4.946	4.509
0.450	7.120	5.904	4.984	4.548
0.500	5.945	4.904	4.109	3.726
0.550	5.377	4.442	3.681	3.302
0.600	6.581	5.486	4.491	3.977
0.650	7.713	6.481	5.272	4.633
0.675	7.875	6.632	5.388	4.728
0.700	6.999	5.891	4.789	4.205
0.750	4.974	4.171	3.399	2.993
0.800	3.217	2.674	2.188	1.937
0.850	2.073	1.707	1.404	1.251

TABLE 143

STEEL MILL EFFLUENT, RADIANCE

SATELLITE ALTITUDE VISIBILITY 23 km

Solar Zenith Angle	Total Radiance ($mw\ cm^{-2} sr^{-1} \mu m^{-1}$) 35°	45°	55°	60°
Wavelength (μm)				
0.400	7.137	6.035	5.087	4.629
0.450	7.150	6.012	5.075	4.622
0.500	5.976	5.001	4.187	3.786
0.550	5.470	4.578	3.788	3.388
0.600	6.833	5.752	4.703	4.154
0.650	8.108	6.863	5.578	4.893
0.675	8.294	7.032	5.709	5.002
0.700	7.353	6.232	5.063	4.438
0.750	5.175	4.374	3.562	3.130
0.800	3.295	2.767	2.261	1.995
0.850	2.078	1.732	1.422	1.262

TABLE 144

STEEL MILL EFFLUENT, RADIANCE

SATELLITE ALTITUDE VISIBILITY 40 km

Solar Zenith Angle	Total Radiance (mw $cm^{-2} sr^{-1} \mu m^{-1}$) 35°	45°	55°	60°
Wavelength (μm)				
0.400	7.259	6.206	5.231	4.752
0.450	7.194	6.128	5.172	4.700
0.500	6.020	5.104	4.269	3.850
0.550	5.571	4.716	3.898	3.476
0.600	7.085	6.014	4.913	4.329
0.650	8.495	7.234	5.877	5.147
0.675	8.702	7.419	6.021	5.267
0.700	7.698	6.562	5.328	4.663
0.750	5.372	4.572	3.720	3.262
0.800	3.374	2.859	2.333	2.053
0.850	2.087	1.759	1.441	1.274

TABLE 145

STEEL MILL EFFLUENT, RADIANCE

SATELLITE ALTITUDE VISIBILITY 60 km

Solar Zenith Angle	Total Radiance ($mw\ cm^{-2} sr^{-1} \mu m^{-1}$) 35°	45°	55°	60°
Wavelength (μm)				
0.400	7.330	6.301	5.311	4.820
0.450	7.223	6.193	5.226	4.744
0.500	6.048	5.162	4.316	3.887
0.550	5.628	4.792	3.958	3.524
0.600	7.222	6.156	5.026	4.423
0.650	8.703	7.434	6.037	5.283
0.675	8.921	7.626	6.188	5.409
0.700	7.883	6.738	5.470	4.784
0.750	5.479	4.678	3.805	3.333
0.800	3.417	2.908	2.372	2.084
0.850	2.093	1.774	1.452	1.281

TABLE 146

PAPER MILL SULFITE LIQUOR, 8% SOLIDS, REFLECTANCE

λ (μm)	ρ
0.400	0.0025
0.450	0.009
0.500	0.025
0.550	0.050
0.600	0.090
0.650	0.120
0.700	0.150
0.750	0.160
0.800	0.140
0.850	0.120
0.900	0.080
0.950	0.055
1.000	0.030

Source: Scherz, J. P., et al. [50, 51, 52, 53].

Laboratory reflectance measurements, Beckman DU-2 spectrophotometer with modification for reflectance measurements, illumination provided by a Sylvania Quartz-Iodine Sun Gun (0.2 μm to 1.2 μm).

TABLE 147

PAPER MILL SULFITE LIQUOR, 8% SOLIDS, RADIANCE

SATELLITE ALTITUDE VISIBILITY 15 km

Solar Zenith Angle	Total Radiance ($mw \cdot cm^{-2} sr^{-1} \mu m^{-1}$) 35°	45°	55°	60°
Wavelength (μm)				
0.400	5.073	4.234	3.685	3.449
0.450	5.180	4.264	3.700	3.458
0.500	4.239	3.454	2.962	2.746
0.550	3.783	3.082	2.598	2.372
0.600	4.386	3.608	2.990	2.683
0.650	4.587	3.801	3.123	2.777
0.700	4.804	4.007	3.276	2.896
0.750	4.523	3.784	3.088	2.724
0.800	3.628	3.028	2.473	2.184
0.850	2.854	2.378	1.945	1.720
0.900	1.877	1.547	1.271	1.131
0.950	1.349	1.101	0.910	0.815
1.000	0.832	0.664	0.553	0.502

TABLE 148

PAPER MILL SULFITE LIQUOR, 8% SOLIDS, RADIANCE

SATELLITE ALTITUDE VISIBILITY 23 km

Solar Zenith Angle	Total Radiance ($mw\ cm^{-2} sr^{-1} \mu m^{-1}$) 35°	45°	55°	60°
Wavelength (μm)				
0.400	4.911	4.170	3.647	3.419
0.450	4.967	4.166	3.628	3.393
0.500	4.077	3.385	2.908	2.692
0.550	3.710	3.074	2.590	2.358
0.600	4.424	3.690	3.053	2.730
0.650	4.694	3.934	3.228	2.861
0.700	4.965	4.181	3.414	3.010
0.750	4.686	3.954	3.224	2.836
0.800	3.740	3.150	2.570	2.263
0.850	2.922	2.458	2.008	1.771
0.900	1.885	1.572	1.289	1.143
0.950	1.325	1.097	0.903	0.805
1.000	0.783	0.636	0.528	0.476

TABLE 149

PAPER MILL SULFITE, 8% SOLIDS, RADIANCE

SATELLITE ALTITUDE VISIBILITY 40 km

Solar Zenith Angle	Total Radiance (mw cm^{-2} sr^{-1} μm^{-1}) 35°	45°	55°	60°
Wavelength (μm)				
0.400	4.761	4.112	3.612	3.391
0.450	4.771	4.078	3.563	3.333
0.500	3.931	3.326	2.861	2.644
0.550	3.649	3.073	2.588	2.348
0.600	4.470	3.774	3.118	2.780
0.650	4.804	4.067	3.332	2.946
0.700	5.125	4.351	3.549	3.121
0.750	4.847	4.120	3.356	2.946
0.800	3.851	3.270	2.665	2.341
0.850	2.991	2.538	2.070	1.820
0.900	1.896	1.599	1.308	1.155
0.950	1.305	1.095	0.899	0.798
1.000	0.740	0.611	0.506	0.453

TABLE 150

PAPER MILL SULFITE, 8% SOLIDS, RADIANCE
SATELLITE ALTITUDE VISIBILITY 60 km

Solar Zenith Angle	Total Radiance ($mw\ cm^{-2} sr^{-1} \mu m^{-1}$) 35°	45°	55°	60°
Wavelength (μm)				
0.400	4.683	4.082	3.595	3.376
0.450	4.670	4.033	3.529	3.302
0.500	3.857	3.296	2.837	2.620
0.550	3.619	3.075	2.588	2.345
0.600	4.497	3.821	3.155	2.808
0.650	4.865	4.139	3.389	2.992
0.700	5.212	4.443	3.622	3.182
0.750	4.934	4.210	3.427	3.006
0.800	3.912	3.334	2.716	2.383
0.850	3.029	2.580	2.103	1.847
0.900	1.903	1.613	1.319	1.162
0.950	1.296	1.094	0.898	0.794
1.000	0.719	0.599	0.495	0.442

TABLE 151

CHEMICAL: CHLOR-ALKALI, REFLECTANCE

λ(μm)	ρ
0.400	0.150
0.450	0.140
0.500	0.140
0.550	0.160
0.600	0.180
0.650	0.180
0.700	0.160
0.750	0.130
0.800	0.090
0.850	0.060

500 mg/1 Cl^-
95 mg/1 Suspended Solids

Source: Wezernak, C. T., and Polcyn, F. C. [49]

Aircraft data, 305 m. altitude, ERIM multispectral scanner.

TABLE 152

CHEMICAL: CHLOR-ALKALI, RADIANCE

SATELLITE ALTITUDE VISIBILITY 15 km

Solar Zenith Angle	Total Radiance ($mw \cdot cm^{-2} sr^{-1} \mu m^{-1}$) 35°	45°	55°	60°
Wavelength (μm)				
0.400	7.026	5.869	4.946	4.509
0.450	8.318	6.916	5.776	5.221
0.500	7.352	6.100	5.055	4.535
0.550	6.705	5.576	4.583	4.077
0.600	6.855	5.721	4.679	4.139
0.650	6.150	5.141	4.197	3.705
0.700	5.048	4.217	3.444	3.041
0.750	3.848	3.204	2.621	2.320
0.800	2.600	2.144	1.761	1.567
0.850	1.738	1.419	1.172	1.050

TABLE 153

CHEMICAL: CHLOR-ALKALI, RADIANCE

SATELLITE ALTITUDE VISIBILITY 23 km

Solar Zenith Angle	Total Radiance ($mw\ cm^{-2} sr^{-1} \mu m^{-1}$) 35°	45°	55°	60°
Wavelength (μm)				
0.400	7.137	6.035	5.087	4.629
0.450	8.498	7.152	5.969	5.381
0.500	7.544	6.334	5.243	4.690
0.550	6.937	5.831	4.787	4.246
0.600	7.134	6.010	4.910	4.332
0.650	6.401	5.398	4.403	3.877
0.700	5.230	4.409	3.597	3.168
0.750	3.953	3.324	2.716	2.397
0.800	2.627	2.193	1.798	1.594
0.850	1.716	1.421	1.171	1.044

TABLE 154

CHEMICAL: CHLOR-ALKALI, RADIANCE

SATELLITE ALTITUDE VISIBILITY 40 km

Solar Zenith Angle	Total Radiance (mw cm^{-2} sr^{-1} μm^{-1}) 35°	45°	55°	60°
Wavelength (μm)				
0.400	7.259	6.206	5.231	4.752
0.450	8.690	7.393	6.165	5.545
0.500	7.744	6.571	5.432	4.846
0.550	7.172	6.084	4.989	4.415
0.600	7.412	6.294	5.137	4.522
0.650	6.649	5.651	4.605	4.046
0.700	5.411	4.597	3.747	3.293
0.750	4.059	3.443	2.810	2.473
0.800	2.657	2.242	1.836	1.621
0.850	1.699	1.425	1.172	1.040

TABLE 155

CHEMICAL: CHLOR-ALKALI, RADIANCE

SATELLITE ALTITUDE VISIBILITY 60 km

Solar Zenith Angle	Total Radiance ($mw\ cm^{-2} sr^{-1} \mu m^{-1}$) 35°	45°	55°	60°
Wavelength (μm)				
0.400	7.330	6.301	5.311	4.820
0.450	8.799	7.527	6.273	5.635
0.500	7.856	6.701	5.536	4.932
0.550	7.302	6.223	5.099	4.507
0.600	7.563	6.448	5.260	4.625
0.650	6.784	5.786	4.713	4.137
0.700	5.509	4.698	3.827	3.360
0.750	4.117	3.507	2.860	2.514
0.800	2.675	2.269	1.856	1.637
0.850	1.692	1.429	1.173	1.039

TABLE 156

TANNERY EFFLUENT, REFLECTANCE

$\lambda(\mu m)$	ρ
0.400	0.015
0.450	0.014
0.500	0.014
0.550	0.017
0.600	0.030
0.650	0.055
0.700	0.050
0.750	0.033
0.800	0.022
0.850	0.018
0.900	0.014
0.950	0.012
1.000	0.012

Source: Scherz, J. P., et al [50, 51, 52, 53]

Laboratory reflectance measurements, Beckman DU-2 spectrophotometer with modification for reflectance measurements, illumination provided by a Sylvania Quartz-Iodine Sun Gun (0.2μm to 1.2μm), concentration and specific nature of effluent are undefined.

TABLE 157

TANNERY EFFLUENT, RADIANCE

SATELLITE ALTITUDE VISIBILITY 15 km

Solar Zenith Angle	Total Radiance ($mw\ cm^{-2} sr^{-1} \mu m^{-1}$) 35°	45°	55°	60°
Wavelength (μm)				
0.400	5.238	4.373	3.792	3.539
0.450	5.300	4.365	3.779	3.526
0.500	3.942	3.201	2.762	2.574
0.550	2.907	2.334	2.003	1.860
0.600	2.740	2.199	1.864	1.713
0.650	2.893	2.349	1.959	1.771
0.700	2.366	1.914	1.594	1.441
0.750	1.664	1.328	1.112	1.012
0.800	1.201	0.942	0.793	0.728
0.850	0.958	0.747	0.631	0.580
0.900	0.762	0.587	0.497	0.459
0.950	0.661	0.509	0.432	0.400
1.000	0.573	0.440	0.373	0.346

TABLE 158

TANNERY EFFLUENT, RADIANCE

SATELLITE ALTITUDE VISIBILITY 23 km

Solar Zenith Angle	Total Radiance ($mw\ cm^{-2} sr^{-1} \mu m^{-1}$) 35°	45°	55°	60°
Wavelength (μm)				
0.400	5.100	4.328	3.769	3.521
0.450	5.102	4.280	3.717	3.469
0.500	3.746	3.103	2.685	2.501
0.550	2.741	2.247	1.932	1.791
0.600	2.618	2.143	1.815	1.663
0.650	2.844	2.347	1.955	1.760
0.700	2.312	1.902	1.581	1.423
0.750	1.584	1.287	1.076	0.975
0.800	1.112	0.890	0.748	0.683
0.850	0.872	0.694	0.585	0.535
0.900	0.681	0.536	0.452	0.416
0.950	0.583	0.458	0.387	0.357
1.000	0.504	0.395	0.334	0.308

TABLE 159

TANNERY EFFLUENT, RADIANCE

SATELLITE ALTITUDE VISIBILITY 40 km

Solar Zenith Angle	Total Radiance ($mw\ cm^{-2} sr^{-1} \mu m^{-1}$) 35°	45°	55°	60°
Wavelength (μm)				
0.400	4.973	4.290	3.750	3.506
0.450	4.921	4.204	3.662	3.417
0.500	3.567	3.015	2.615	2.433
0.550	2.591	2.170	1.867	1.729
0.600	2.509	2.094	1.773	1.618
0.650	2.805	2.351	1.954	1.753
0.700	2.266	1.895	1.572	1.409
0.750	1.512	1.253	1.045	0.941
0.800	1.033	0.844	0.708	0.642
0.850	0.795	0.647	0.543	0.494
0.900	0.608	0.489	0.412	0.376
0.950	0.512	0.411	0.347	0.318
1.000	0.442	0.354	0.298	0.273

TABLE 160

TANNERY EFFLUENT, RADIANCE

SATELLITE ALTITUDE VISIBILITY 60 km

Solar Zenith Angle	Total Radiance ($mw\ cm^{-2} sr^{-1} \mu m^{-1}$) 35°	45°	55°	60°
Wavelength (μm)				
0.400	4.907	4.270	3.740	3.499
0.450	4.828	4.166	3.634	3.391
0.500	3.475	2.971	2.579	2.399
0.550	2.515	2.131	1.835	1.696
0.600	2.454	2.070	1.752	1.596
0.650	2.786	2.355	1.955	1.751
0.700	2.245	1.892	1.568	1.402
0.750	1.477	1.236	1.029	0.925
0.800	0.992	0.821	0.687	0.622
0.850	0.756	0.623	0.522	0.473
0.900	0.570	0.465	0.391	0.356
0.950	0.476	0.388	0.326	0.297
1.000	0.411	0.333	0.280	0.255

3.7 OTHER AQUEOUS SOLUTIONS

Laboratory measurements of the specular reflectance of aqueous solutions of NaCl, K_2SO_4, $ZnSO_4$, $(NH_4)_2SO_4$, and $NH_4H_2PO_4$ were performed by Querry and co-workers [54]. The solution concentrations used were very high and far exceed values found in surface waters. Furthermore, the measurements were performed in the infrared, outside the spectral region of interest in this report.

For somewhat similar reasons, data regarding salinity measurement is not included in this report. Salinity measurement by remote sensing is generally considered a microwave measurement problem.

RESEARCH NEEDS

The potential of passive remote sensing for the measurement of specific cations, anions, organics, and other parameters as expressed in Standard Methods [55] or The Report of the Committee on Water Quality Criteria [56], at the concentration of interest, is extremely limited. It is important to distinguish between water chemistry and a general characterization as exemplified by the typical passive remote sensing data record.

A considerable amount of information can be derived regarding various aqueous solutions and suspensions through an analysis of their reflectance characteristics. The development of suitable remote sensing systems for this purpose requires considerably more data than contained in this report. The amount of suitable information contained in the literature was found to be very limited. Complete water quality information as well as pertinent information regarding the conditions of data collection were found to be generally lacking. This underscores the need for laboratory and field measurements to determine the optical properties of a wide range of water bodies and their major constituents, industrial effluents, wastes disposed of by ocean dumping, and substances which gain entry into the aquatic environment through the mechanism of surface runoff.

Remote sensing technology has the potential for making a major contribution in limnology in terms of trophic-state assessment. Development of suitable data analysis procedures requires data regarding the optical properties of a variety of lake waters. The latter should include clear as well as colored lakes in various states of eutrophy.

Large volumes of hazardous polluting substances are transported by water for use in various industrial processes [57]. These substances gain entry into surface waters from offshore and onshore facilities by reason of accident, deliberate discharge, employee error, and/or improper facilities, faulty equipment or careless handling. The optical properties of these, together with the optical properties of effluents from major industrial processes should be determined. However, it must be recognized that the apparent reflectance of effluents and other discharges is a function of concentration and the properties of the receiving waters.

In addition to the need for acquisition of data regarding the optical properties of various water bodies and pollutants, an effort is also required to (1) examine target-background relationships and their effect on radiance at satellite altitude, and (2) the non-Lambertian property of selected targets.

In the analysis of multispectral remote sensing data of water bodies it is important to realize that surface materials outside the instantaneous field of view can affect the target radiance as a result of atmospheric scattering. Failure to account for this effect could result in a misinterpretation of the target data. In a previous study [58] an estimate was made of the target- background interaction for singly-scattered radiation arising from a spatially inhomogeneous surface. It was found, in one case that the change in radiance was as much as 85 percent for a small dark target surrounded by a bright background. The magnitude of the effect depends upon the size of the target and background elements, the reflectances of the materials, the spatial configuration, the sun angle, and the atmospheric turbidity. This effect should be of considerable importance for a water target near a brighter background such as a sandy beach or vegetative shoreline.

For many satellite investigations of the earth's surface it is not a good approximation to assume Lambertian reflectance. A surface, particularly a water surface, may have a distinctly bidirectional character to its reflectance. In general, the spectral radiance L_o is given by the following:

$$L_o(\lambda,\tau_o,\mu,\phi,\mu_o) = \int_0^{2\pi}\int_0^1 \mu'\rho(\lambda,\mu,\phi,-\mu',\phi')L_S(\lambda,\tau_o,\mu_o,\phi_o)d\mu'd\phi'$$

$$+ \int_0^{2\pi}\int_0^1 \mu'\rho(\lambda,\mu,\phi,-\mu',\phi')L_D(\lambda,\tau_o,-\mu',\phi',\mu_o)d\mu'd\phi' \tag{63}$$

where L_S is the direct solar radiance, given by

$$L_S(\lambda,\tau_o,\mu_o,\phi_o) = E_o(\lambda)e^{-\tau_o/\mu}\delta(\mu-\mu_o)\delta(\phi-\phi_o) \tag{64}$$

and L_D is the diffuse sky radiance. Therefore, in general we have

$$L_o(\lambda,\tau_o,\mu,\phi,\mu_o) = \mu_o E_o(\lambda)e^{-\tau_o/\mu}\rho(\lambda,\mu,\phi,-\mu_o,\phi_o)$$
$$+ \int_0^{2\pi}\int_0^1 \mu'\rho(\lambda,\mu,\phi,-\mu',\phi')L_D(\lambda,\tau_o,-\mu',\phi',\mu_o)d\mu'd\phi' \tag{65}$$

where the term $\rho(\lambda,\mu,\phi,-\mu_o,\phi_o)$ is the bidirectional reflectance. For a Lambertian surface Eq. (65) reduces to

$$L_o(\lambda, \lambda_o, \mu_o) = \frac{\rho(\lambda)}{\pi}\tilde{E}_-(\lambda, \tau_o, \mu_o, \rho) \tag{66}$$

where ρ is the surface albedo. How the non-Lambertian property of the surface manifests itself in terms of spectral radiance at satellite altitudes is largely unknown.

5
CONCLUSIONS AND RECOMMENDATIONS

The material compiled in this report provides information regarding the spectral characteristics of a limited number of water bodies, water constituents, and effluent streams. Likewise, radiance calculations at satellite altitude provide data regarding the radiance levels to be expected from water targets under specified conditions.

The amount of suitable material contained in the professional literature is extremely limited. Much of the remote sensing literature consists of imagery and/or data obtained under unspecified conditions, uncalibrated, and generally unsupported by good ground truth data. As a consequence, a field and laboratory program is required to determine the optical properties of a selected number of water bodies, their major constituents, and aqueous wastes.

Concurrent with the above, an analysis of the effect of target-background relationships on radiance levels at satellite altitude is required. This can be expected to have a significant effect in coastal areas. Likewise, the influence of bottom reflectance must be considered. The potential implications of the non-Lambertian property of a number of water targets also requires examination.

In summary, the material presented in this report is regarded simply as an initial step in the development of a suitable data base which can serve as the basis for the development of remote sensing systems for monitoring the aquatic environment.

REFERENCES

1. R.M. Goody, Atmospheric Radiation, Oxford University Press, New York, 1964.

2. V. Ye. Zuyev, Propagation of Visible and Infrared Waves in the Atmosphere, NASA TTF-707, NTIS. U.S. Department of Commerce, Springfield, VA., 1970.

3. U.S. Standard Atmosphere Supplements, U.S. Government Printing Office, Washington, 1966.

4. G.M. Hidy and J.R. Brock, An Assessment of the Global Sources of Tropospheric Aerosols, Academic Press, New York, 1971, p. 1088.

5. F.E. Volz, Infrared Absorption by Atmospheric Aerosol Substances, J. Geophys. Res., 77, No. 6, 1972, p. 1017.

6. F.E. Volz, Infrared Optical Constants of Ammonium Sulfate, Sahara Dust, Volcanic Pumice, and Flyash, Appl. Optics, 12, No. 3, 1973, p. 564.

7. G.W. Grams, I.H. Blifford, Jr., B.G. Schuster, and J.J. DeLuisi, Complex Index of Refraction of Airborne Flyash Determined by Laser Radar and Collection of Particles at 13 km, J. of Atmos. Sciences, 29, 1972, p. 900.

8. D.F. Flanigan and H.P. DeLong, Spectral Absorption Characteristics of the Major Components of Dust Clouds, Appl. Optics, 10, No. 1, 1971, p. 51.

9. C.E. Junge, Journal Meteorol., 12, 1955, p. 13.

10. D. Deirmendjian, Electromagnetic Scattering on Spherical Polydispersions, Elsevier, New York, 1969, p. 78.

11. A.C. Holland and G. Gagne, The Scattering of Polarized Light by Polydisperse Systems of Irregular Particles, Appl. Optics, 9, No. 5, 1970, p. 1113.

12. R.S. Powell, R.R. Circle, D.C. Vogel, P.D. Woodson III, and B. Donn, Optical Scattering from Non-Spherical Randomly Aligned, Polydisperse Particles, Planet. Space Sc., 1967, p. 1641.

13. D.M. Ruthven and K.F. Loughlin, Effects of Particle Shape and Size Distribution on the Transient Solution of the Diffusion Equation, Nature Phys. Sc., 230, 1971, p. 69.

14. C. Junge, Chemical Composition and Radioactivity of the Atmosphere, World Publishing Co., Cleveland, 1963.

15. L.S. Ivlev, Aerosol Model of the Atmosphere, Prob. Fiz. Atmos. Leningrad, No. 7, 1967, pp. 125-160.

16. B.J. Mason, The Physics of Clouds, Clarendon Press, Oxford, 1971.

17. N.A. Fuchs, The Mechanics of Aerosols, Pergamon, Elmsford, N.Y., 1964.

18. C.N. Davies, Aerosol Science, Academic Press, New York, 1966.

19. H.L. Green and W.R. Lane, Particulate Clouds, Dusts, Smokes, and Mists, 2nd Edition. D. Van Nostrand, Inc., Princeton, 1964.

20. F. Linke, Handbuch der Geophysik, Vol. VIII, Springer-Verlag, Berlin, 1943.

21. K. Ya. Kondratyev, Radiation in the Atmosphere, Academic Press, New York, 1969.

22. D.T. Chang and R. Wexler, Relation of Aerosols to Atmospheric Features, Final Report AFCRL-68-0360, AD 674 629, Air Force Cambridge Research Laboratories, Bedford, Mass., 1968.

23. L. Elterman, An Atlas of Aerosol Attenuation and Extinction Profiles for the Troposphere and Stratosphere, Environmental Research Papers No. 241, Air Force Cambridge Research Laboratories, Bedford, Mass., 1966.

24. W.E.K. Middleton, Vision Through the Atmosphere, University of Toronto Press, Toronto, 1952.

25. P.N. Tverskoi, Physics of the Atmosphere, A Course in Meteorology NASA TTF-288, TT65-50114, U.S. Department of Commerce, Washington, 1965.

26. Lord Rayleigh, Phil., Mag., 47, 375, 1899.

27. L. Elterman, U.V., Visible and IR Attenuation for Altitudes to 50 km Report No. AFCRL-68-0153, Air Force Cambridge Research Laboratories, Office of Aerospace Research, Bedford, Mass., 1970.

28. L. Elterman, Vertical-Attenuation Model with Eight Surface Meteorological Ranges 2 to 13 Kilometers, Report No. AFCRL-70-0200, Air Force Cambridge Research Laboratories, Office of Aerospace Research, Bedford, Mass., 1970.

29. R.E. Turner, Radiative Transfer in Real Atmospheres, Report 190100-24-T, Environmental Research Institute of Michigan, Ann Arbor, 1974.

30. W.A. Malila, R.B. Crane, C.A. Omarzu, and R.E. Turner, Studies of Spectral Discrimination. Report WRL 31650-22-T, Willow Run Laboratories University of Michigan, Ann Arbor, 1971.

31. K.L. Coulson, J.V. Dave, and Z. Sekera, Tables Relating to Radiation Emerging from a Planetary Atmosphere with Rayleigh Scattering, University of California Press, Berkeley, 1960.

32. S. Chandrasekhar, Radiative Transfer, Dover Publications, New York, 1960.

33. G.L. Clarke, G.C. Ewing, and C.J. Lorenzen, Spectra of Back-scattered Light from the Sea Obtained from Aircraft as a Measure of Chlorophyll Concentration, Science, Vol. 167, No. 3921, February 1970, pp. 1119-1121.

34. L.V. Strees, The Tongue of the Ocean as a Remote Sensing Ocean Color Calibration Range. Fourth Annual Earth Resources Program Review: Vol. 4, Manned Spacecraft Center, Houston, Texas, January 17 - 21, 1972, pp. 113-1 through 113-13.

35. J.P. Millard and J.C. Arvesen, Results of Airborne Measurements to Detect Oil Spills by Reflected Sunlight, in Remote Sensing of Southern California Oil Pollution Experiment, U.S. Coast Guard, Washington, D.C., 1971, pp. 38-62.

36. Peter G. White, High Altitude Remote Spectroscopy of the Ocean, in Remote Sensing of Earth Resources and the Environment, Proceedings of the Society of Photo-Optical Instrumentation Engineers, Vol. 27, Palo Alto, California, November 1971, pp. 111-114.

37. R.W. Austin, Inherent Spectral Radiance Signatures of the Ocean Surface, in Ocean Color Analysis, technical Report SIO Ref. 74-10, Scripps Institution of Oceanography, University of California San Diego, 1974.

38. P.G. White, Experimental Results of the Remote Measurement of Ocean Color, Second Annual Earth Resources Aircraft Program Status Review, NASA Manned Spacecraft Center, Houstin, Texas, Vol. III, September 1969, pp. 50-1 through 50-9.

39. J.S. Bailey and P.G. White, Remote Sensing of Ocean Color, in Advances in Instrumentation, Proceedings of the 24th Annual ISA Conference, Vol. 24, Part 3, Houston, October 1969, pp. 635-1 to 635-7.

40. J.P. Scherz, W.C. Boyle, and D.R. Graff, Aerial Photographic Techniques in Pollution Detection, Proceedings 23rd Industrial Waste Conference, Purdue University, West Lafayette, May 1968, pp. 87-100.

41. M. Griggs, A Method to Measure the Atmospheric Aerosol Content Using ERTS-1 Data, Third Earth Resources Technology Satellite-1 Symposium, Vol. 1: Technical Presentations, Goddard Space Flight Center, December, 1973, pp. 1509-1518.

42. J.D.H. Strickland, Measuring the Production of Marine Phytoplankton, Bulletin No. 122, Fisheries Res. Board of Canada, Ottawa, 1960.

43. H.H. Seliger and W.D. McElroy, Light: Physical and Biological Action, Academic Press, New York, 1965.

44. V. Klemas, M. Otley, W. Philpot, C. Wethe, R. Roberts, and N. Shah, Correlation of Coastal Water Turbidity and Current Circulation with ERTS-1 and Skylab Imagery, Proceedings Ninth International Symposium on Remote Sensing of Environment, Environmental Research Institute of Michigan, Ann Arbor, April 1974, pp. 1289-1317.

45. R. Horvath, W.L. Morgan, and S.R. Stewart, Optical Remote Sensing of Oil Slicks: Signature Analysis and Systems Evaluation, Final Report, Willow Run Laboratories of the Institute of Science and Technology, The University of Michigan, Ann Arbor, October 1971.

46. R. Horvath and S.R. Stewart, Analysis of Multispectral Data from the California Oil Experiment of October 1970, in Remote Sensing of Southern California Oil Pollution Experiment, U.S. Coast Guard Washington, D.C., 1971, pp. 91-106.

47. P.G. White, Visible Region Remote Spectroscopy of Polluted Water, Third Annual Earth Resources Program Review, NASA Manned Spacecraft Center, Houston, Texas, Vol. III, December 1970, pp. 63-1 through 63-15.

48. American Chemical Society, Cleaning Our Environment, The Chemical Basis for Action, Washington, D.C., 1969.

49. C.T. Wezernak and F.C. Polcyn, Multispectral Remote Sensing Study of Industrial Discharges, Proceedings, 25th Industrial Waste Conference, Purdue University, West Lafayette, Indiana, May 1970, pp. 708-720.

50. J.P. Scherz, W.C. Boyle, and D.R. Graff, Aerial Photographic Techniques in Pollution Detection, Proceedings 23rd Industrial Waste Conference, Purdue University, West Lafayette, May 1968, pp. 87-100.

51. J.P. Scherz, Photographing Water Pollution, Paper No. 68-264 ACSM-ASP Convention of 1968, Washington, D.C., March 1968.

52. J.P. Scherz, D.R. Graff, and W.C. Boyle, Photographic Characteristics of Water Pollution, Photogrammetric Engineering, Vol. XXV, No. 1, January 1969, pp. 38-43.

53. J.P. Scherz, Monitoring Water Pollution by Means of Remote Sensing Techniques, Preprint 1317 ASCE National Water Resources Engineering Meeting, Phoenix, Arizona, January 1971.

54. M.R. Querry, R.C. Waring, W.E. Holland, and G.R. Mansell, Specular Reflectance of Aqueous Solutions, in Proceedings 7th International Symposium on Remote Sensing of the Environment, University of Michigan, Ann Arbor, 1970, pp. 1052-1070.

55. American Public Health Association, Standard Methods for the Examination of Water and Wastewater, 13th Edition, New York, 1971.

56. Federal Water Pollution Control Administration, Report of the Committee on Water Quality Criteria, Washington, D.C. 1968.

57. U.S. Coast Guard, Control of Hazardous Polluting Substances, Report to the 92nd Congress of the United States, House Document 92-70, Washington, D.C.

58. R.E. Turner, Atmospheric Effects in Multispectral Remote Sensing Data, Report 109600-15-F, Environmental Research Institute of Michigan, Ann Arbor, March 1975.

*U.S. GOVERNMENT PRINTING OFFICE: 1976 - 635-275/98